

## SPECTROSCOPY OF LIGHT AND HEAVY QUARKS\*

S. COOPER

Stanford Linear Accelerator Center  
Stanford University, Stanford, California 94305

New results on various controversial light mesons are reviewed, including the glueball candidates  $f_2(1720)$  and  $\eta(1460)$ , the  $1^{++}-0^{-+}$  mass "coincidences"  $f_1(1285)-\eta(1275)$  and  $f_1(1420)-\eta(1420)$ , as well as evidence for the  $X(3100)\rightarrow\Lambda\bar{p}+n\pi$  and the  $\rho(1480)\rightarrow\phi\pi$ , which have quantum numbers not allowed for  $q\bar{q}$ . The  $\gamma\gamma\rightarrow VV$  effects move out of the threshold region with data on  $\gamma\gamma\rightarrow\omega\rho$ . Statistically weak data on  $\Gamma_{\gamma\gamma}(\eta_c)$  and the search for heavy quark  ${}^1P_1$  states are presented.  $\Gamma_{ee}$ ,  $B_{\mu\mu}$ , and  $\Gamma_{tot}$  for the  $\Upsilon(1S)$ ,  $\Upsilon(2S)$ , and  $\Upsilon(3S)$  are updated using new data and a consistent treatment of the radiative corrections for  $\Gamma_{ee}$ . New data on the mass splittings of the  $\chi_b(2P)$  compare favorably with the scalar confinement model, which may however have new trouble.

This review was supposed to cover all the spectroscopy presented in 3 parallel sessions:  $\gamma\gamma$  Interactions, Heavy Bound-Quark States, and a particularly full session on Hadron Spectroscopy. It was too much, even after the usual restriction to things I found interesting and could understand, and in desperation I decided to exclude baryons and  $Q\bar{q}$  mesons. I sincerely hope the next conference offers those fields better treatment (and more time!)

The light mesons part of this paper may be more than the casual reader wants to digest. There are many details, and few firm conclusions. However to simplify would be to mislead. Heavy mesons are a lot easier to deal with, and the last pages are devoted with relief to them.

## 1 New Meson Names

Starting this year the Particle Data Group asks us to use their new naming scheme for hadrons [1]. New and old names are compared in Table 1. Much of this talk is devoted to the  ${}^3P_J$  states, which have  $J^{PC} = 0^{++}, 1^{++},$  and  $2^{++}$ . The new scheme unifies them, with a subscript to label the spin.  $f$  stands for  $I=0$  and  $a$  for  $I=1$ . If you can remember that  $S^*$  and  $\delta$  were  $0^{++}$  mesons with  $I=0$  and 1, you know that they are now  $f_0$  and  $a_0$ . The first step is harder than the second, demonstrating the need for new names. However progress is always accompanied by some pain.  $f'$  and  $\Theta$  were a lot easier than  $f_2(1525)$  and  $f_2(1720)$ .

\*Work supported by the Department of Energy, contract DE-AC03-76SF00515.

<sup>1</sup>Their original names were  $i$ ,  $\Theta$ ,  $g_T$  and  $G$ .

2  $K\bar{K}$  and  $\eta\eta$  Resonances

## 2.1 Glueball Production in Hadron-Hadron Scattering

The search for glueballs has occupied many people over the last several years. At first there was hope that a candidate would be found satisfying all the criteria naively expected of a pure glueball:

- no place in a  $q\bar{q}$  nonet
- flavor symmetric decay (equal coupling to u, d, s quarks)
- copious production in glue-enhanced channels like radiative  $J/\psi$  decay
- not produced in  $\gamma\gamma$  scattering
- not produced in hadron scattering

Of the various candidates<sup>1</sup> that have turned up: the  $\eta(1460)\rightarrow K\bar{K}\pi$  and  $f_2(1720)\rightarrow\eta\eta, K\bar{K}$  in radiative  $J/\psi$  decay, the  $f_2(2050, 2300, 2350)\rightarrow\phi\phi$  [2] and the  $f_0(1590)\rightarrow\eta\eta, \eta\eta'$  [3] in hadronic collisions, none clearly satisfies all of the above. The lack of an ideal glueball has not shaken our faith that QCD gives states of bound glue. Instead we have begun to question how valid the above criteria are. Inspired by a contribution to this conference [4], I would like to re-examine the last of the criteria: **Do we expect to see glueballs in hadron-hadron collisions?** The standard answer is **NO!** Glueballs have no quark content, and therefore don't couple to ordinary hadrons. Hadron scattering is thought of in terms of quark line diagrams, as in

Invited talk presented at the XXIII International Conference on High Energy Physics, Berkeley, California, July 16-23, 1986.

Table 2: Properties of the  $f_2(1720)$  in Radiative  $J/\psi$  Decay.

|  | Crystal Ball [6] | Mark II [7] | Mark III [8] | DM2 [12]    | average |
|--|------------------|-------------|--------------|-------------|---------|
| Number of Events   | 39±11            | ~50         | 192±25       | 410         |         |
| Mass in MeV  | [1720]           | 1700±30     | 1720±10±10   | 1707±10     | 1711±8  |
| Width in MeV   | [130]            | 156±20      | 130±20       | 166±33      | 147±13  |
| $10^4 \times B(J/\psi \rightarrow \gamma f_2, f_2 \rightarrow \eta\eta)$ | 2.6±0.8±0.7      |             |              |             | 2.6±1.1 |
| $K\bar{K}$   |                  | 12±2±5      | 9.6±1.2±1.8  | 9.2±1.4±1.4 | 9.6±1.4 |
| $\pi\pi$   | 2.3±0.7±0.8      | <3.2        | 2.4±0.6±0.5  | 1.8±0.3±0.3 | 2.0±0.4 |
| $\rho\rho$   |                  |             | <5.5 [9]     |             |         |
| $\omega\omega$   |                  |             | <2.4 [10]    |             |         |
| $K^*K^*$   |                  |             | <4.5 [11]    |             |         |
| $\eta\eta'$  |                  |             | <2.1 [11]    |             |         |
| $K\bar{K}\pi$  |                  |             | <2.8 [11]    |             |         |

In the decay  $J/\psi \rightarrow \gamma X$ ,  $I=0$  is preferred for the state  $X$ , and  $0^{++}$ ,  $0^{-+}$ , and  $2^{++}$  are expected to dominate. For  $I=0$  and  $X$  a meson anti-meson pair,  $J^{PC}(X) = (\text{even})^{++}$ . The angular distributions of the 1720 prefer  $2^{++}$  over  $0^{++}$  [13,7,8,12], although sometimes not by as much as one would like [13,12,14]. This might be due to some production of the  $f_0(1730)$  [4,15,1]. The branching ratios assume  $I=0$ ,  $C=+$ , thus  $K\bar{K} = \frac{1}{2}K^+K^- + \frac{1}{4}K_s K_s + \frac{1}{4}K_L K_L$  and  $\pi\pi = \frac{2}{3}\pi^+\pi^- + \frac{1}{3}\pi^0\pi^0$ . Upper limits are 90% confidence level. The average mass and width use  $K^+K^-$  data only. The  $K^+K^-$  results are all from fits to the  $f_2(1525) + f_2(1720)$ , neglecting interference.

The  $f_2(1720)$  was discovered [13] in  $J/\psi \rightarrow \gamma\eta\eta$  with  $M = 1640 \pm 50$  MeV,  $\Gamma = 220^{+100}_{-70}$  MeV, and  $B(J/\psi \rightarrow \gamma 1640, 1640 \rightarrow \eta\eta) = (4.9 \pm 1.4) \times 10^{-4}$ . That is a lower mass and larger width than later seen in the higher statistics  $\gamma K\bar{K}$  measurements. The  $\gamma\eta\eta$  signal may be contaminated by the  $f_2(1525)$ , which is  $2^{++}$  but with unknown rate to  $\eta\eta$  [3], or by the  $f_0(1590)$ , which does decay to  $\eta\eta$  but is  $0^{++}$  [3]. Thus we should probably regard the original branching ratio as an upper limit for the  $f_2(1720) \rightarrow \eta\eta$ . Indeed a fit including the  $f_2(1525)$  gave  $M = 1670 \pm 50$ ,  $\Gamma = 160 \pm 80$ , and  $B(J/\psi \rightarrow \gamma 1670, 1670 \rightarrow \eta\eta) = (3.8 \pm 1.6) \times 10^{-4}$  [16]. The branching ratio in the table is from a third fit where the masses and widths were fixed at the Mark III values.

The  $\pi\pi$  branching ratios are from fits to  $f_2(1270) + f_2(1720) + X(\sim 2100)$ , neglecting interference, which can reduce the  $f_2(1720)$  branching ratio by at least a factor of 2 [11]. Only the  $f_2(1270)$  spin has been determined in  $J/\psi \rightarrow \gamma\pi\pi$ , so the identification of the 1720 peak with the  $f_2(1720)$  is tentative, and may be contradicted by  $\pi\pi \rightarrow K\bar{K}$  data [4], as discussed in the text.

there are other decays not seen yet. Thus  $K\bar{K}$  scattering should produce one of our favorite glueball candidates about as strongly as it does one of our better understood  $q\bar{q}$  mesons. The equality of the quantum numbers and near equality of the masses reduces most kinematic effects. For example, the  $1/p_K^2$  in the B-W gives a suppression of only 0.7 for  $f_2(1720)/f_2(1525)$ .

Although we expect to produce about the same number of  $f_2(1525)$  and  $f_2(1720)$  mesons, if we require the final state to be  $K\bar{K}$ , they will be seen in the ratio of their  $K\bar{K}$  branching ratios. Furthermore if a fit has not been done to the spectrum, we have to rely on our eyes, which are more sensitive to peak height than to area. The peak height scales as  $1/\Gamma_{\text{tot}}$  for equal area. Including the  $1/p_K^2$  factors from the Breit-Wigner scattering formula, we find that the peak height of each  $f_2$  is proportional to  $B_{KR}^2/p_K^2$ . This gives a ratio  $f_2(1720)/f_2(1525) \sim 1/2$  (with a large error due to the poorly known branch-

ing ratios.)

Lacking a  $K\bar{K}$  collider, we turn to the reaction of Fig. 1,  $K^-p \rightarrow K\bar{K}\Lambda$ , since the upper vertex looks like  $K\bar{K}$  scattering. The  $K_s K_s$  final state can only be  $0^{++}$ ,  $2^{++}$ , etc., so it is preferable to  $K^+K^-$  for the study of  $2^{++}$  mesons. The new LASS data [18] is shown in Fig. 2. The  $f_2(1525)$  is prominent in the spectrum, but the  $f_2(1720)$  is in one of the lowest bins around. We would like to use this result to gain quantitative information on the  $f_2$  branching ratios.

In the  $K$  exchange picture we have assumed, there is additional mass dependence of the effective virtual kaon flux which must be calculated correctly, and tested against data on known mesons. The Watson theorem [19] gives the total production of a resonance  $R$  in  $K^-p \rightarrow R\Lambda$  as [20]

$$\sigma_R = \frac{2\pi M_R}{(p_K)^{2J+1}} \Gamma_{KR} \quad (3)$$

Table 1: New Meson Names

| $J^{PC}$                   | New Names (masses in MeV, if known) |              |                    |               | Old Names |          |            |         |
|----------------------------|-------------------------------------|--------------|--------------------|---------------|-----------|----------|------------|---------|
| $0^{-+}$                   | K (494)                             | $\pi$ (140)  | $\eta$ (549)       | $\eta'$ (958) | K         | $\pi$    | $\eta$     | $\eta'$ |
| $^1S_0 \downarrow\uparrow$ | $D_s$ (1971)                        | D (1860)     | $\eta_c$ (2981)    |               | F         | D        | $\eta_c$   |         |
|                            | $B_s$                               | B (5271)     | $\eta_b$           |               | $B_s$     | B        | $\eta_b$   |         |
| $1^{--}$                   | $K^*$ (892)                         | $\rho$ (770) | $\omega$ (783)     | $\phi$ (1020) | $K^*$     | $\rho$   | $\omega$   | $\phi$  |
| $^3S_1 \uparrow\uparrow$   | $D_s^*$ (2109)                      | $D^*$ (2010) | J/ $\psi$ (3097)   |               | F*        | D*       | J/ $\psi$  |         |
|                            | $B_s^*$                             | $B^*$ (5325) | $\Upsilon$ (9460)  |               | $B_s^*$   | $B^*$    | $\Upsilon$ |         |
| $1^{+-}$                   | $K_1$ (1400)                        | $b_1$ (1235) | $h_1$ (1190)       | $h'_1$        | $Q_2$     | B        | H          |         |
| $^1P_1 \downarrow\uparrow$ |                                     |              | $h_c$              |               |           |          |            |         |
|                            |                                     |              | $h_b$              |               |           |          |            |         |
| $0^{++}$                   | $K_0^*$ (1350)                      | $a_0$ (980)  | $f_0$ (1300)       | $f_0$ (975)   | $\kappa$  | $\delta$ | $\epsilon$ | $S^*$   |
| $^3P_0 \uparrow\uparrow$   |                                     |              | $\chi_{c0}$ (3415) |               |           |          | $\chi$     |         |
|                            |                                     |              | $\chi_{b0}$ (9860) |               |           |          | $\chi_b$   |         |
| $1^{++}$                   | $K_1$ (1280)                        | $a_1$ (1270) | $f_1$ (1285)       | $f_1$ (1420)  | $Q_1$     | $A_1$    | D          | E       |
| $^3P_1 \uparrow\uparrow$   |                                     |              | $\chi_{c1}$ (3510) |               |           |          | $\chi$     |         |
|                            |                                     |              | $\chi_{b1}$ (9892) |               |           |          | $\chi_b$   |         |
| $2^{++}$                   | $K_2^*$ (1425)                      | $a_2$ (1320) | $f_2$ (1270)       | $f'_2$ (1525) | $K^*$     | $A_2$    | $f^0$      | $f'$    |
| $^3P_2 \uparrow\uparrow$   |                                     |              | $\chi_{c2}$ (3556) |               |           |          | $\chi_c$   |         |
|                            |                                     |              | $\chi_{b2}$ (9913) |               |           |          | $\chi_b$   |         |

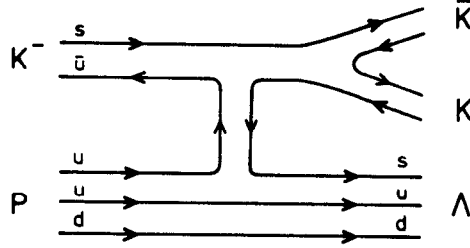

 Figure 1: Quark diagram for  $K^- p \rightarrow \bar{K} K \Lambda$ .

Fig. 1. A glueball has no place in such a diagram, at least to the extent that  $\alpha_s$  is small. The suppression is expected to be approximately the square root of the normal OZI suppression. It should lead to a narrow width for glueballs, since their only possible decay, to hadrons, is suppressed. However, a wide glueball has by definition a large coupling to hadrons. The strength of its decay to hadrons is related by time reversal to the strength of its formation in collisions of those hadrons.

In  $K\bar{K}$  collisions we should see resonances which couple to  $K\bar{K}$ . The relativistic Breit-Wigner scattering formula is [5]

$$\sigma(W) = \frac{4\pi g}{p_i^2} \frac{M^2 \Gamma_i \Gamma_f}{(W^2 - M^2)^2 + M^2 \Gamma_{tot}^2} \quad (1)$$

where  $p_i$  is the momentum of the initial particles in their center of mass frame and  $W$  is the total center of mass energy;  $M$  is the mass of the resonance,  $\Gamma_{tot}$  is its total width, and  $\Gamma_i$  and  $\Gamma_f$

its partial widths to the initial and final states.  $g = (2J + 1) / [(2s_1 + 1)(2s_2 + 1)]$  is the spin factor for a spin  $J$  resonance formed by spin  $s_1$  and  $s_2$  initial state particles.

To calculate the total production rate of a resonance in  $K\bar{K}$  collisions we sum over the final states  $\sum \Gamma_f = \Gamma_{tot}$ , and integrate over  $W$  to obtain (for a narrow resonance)

$$\sigma_R = \int \sigma(W) dW = \frac{2g\pi^2}{p_K^2} \Gamma_{KK}. \quad (2)$$

Thus the production rate of a resonance is determined by its partial width to the initial state, entirely independent of whether the resonance is  $q\bar{q}$  or  $gg$ . Now we can correctly answer the question above with **Yes, we expect a wide glueball to be produced in hadronic collisions, at least when the input channel corresponds to one of its dominant decays.**

## 2.2 Properties of the $f_2(1720)$

Consider two resonances with the same quantum numbers which couple strongly to  $K\bar{K}$ : the  $f_2(1525)$  and the  $f_2(1720)$ . You know these as the  $f'(1525)$   $s\bar{s}$  resonance and the  $\Theta(1720)$  glueball candidate seen in radiative J/ $\psi$  decays. The  $f_2(1525)$  decays dominantly to  $K\bar{K}$ . A predicted [17] 13% branching ratio to  $\eta\eta$  may have been observed [3]. Using Ref. [17] let us assume  $\Gamma_{K\bar{K}}^{1525} = 0.8 \times \Gamma_{tot}^{1525} = 0.8 \times (70 \pm 10)$  MeV. The observed  $f_2(1720)$  branching ratios are listed in Table 2.  $K\bar{K}$  is  $\sim 70\%$  of the total observed, giving  $\Gamma_{K\bar{K}}^{1720} \sim 0.7 \times 147 = 100$  MeV, less if

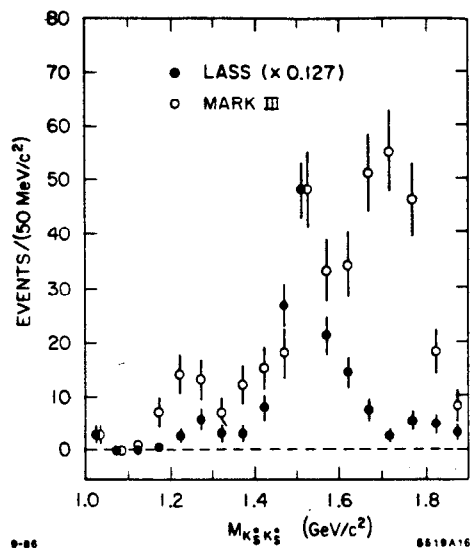


Figure 2:  $K_s K_s$  mass distributions [18] from (open circles) Mark III uncorrected  $J/\psi \rightarrow \gamma K_s K_s$  data and (solid circles) LASS acceptance corrected  $K^- p \rightarrow K_s K_s \Lambda$ . The LASS data have been multiplied by 0.127 to match the Mark III data in the 1525 MeV bin. LASS used a 11 GeV/c  $K^-$  beam, and for this plot required  $|t'| < 2 \text{ GeV}^2$ , where  $t' \equiv t - t_{\min}$ .

This leads to a suppression from the  $p_K$  factors of 0.4 rather than 0.7. I don't understand the origin of Eq. (3), but it gives the strongest suppression that has been suggested to me, so I quote it to show that even the extreme case is not very dramatic.

More critical is the validity of the K exchange picture itself. The analogous  $\pi$  exchange mechanism has been well tested, but K exchange has not. Data comparing production of the  $u\bar{u} + d\bar{d}$   $f_2(1270)$  with the  $s\bar{s}$   $f_2(1525)$  in  $\pi^- p \rightarrow f_2 n$  and  $K^- p \rightarrow f_2 \Lambda$  indicate a factor of two problem in the K exchange picture [20,21]. In contrast to the pion, the kaon may not be light enough to dominate over other strange meson exchanges. Fits to  $t$ -distributions, and polarised target data, may help to separate the various contributions [20].

If the strangeness exchange process can be understood, it could provide useful information on the absolute  $f_2(1720)$  decay branching ratios. That, combined with the data in Table 2, would give the total rate for  $J/\psi \rightarrow \gamma f_2(1720)$ . The more the  $f_2(1720)$  is produced in that glue-enriched channel, the more glueball character we are willing to attribute to it. In principle the total  $J/\psi \rightarrow \gamma f_2(1720)$  rate could be measured from the inclusive  $\gamma$  spectrum in  $J/\psi \rightarrow \gamma + X$  shown in Fig. 3. It would appear at  $E_\gamma \sim 1070 \text{ MeV}$  with a full width of  $\sim 70$

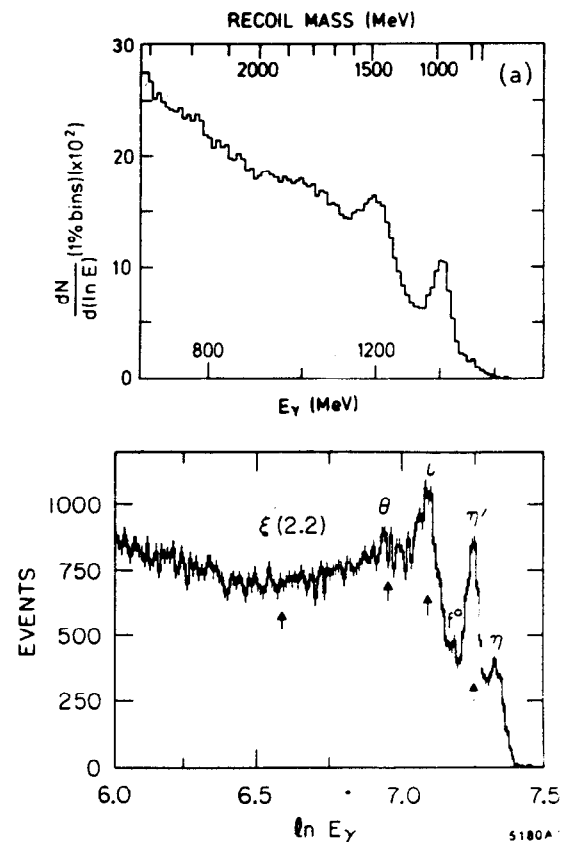


Figure 3: Crystal Ball inclusive  $\gamma$  spectra, without efficiency correction or background subtraction, from (a)  $J/\psi \rightarrow \gamma + \text{hadrons}$  [22], and (b)  $J/\psi \rightarrow \gamma + X$  [23].

MeV. However here no spin-parity analysis is possible, so that it would be difficult to cleanly isolate the  $f_2(1720)$  signal from all the other radiative  $J/\psi$  decays. Knowledge of the  $\gamma$  background from  $\pi^0$  decays might help.

While one-kaon exchange may have its problems, one-pion exchange (OPE) is well established. One could therefore use the  $J/\psi \rightarrow \gamma K\bar{K}$  data to determine the mass and  $\Gamma_{\text{tot}}$  of the  $f_2(1720)$ , and  $\pi\pi \rightarrow \pi\pi$  to get  $\Gamma_{\pi\pi}^2$ , and thus  $B(f_2(1720) \rightarrow \pi\pi)$ .  $\pi\pi \rightarrow K\bar{K}$  similarly yields  $\Gamma_{\pi\pi}\Gamma_{K\bar{K}}$ .

Longacre *et al.* [4] have done a partial wave analysis to extract the  $2^{++}$  contribution from their new  $\pi^- p \rightarrow K_s K_s n$  data (Fig. 4). Using OPE they extrapolate to the pion pole to get the  $\pi\pi \rightarrow K\bar{K}$   $2^{++}$  intensity. They then make a simultaneous fit to that and to older  $2^{++}$   $\pi\pi \rightarrow \pi\pi, \eta\eta$ , and (assumed)  $K\bar{K} \rightarrow K\bar{K}$  data, as well as to the total (not

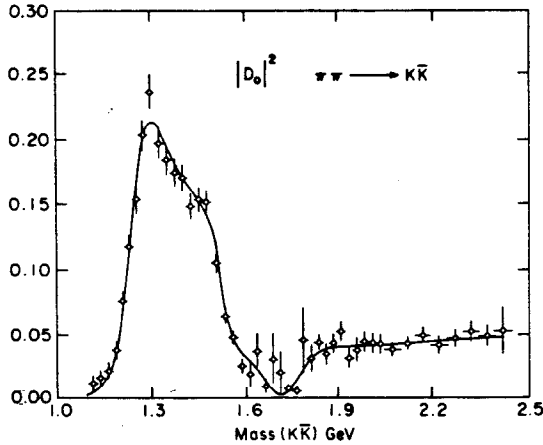


Figure 4:  $\pi\pi \rightarrow K_s K_s$ ,  $2^{++}$  intensity extrapolated using OPE from 22 GeV/c  $\pi^- p \rightarrow K_s K_s n$  data with  $|t'| < 0.1$  GeV<sup>2</sup> [4]. The curve is the fit described in the text. It has destructive interference between the  $f_2(1525)$  and  $f_2(1720)$  to give the maximum  $f_2(1720) \rightarrow \pi\pi$  branching ratio.

spin-separated)  $J/\psi \rightarrow \gamma K\bar{K}, \gamma\pi\pi, \gamma\eta\eta$ . The hadronic scattering data have no need for the  $f_2(1720)$ , and an upper limit of 4% for the branching ratio  $f_2(1720) \rightarrow \pi\pi$  is obtained.<sup>2</sup> This is in contradiction to the  $\pi\pi$  fraction of the observed branching ratios in Table 2, which were however obtained without spin analysis and interference. Allowing interference can reduce  $\pi\pi$  to  $(8 \pm 3)\%$  of the observed decays. A glueball candidate which decays dominantly to  $K\bar{K}$  and  $< 4\%$  to  $\pi\pi$  isn't doing very well at passing the test of flavor symmetric decay. It would be interesting to repeat this fit with the newer  $\pi\pi \rightarrow \eta\eta$  [3] and  $K\bar{K} \rightarrow K\bar{K}$  [18] data, as well as spin-analysed radiative  $J/\psi$  decay data, should that become available. It may also be possible to use double-Pomeron scattering data [24], as done in Ref. [25] for the  $0^{++}$  system.

DM2 [28,12] and Mark III [29,26,27] have compared tensor resonance production in  $J/\psi \rightarrow \gamma X$  with  $J/\psi \rightarrow \omega X$  and  $J/\psi \rightarrow \phi X$ . The first channel presumably goes via  $\gamma gg$  and therefore enhances glueball production, while the presence of the  $\omega$  and  $\phi$  in the last two select  $u\bar{u}d\bar{d}$  and  $s\bar{s}$  mesons respectively (see Fig. 5). They look for the  $f_2(1720)$  in events where  $X$  is  $K\bar{K}$  or  $\pi\pi$ . The Mark III spectra with  $X = K^+K^-$  are shown in Fig. 6. The  $f_2(1720)$  is seen clearly in the  $J/\psi \rightarrow \gamma K^+K^-$  spectrum, where it has been determined to be  $2^{++}$ . The  $\omega K^+K^-$  spectrum shows a peak with the same mass and width, but no spin analysis has been done. Since

<sup>2</sup>The limit depends on the assumption of K exchange.

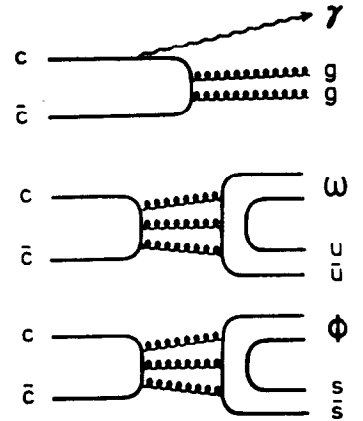


Figure 5: Quark diagrams for  $J/\psi \rightarrow \gamma X$ ,  $J/\psi \rightarrow \omega X$ , and  $J/\psi \rightarrow \phi X$ .

there is evidence [1,4,15] for a  $0^{++}$   $K\bar{K}$  resonance  $f_0(1730)$ , it is not safe to assume that the peak in  $J/\psi \rightarrow \omega K^+K^-$  is the  $f_2(1720)$ . Let us call it X. Then  $B(J/\psi \rightarrow \gamma f_2, f_2 \rightarrow K\bar{K}) \approx 2 \times B(J/\psi \rightarrow \omega X, X \rightarrow K\bar{K})$ . The values are given in Table 3. It is rather peculiar that X is produced so strongly with  $\omega$ , which should suppress  $s\bar{s}$  resonances, yet decays to  $K\bar{K}$ . The  $J/\psi \rightarrow \phi K^+K^-$  spectrum is dominated by the  $f_2(1525)$  (expected here since it is  $s\bar{s}$ ) with a shoulder on its high mass side. In looking for the  $f_2(1720)$  here, not only do we have to worry about interference with the  $f_2(1525)$ , but also about the apparent (but low-statistics) disagreement between the  $K^+K^-$  and  $K_s K_s$  spectra<sup>3</sup> (see Fig. 7). If the same X is being seen in the DM2  $\phi K_s K_s$  and the Mark III  $\omega K^+K^-$  spectra, it is being produced with  $\phi$  and  $\omega$  at about the same rate. Using  $\phi K^+K^-$  gives considerably less. These data and those with  $X = \pi\pi$ , especially when spin-analysed, will provide a wealth of information.

### 2.3 $f_2$ States Near 2.2 GeV

There is quite a bit of action in the  $2^{++}$  system above 2 GeV. There are three wide  $2^{++}$   $\phi\phi$  resonances originally named<sup>4</sup>  $g_T$ :

|       |                             |                                  |
|-------|-----------------------------|----------------------------------|
| $g_T$ | $M = 2050^{+90}_{-50}$ MeV  | $\Gamma = 200^{+160}_{-50}$ MeV  |
| $g_T$ | $M = 2300^{+20}_{-100}$ MeV | $\Gamma = 200^{+80}_{-50}$ MeV   |
| $g_T$ | $M = 2350^{+20}_{-30}$ MeV  | $\Gamma = 270^{+270}_{-130}$ MeV |

seen in  $\pi^- p \rightarrow \phi\phi n$  [2]. The  $g_T(2050)$  is the dom-

<sup>3</sup>In  $J/\psi \rightarrow \phi X$ , isospin conservation requires that X have  $I=0$ , and therefore  $J^{PC} = 0^{++}, 2^{++}$ , etc. for both  $K^+K^-$  and  $K_s K_s$ . However the  $K_s K_s$  spectrum is nearly background free, while  $K^+K^-$  is not.

<sup>4</sup>They should be called  $f_2$ . I use  $g_T$  here as a generic name for all three  $\phi\phi$  resonances, and to avoid hopelessly confusing them with Mark III's  $f_2(2230)$ .

Table 3: Comparison of  $f_2(1525)$  and  $f_2(1720)$  production in  $J/\psi$  decays and  $\gamma\gamma$  Collisions.

| V  | $10^4 \times B(J/\psi \rightarrow Vf_2, f_2 \rightarrow K\bar{K})$ |                        | Spin known? |                       |
|--|--|------------------------|-------------|-----------------------|
|  | $f_2(1525)$  | $f_2(1720)$            |             |                       |
| $\gamma$   | $6.0 \pm 1.4 \pm 1.2$  | $9.6 \pm 1.2 \pm 1.8$  | yes         | Mark III [8]          |
|  | $5.0 \pm 1.2 \pm 0.8$  | $9.2 \pm 1.4 \pm 1.4$  | yes         | DM2 [28,12]           |
|  | $6.0 \pm 1.2 \pm 1.2$  | $12.4 \pm 2.8 \pm 2.4$ | no          | $K_s K_s$ DM2 [28,12] |
| $\omega$   | $< 1.2$ (90% C.L.)   | $4.5 \pm 1.2 \pm 1.0$  | no          | Mark III [29,27]      |
| $\phi$   | $6.4 \pm 0.6 \pm 1.6$  | $\sim 1.4^{\dagger}$   | no          | Mark III [29,27]      |
|  | $4.6 \pm 0.5$  |                        | no          | DM2 [28,12]           |
|  | $4.3 \pm 0.7 \pm 0.9$  | $3.6 \pm 0.7 \pm 0.7$  | no          | $K_s K_s$ DM2 [28,12] |
| $\Gamma_{\gamma\gamma} \times B(f_2 \rightarrow K\bar{K})$ | $0.11 \pm 0.02 \pm 0.04$ keV                                       | $< 0.3$ keV            |             | TASSO [30]            |
|  | $0.12 \pm 0.07 \pm 0.04$ keV                                       | $< 0.2$ keV            |             | TPC/2 $\gamma$ [31]   |
|  | $0.10 \pm 0.04$ keV  |                        |             | (prel.) Mark II [32]  |

Branching ratios have been converted to  $K\bar{K}$  assuming  $I = 0, C = +$ :  $K\bar{K} = \frac{1}{2}K^+K^- + \frac{1}{4}K_s K_s + \frac{1}{4}K_L K_L$ . They were measured in  $K^+K^-$  unless indicated otherwise.

$\dagger$  Mark III and DM2 quote  $B(J/\psi \rightarrow \phi f_2(1720))$  from fits to  $K^+K^-$  without  $f_2(1720)$ - $f_2(1525)$  interference. Their  $f_2(1720)$  masses come out 1671 and 1643 MeV, respectively, which I find too far off to be meaningful. Interference moves the mass up some, but it stays below 1700. Mark III [27] say they can accommodate a "standard"  $f_2(1720)$  with interference, for which B goes down a factor of  $\sim 2.5$ . From that I derive the  $\sim 1.4$ .

inant one, and its  $\phi\phi$  decay is mostly  $L=0$ . The others are mostly  $L=2$ . The  $g_T$  are glueball candidates because production of  $q\bar{q}$  resonances is suppressed by OZI in  $\pi^- p \rightarrow \phi\phi n$ . Three  $2^{++}$  glueballs with similar masses can be described by theory, e.g. a strong coupling calculation [33]. However so far these states have not taught us much about glueballs, since they have only been seen in this production and this decay. For a new evaluation of the  $g_T$ 's and the rest of the  $f_2$  system see Ref. [34].

DM2 [12] and Mark III [29] have some  $J/\psi \rightarrow \gamma\phi\phi$  events. Mark III [35] also have  $J/\psi \rightarrow \gamma\phi\omega$ . Further efforts at increasing the  $\phi$  reconstruction efficiency may yield enough events to compare them to the  $g_T$  resonances and to Mark III's  $f_2(2230)$ .

If the matrix element for the  $g_T$  decay to  $K\bar{K}$  were the same as that for  $\phi\phi$ , the  $p^{2L+1}$  phase space factor would give  $\sim 30$  times more  $K\bar{K}$  than  $\phi\phi$  for the  $L=2$   $g_T(2300)$ , although this factor gets much smaller if damped by an interaction radius [20]. The measured [4]  $D_0$  waves in  $\pi^- p \rightarrow K\bar{K}n$  and  $\pi^- p \rightarrow \phi\phi n$  are in the ratio  $\sim 20:1$  and the  $K\bar{K}$  is flat above 1.9 GeV. Very preliminary MIS ITEP data [15] on the  $2^{++}$   $K_s K_s$  in 40 GeV/c  $\pi^- p \rightarrow K_s K_s n$  look different, going to zero at 2 GeV and rising again to a  $\sim 70$  MeV wide peak at  $\sim 2230$  MeV. However the region above 1.9 GeV is subject to ambiguities in the PWA, so that comparisons between experiments cannot be made before seeing all the waves and their phases [20,36].

GAMS have seen a narrow peak ( $\Gamma < 80$  MeV) at  $2220 \pm 10$  MeV in their  $\eta\eta'$  spectrum from 38 and 100 GeV/c  $\pi^- p \rightarrow \eta\eta' n$  data [37]. The anisotropy of

the decay angular distribution suggests  $J \geq 2$ . If GAMS and MIS ITEP are seeing the same state, its branching ratio to  $\eta\eta'$  is at least twice as large as to  $K\bar{K}$  [15]. This would be evidence against its interpretation as an  $L=3$   $s\bar{s}$  state, an explanation put forward [38] for Mark III's  $f_2(2230)$ .

The  $K_s K_s$  spectrum from the LASS  $K^- p \rightarrow K\bar{K}A$  data shows evidence for a peak at  $\sim 2.2$  GeV with spin  $\geq 2$ , and the moments of their  $K^+K^-$  indicate a  $J \geq 4$  state at  $2193 \pm 25$  GeV with a width of  $83 \pm 101$  GeV [18].

The above can be compared to the  $f_2(2230)$  a narrow  $2^{++}$   $K\bar{K}$  resonance<sup>5</sup> seen by Mark III [39] - but not by DM2 [28,12] - in  $J/\psi \rightarrow \gamma K\bar{K}$ . The discrepancy was not settled at this conference. Mark III [14] have shown that its spin is more likely  $\geq 2$  than 0. (Only  $J^{PC} = (\text{even})^{++}$  is allowed for  $J/\psi \rightarrow \gamma K\bar{K}$ .)

A search for the  $f_2(2230)$  in  $p\bar{p}$  annihilation gave a limit on  $B(f_2 \rightarrow p\bar{p}) \times B(f_2 \rightarrow K\bar{K})$  ranging from  $< 2 \times 10^{-4}$  if its width is 35 MeV to twice that for a width of 7 MeV [40].

Both Mark III and DM2 see a wide (100-300 GeV) enhancement at 2100-2200 MeV in their  $K_s K_s$  data, which is nearly background-free. This wide resonance also seems to have  $J \geq 2$  [28,14]. The  $\pi\pi$  mass distributions in radiative  $J/\psi$  decay also have a wide enhancement at  $\sim 2100$  MeV. This last is consistent in mass and width with the  $4^{++}$   $f_4(2030)$ , but such high spin resonances are not expected in radiative  $J/\psi$  decays.

<sup>5</sup>originally called  $\xi$

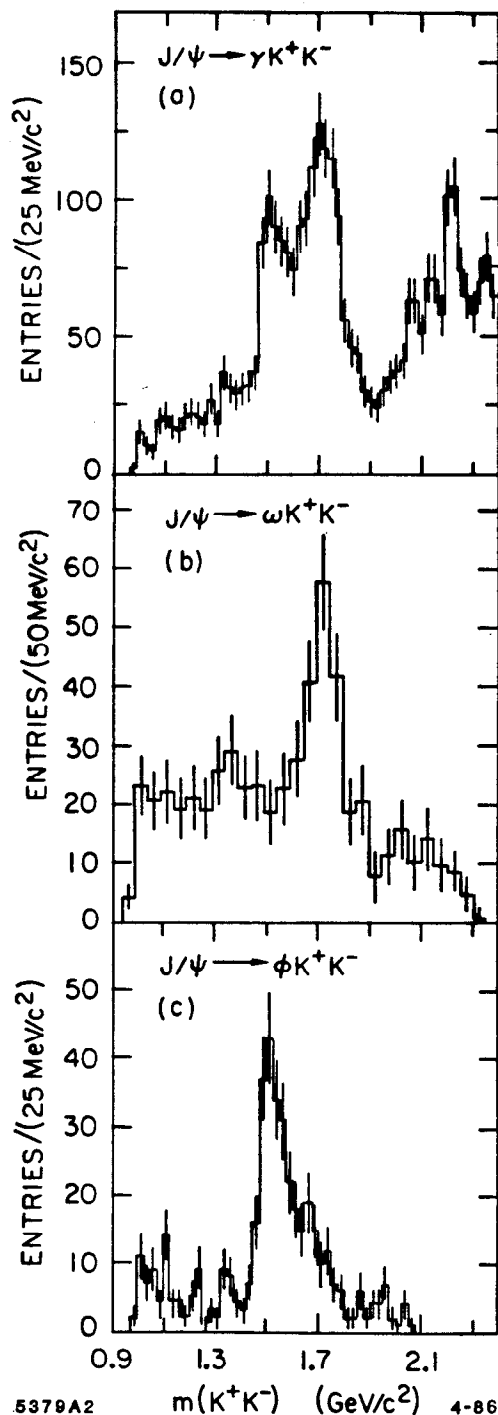


Figure 6: Mark III [27]  $K^+K^-$  mass spectra from (a)  $J/\psi \rightarrow \gamma K^+K^-$ , (b)  $J/\psi \rightarrow \omega K^+K^-$ , (c)  $J/\psi \rightarrow \phi K^+K^-$ .

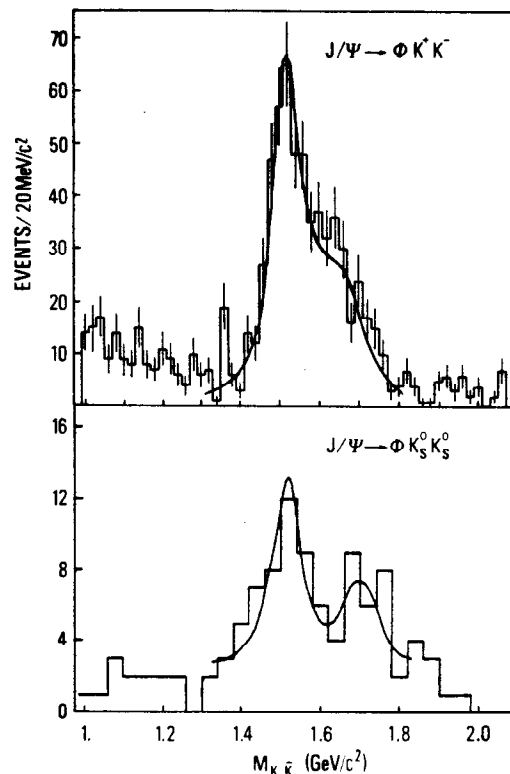


Figure 7: DM2 [28]  $K\bar{K}$  mass spectra from (a)  $J/\psi \rightarrow \phi K^+K^-$  and (b)  $J/\psi \rightarrow \phi K_s^0 K_s^0$ .

## 2.4 $f_0(1590)$

A discussion of the GAMS  $f_0(1590)$  glueball candidate<sup>6</sup> was given by Obraztsov [15,3,41]. Its decay rates are in the proportion  $\eta\eta':\eta\eta:K\bar{K}:\pi\pi \sim 3:1:<1:<1$ . Its  $t$  distribution in  $\pi^-p \rightarrow \eta\eta n$  is in good agreement with dominant one-pion exchange, which can be used to show that the  $f_0(1590)$  branching ratio to  $\pi\pi$  must be between 3.6 and 6%.

## 3 Mystery Mesons

### 3.1 $\rho(1480) \rightarrow \phi\pi$

Lepton-F [15,42] have further studied their  $\rho(1480) \rightarrow \phi\pi^0$  resonance<sup>7</sup>. It has  $M = 1480 \pm 40$  MeV,  $\Gamma = 130 \pm 60$  MeV,  $J^{PC} = 1^{--}$ , and has been seen in 32 GeV  $\pi^-p \rightarrow \phi\pi^0 n$  with  $|t'| < 0.2$  GeV<sup>2</sup>. An  $I=1$   $q\bar{q}$  resonance should decay much more readily to  $\omega\pi^0$  than to  $\phi\pi^0$ , but comparing with GAMS data they find  $B(1480 \rightarrow \omega\pi^0) < 2 B(1480 \rightarrow \phi\pi^0)$ . This resonance is a good candidate for a 4-quark or a  $q\bar{q}g$  state.

<sup>6</sup>originally called G

<sup>7</sup>originally called C

### 3.2 Search for $1^{-+}$ Hybrids

The Primakoff effect [43] has been used [44] to measure  $\Gamma(\rho \rightarrow \gamma \pi)$ . The reaction is  $200 \text{ GeV}/c \pi N \rightarrow \rho N$ , where the incident pion interacts with a virtual  $\gamma$  in the Coulomb field of the nucleus  $N$ :  $\pi \gamma \rightarrow \rho$ . Using vector dominance to replace the virtual  $\gamma$  by a virtual  $\rho$ , one can look for a  $\bar{\rho}$  which couples to  $\pi \rho$ :  $\pi \rho \rightarrow \bar{\rho}$ . The interest in this channel comes from predictions of  $I = 1, J^{PC} = 1^{-+}$  hybrid mesons which are expected to have a large branching ratio to  $\rho \pi$ . The upper limits from such a search up to  $M \sim 1.5 \text{ GeV}$  are in "mild" conflict with predictions. Details are given in the talk of Ferbel [45].

### 3.3 $X(3100) \rightarrow \Lambda \bar{p} +$ pions

Evidence for an unexpected meson<sup>8</sup> has been obtained by WA62 using a  $135 \text{ GeV}/c \Sigma^-$  beam on a beryllium target [46]. They observe a peak in  $\Lambda \bar{p} \pi^+ \pi^+$  at  $3100 \text{ MeV}$  of width compatible with their  $24 \text{ MeV}$  FWHM resolution (Fig. 8). Choosing a  $30 \text{ MeV}$  wide bin centered at  $3105 \text{ MeV}$  they have a signal of 53 events over a background of 136. By tightening the  $\bar{p}$  cuts, they get 46 events over 52. Signals are also seen in two other charge states. The results, corrected for double counting, are shown in Table 4, along with the Monte Carlo calculations of the probability that they are statistical fluctuations. These calculations take into account choosing the bin position to maximise the signal, but cannot correct for the effect of choosing the  $\bar{p}$  cuts.

Now BIS-2 [47] also report seeing the  $X(3100)$ , in their case centered at  $3060 \pm 40 \text{ MeV}$ . They use a  $40 \text{ GeV}$  neutral beam composed mainly of neutrons incident on  $\text{H}_2$ ,  $\text{C}$ ,  $\text{Al}$ , and  $\text{Cu}$  targets, and have so far analysed  $1/4$  of their data. They see their strongest signal in  $X^0 \rightarrow \Lambda \bar{p} \pi^+$ , where WA62 sees none, and nothing significant in  $X^+ \rightarrow \Lambda \bar{p} \pi^+ \pi^+$ , WA62's best channel. This difference is puzzling, at best. The BIS-2 signals, after  $\bar{p}$  and  $\pi^+$  cuts, are shown in Table 4 and Fig. 9.

If the  $X^+$  (seen only by WA62) decays strongly to  $\Lambda \bar{p} \pi^+ \pi^+$ , it is a four quark state ( $sudd$ ), and its narrowness is striking. If not, the absence of a strong decay must be explained.

When the WA62 result first became known, it was assumed that its strange dibaryon composition meant a hyperon beam was needed to produce it. Now that BIS-2 have seen it with a neutron beam, there are presumably many other experiments which can see this object (if it is real) and give more information about its nature.

<sup>8</sup>They named it the  $U(3100)$ , but the PDG say unknown particles should be called  $X$ .

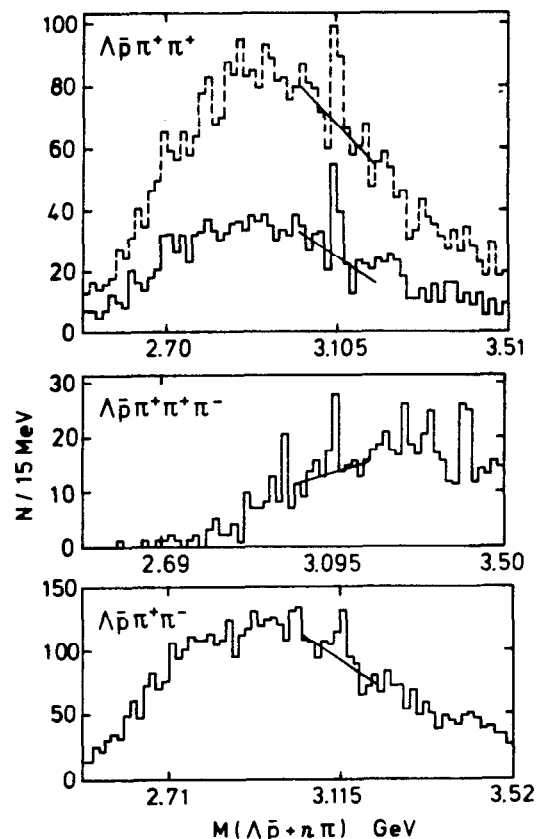


Figure 8: WA62 [46]  $X(3100)$  signals in  $+, 0, -$  charge states from the reaction  $\Sigma^- N \rightarrow \Lambda \bar{p} +$  pions + anything. The bin position is adjusted in each plot to maximise the signal. The dashed histogram for  $X^+$  is the original signal; the solid histograms are after additional  $\bar{p}$  cuts.

### 3.4 $\gamma \gamma \rightarrow VV$

A puzzling surprise in  $\gamma \gamma$  collisions has been the large cross section for  $\gamma \gamma \rightarrow \rho^0 \rho^0$  at threshold, which was first seen by TASSO [48], and since by other groups [49,50]. The TASSO  $J^P$  analysis indicated that the enhancement has mostly positive parity, but is not dominated by a single spin. TPC/2 $\gamma$  [50] also find  $0^+$  and  $2^+$ .

Initial thoughts of a resonance were somewhat shaken by the lack of a clearly dominant  $J^P$ , and by the lack of an obvious resonance shape. (The continuation of the cross section below  $\rho \rho$  threshold implies a strongly rising matrix element.) One naively wonders if this is not some kind of threshold effect, perhaps having something to do with the fact that  $\rho^0$ 's are broad, and couple directly to  $\gamma$ 's in the Vector Dominance Model.

The analyses are made difficult by the width of the  $\rho$ , the necessity to accommodate Bose-Einstein



Table 4: X(3100) Signals

| Charge State   | Decay Mode                      | WA62 [46]        |               |                   |                         | BIS-2 [47]  |               |                   |
|----------------|---------------------------------|------------------|---------------|-------------------|-------------------------|-------------|---------------|-------------------|
|                |                                 | Bin Center [MeV] | Signal Events | Background Events | Statistical Probability | Mass [MeV]  | Signal Events | Background Events |
| X <sup>+</sup> | $\Lambda\bar{p}\pi^+\pi^+$      | 3105             | 45            | 50                | $6 \times 10^{-6}$      | $\sim 3060$ | 10            | 16                |
| X <sup>0</sup> | $\Lambda\bar{p}\pi^+\pi^+\pi^-$ | 3095             | 19            | 28                | 0.2                     | $\sim 3060$ | 10            | 7                 |
|                | $\Lambda\bar{p}\pi^+$           |                  | <20           | $\sim 115$        |                         | $\sim 3050$ | 73            | 168               |
| X <sup>-</sup> | $\Lambda\bar{p}\pi^+\pi^-$      | 3105             | 62            | 187               | $9 \times 10^{-3}$      | $\sim 3070$ | 32            | 49                |

BIS-2 say all their peaks are near 3060; the masses here are my own best guess from the histograms. They do not consider their X<sup>+</sup> signal significant. The WA62 uncertainty in the mass scale is  $\pm 20$  MeV; that of BIS-2 is 40 MeV. No X<sup>++</sup> or X<sup>--</sup> has been seen.

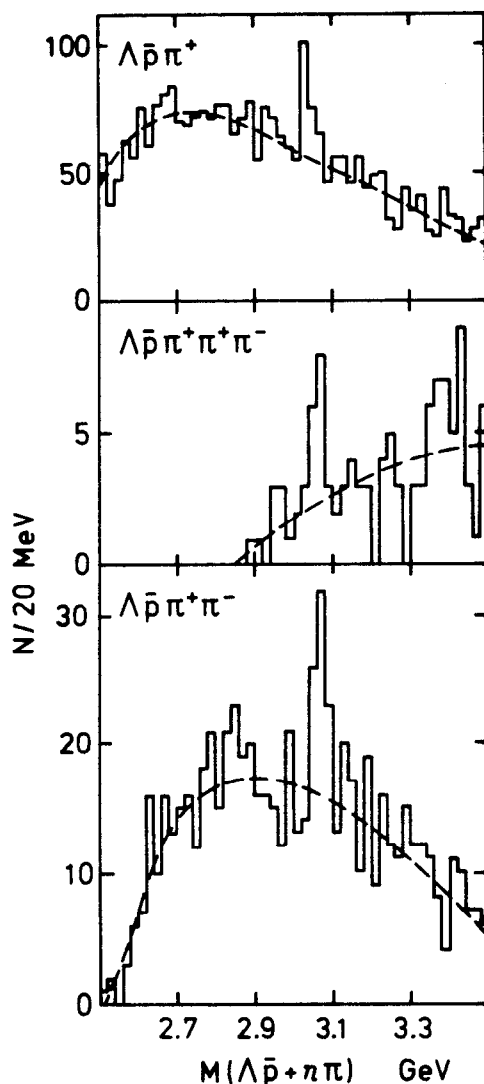


Figure 9: BIS-2 [47] X(3100) signals in 0,0,- charge states from  $nN \rightarrow \Lambda\bar{p} + \text{pions} + \text{anything}$ .

statistics among the 4  $\pi$ 's, and the presence of  $\rho^0\pi\pi$  and  $4\pi$  backgrounds to the  $\rho^0\rho^0$ . Interference between the various channels was ignored. It has been pointed out [51] that the  $\rho^0\pi\pi$  channel must have the  $\pi\pi$  in an L=odd state. This effect, which changes the shape of the  $\rho^0\pi\pi$  background and also increases the chances that it should interfere with  $\rho^0\rho^0$ , was not included in the TASSO analysis [48]. Until its effect is studied, we must admit the possibility that a correct analysis might show a dominant  $J^P$  after all.

If the  $\rho^0\rho^0$  enhancement is due to a resonance, some values of isospin can be ruled out. The lack of a similar enhancement in  $\rho^+\rho^-$  [52] rules out an I=0 resonance as the explanation of the  $\rho^0\rho^0$  signal. A neutral I=1 resonance is conveniently forbidden by its Clebsch-Gordan coefficient to decay to  $\rho^0\rho^0$ . I=2 and I=0 resonances interfering were predicted to cause a large  $\rho^0\rho^0/\rho^+\rho^-$  ratio [51] and I=2 occurs naturally among  $q\bar{q}q\bar{q}$  states. An alternate explanation [53] relating  $\gamma\gamma \rightarrow VV$  to photon production of vector mesons and to nucleon-nucleon scattering, assuming t-channel exchange and factorisation, has been revised [54] to accommodate later  $\gamma\gamma$  data.

For more information one looks to other  $\gamma\gamma \rightarrow VV$  reactions. In  $\gamma\gamma \rightarrow K^+K^-\pi^+\pi^-$ , single K\*'s and  $\phi$ 's are seen [55]. ARGUS [56] have now reported a smooth  $K^0\bar{K}^0$  cross section at the level of  $\sim 25\%$  of the total  $K^+K^-\pi^+\pi^-$  (Fig. 10).

More exciting is the new ARGUS [56] evidence for  $\gamma\gamma \rightarrow \rho\omega$ . The signal is among their  $\gamma\gamma \rightarrow \pi^+\pi^-\pi^+\pi^-\pi^0$  events, for which they estimate a  $\sim 12\%$  background from other processes. They extract the number of  $\omega \rightarrow \pi^+\pi^-\pi^0$  decays as a function of total mass  $M(5\pi)$ , obtaining the cross section for  $\gamma\gamma \rightarrow \omega\pi^+\pi^-$  shown in Fig. 11a. For events with  $M(5\pi) > 1.7$  GeV the mass distribution of the  $\pi^+\pi^-$  not included in the  $\omega$  is shown in Fig. 11b. A clear  $\rho$  is seen with no noticeable background. The  $\omega$ -sidebands show no such  $\rho$  signal. Thus above 1.7

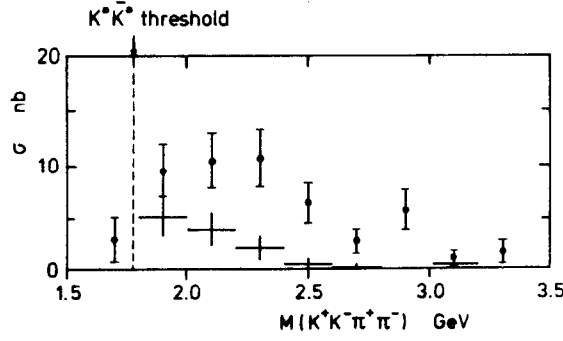


Figure 10: Preliminary ARGUS [56] cross section for  $\gamma\gamma \rightarrow K^+K^-\pi^+\pi^-$  with  $\phi\pi^+\pi^-$  removed ( $\bullet$ ), and  $\gamma\gamma \rightarrow K^{*0}\bar{K}^{*0}\pi^+\pi^-$  ( $+$ ).

GeV the  $\omega\pi^+\pi^-$  cross section is dominantly  $\omega\rho$ .

What is intriguing here is that the  $\rho\omega$  does not peak at threshold, but considerably above it. Its shape even resembles a resonance, unlike the  $\rho^0\rho^0$ .

Neither of the above models predicted this  $\rho\omega$  behaviour; it will be interesting to see if they can accommodate it. A successful description should also deal with (or explain why not) other production mechanisms for  $VV$ , such as radiative  $J/\psi$  decay where there is new data on  $\omega\phi$  [35] and  $\rho^0\rho^0$  [28], central production in  $\pi^+p$ , where  $\phi\phi$  and  $K^*K^*$  have been reported [57], and the  $\phi\phi$  resonances seen in  $\pi^-p$  [2]. There is also evidence from  $\bar{p}$  annihilation in deuterium for a  $\rho\rho$  resonance at 1485 MeV [58], which has been compared to the  $\gamma\gamma \rightarrow \rho^0\rho^0$  enhancement [59]. These  $VV$  reactions may not all be related, but it would be unaesthetic to propose a different explanation for each.

## 4 $K\bar{K}\pi$ and $\eta\pi\pi$ Resonances

Table 5: Isobars for  $K\bar{K}\pi$  and  $\eta\pi\pi$ .

|                                  | $G^*$ | $I$   | $J^P$ |       |       |       |       |
|----------------------------------|-------|-------|-------|-------|-------|-------|-------|
|                                  |       |       | $0^-$ | $1^+$ | $1^-$ | $2^+$ | $2^-$ |
| $K\bar{K}\pi$ :                  |       |       |       |       |       |       |       |
| $K_{ch}^*K + K_{neut}^*K$        | +     | 0,1   | P     | S,D   | P     | D     | P     |
| $K_{ch}^*K - K_{neut}^*K$        | -     | 0,1   | P     | S,D   | P     | D     | P     |
| $K\bar{K}\pi$ and $\eta\pi\pi$ : |       |       |       |       |       |       |       |
| $a_0(980)\pi$                    | +     | 0,1,2 | S     | P     | -     | -     | D     |
| $\eta\pi\pi$ :                   |       |       |       |       |       |       |       |
| $f_0\eta$                        | +     | 0     | S     | P     | -     | -     | D     |
| $\rho\eta$                       | +     | 1     | P     | S     | P     | D     | P     |

$$* C = G(-1)^I$$

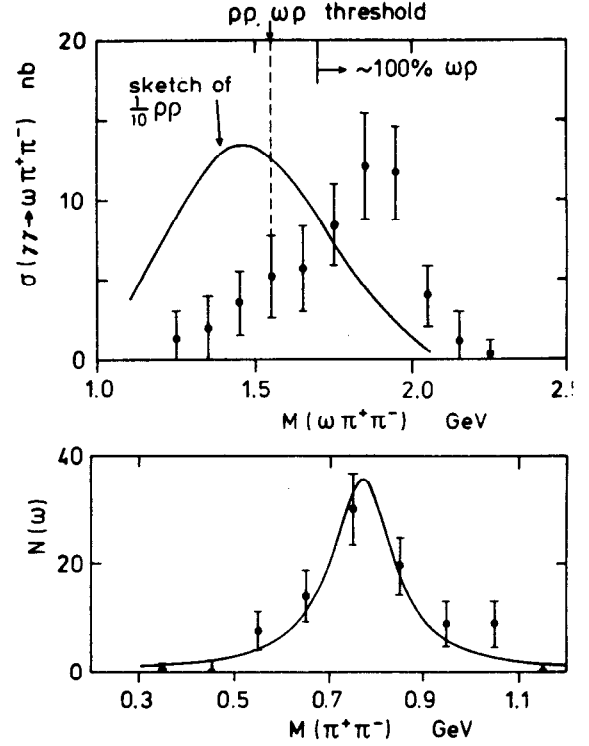


Figure 11: ARGUS [56] evidence for  $\gamma\gamma \rightarrow \rho\omega$ . (a) cross section for  $\gamma\gamma \rightarrow \omega\pi^+\pi^-$ . For comparison I have roughly sketched in the  $\gamma\gamma \rightarrow \rho^0\rho^0$  cross section. (b) For  $M(5\pi) > 1.7$  GeV, the  $\pi^+\pi^-$  mass spectrum accompanying the  $\omega$ .

### 4.1 1400 MeV Region

The  $K\bar{K}\pi$  system in the 1.4 GeV region has been a source of much controversy. There is evidence, perhaps contradictory, for both<sup>9</sup> a  $0^{-+} \rightarrow a_0\pi$  and a  $1^{++} \rightarrow \bar{K}K^*$  meson at  $\sim 1420$  MeV in hadron collisions, and a very strong, somewhat wider  $0^{-+} \rightarrow "a_0"\pi$  peak at 1460 MeV in radiative  $J/\psi$  decays.

Diagrams of the various meson production mechanisms are shown in Fig. 12, and the decay channels are listed in Table 5. The data from hadron collisions are summarised in Table 6. Some of these experiments are not sensitive to the isospin, and therefore determine  $J^{PG}$  rather than  $J^{PC}$ . However all isospin measurements of the 1420 peak have given  $I=0$ , in which case  $C=G$ . The  $J^{PG}$  determinations here rely on the isobar model, i.e. the assumption that all 3 body decays go via two body intermediate states. Those allowed for the  $K\bar{K}\pi$  final state are  $a_0\pi$  and  $\bar{K}K^*$ . Since the  $a_0(980)$  decays

<sup>9</sup>The old  $\delta$  is now called  $a_0(980)$ .

Table 6: Spin Analyses of  $E \rightarrow \bar{K}\bar{K}\pi$  peak at  $\sim 1420$  MeV in Hadron Collisions

| Experiment   | 81 cm HBC<br>CERN              | 2 m HBC<br>CERN                   | $\Omega$ Spectr.<br>CERN WA76                             | Multi-Particle Spectrometer<br>BNL AGS-771 |                                       |
|--|--------------------------------|-----------------------------------|---|--|---------------------------------------|
| Reference  | Baillon [60]                   | Dionisi [61]                      | Armstrong [62]  | Chung [63]                                 | Reeves [64]                           |
| Process  | $\bar{p}p \rightarrow E\pi\pi$ | $\pi^-p \rightarrow E n$          | $\pi^+p \rightarrow \pi^+ E p$<br>$p p \rightarrow p E p$ | $\pi^-p \rightarrow E n$                   | $\bar{p}p \rightarrow E X$            |
| E $\rightarrow$<br>beam energy                       | $\bar{K}\bar{K}\pi$<br>at rest | $K_s K^\pm \pi^\mp$<br>3.95 GeV/c | $K_s K^\pm \pi^\mp$<br>85 GeV/c                           | $K_s K^\pm \pi^-$<br>8 GeV/c               | $K_s K^\pm \pi^-$<br>6.6 GeV/c        |
| Fit to all $\bar{K}\bar{K}\pi$ :                     |                                |                                   |   |  |                                       |
| E mass [MeV]   | $1425 \pm 7$                   | $1426 \pm 6$                      | $1425 \pm 2$  | $1421 \pm 3$                               | $1424 \pm 3$                          |
| E width [MeV]  | $80 \pm 10$                    | $40 \pm 15$                       | $62 \pm 5$  | $70 \pm 8$                                 | $60 \pm 10$                           |
| no. events<br>in E peak<br>background                | $\sim 800$<br>$\sim 70$        | $152 \pm 25$<br>$\sim 200$        | $\sim 1000$<br>$\sim 1000$                                | 4240<br>$\sim 4000$                        | $620 \pm 50$<br>$\sim 1700$           |
| Isospin  | 0                              | 0                                 |   |  |                                       |
| $J^{PG}(E)$<br>for $M(\bar{K}\bar{K}\pi)$            | $0^{-+}$<br>unbinned           | $1^{++}$<br>1390-1470             | $1^{++}(\sim 10\% 0^{-})$<br>40 MeV bins                  | $0^{-+}$<br>20 MeV bins                    | $0^{-+}(<20\% 1^{++})$<br>40 MeV bins |
| $J^{PG}_s$ tried                                     | $0^-, 1^+, 2^-$                | $0^-, 1^\pm, 2^\pm$               | $0^{-+}, 1^\pm$   | $0^\pm, 1^\pm, 1^{-\pm}$                   | $0^{-+}, 1^{++}, 1^{+-}$              |
| $\bar{K}\bar{K}\pi$ P.S.                             | no                             | yes                               | yes   | yes  | yes                                   |
| Flatté $a_0$   |                                | yes                               | yes   | yes  | yes                                   |
| $E \rightarrow a_0\pi / \bar{K}\bar{K}\pi$           | $\sim 0.5$                     |                                   | $0.02 \pm 0.02$   | dominant                                   | $> 75\%$                              |
| $E \rightarrow \bar{K}\bar{K}^* / \bar{K}\bar{K}\pi$ | $\sim 0.5$                     | $0.86 \pm 0.12$                   | 0.98  |  |                                       |

to both  $\bar{K}\bar{K}$  and  $\eta\pi$ , any signal in  $a_0\pi$  leads us to look also in the  $\eta\pi\pi$  channel, where the isobars<sup>10</sup> are  $a_0\pi$ ,  $\rho\eta$ , and  $f_0\eta$ .

While discussing the indeterminateness of the spin, it is convenient to use the historic name  $E$  for the particle seen in hadronic collisions. A  $1^{++}$  resonance would properly be called  $f_1(1420)$ , and a  $0^{-+}$  would be  $\eta(1420)$ . Similarly the  $\iota$  seen in radiative  $J/\psi$  decay is now called the  $\eta(1460)$ .

#### 4.1.1 $\bar{p}p \rightarrow \eta(1420) \pi^+\pi^-$

The  $E(1420)$  was first seen in  $\bar{p}p$  annihilation at rest, and determined to have  $J^{PG}=0^{-+}$ ,  $I=0$ , with about equal decays to  $a_0\pi$  and  $\bar{K}\bar{K}^*$  [60]. More recently AGS-771 have observed the  $E$  in  $p\bar{p}$  annihilation in flight with the Multiparticle Spectrometer (MPS) [64]. Their data also favor  $0^{-+}$ , this time with the  $a_0\pi$  decay dominant.

#### 4.1.2 $\pi^-p \rightarrow \eta(1420) n$

Dionisi *et al.* [61] studied the  $E(1420)$  in a 4 GeV/c  $\pi^-p \rightarrow (K_s K^\pm \pi^\mp) n$  bubble chamber experiment at CERN. They performed a Dalitz plot analysis in a 80 MeV wide  $M(\bar{K}\bar{K}\pi)$  bin centered on the  $E$  signal, and found it to be  $1^{++}$  decaying into  $\bar{K}\bar{K}^*$ .

<sup>10</sup>The old  $\epsilon \rightarrow \pi\pi$  resonance, at whatever mass it may be, is now called  $f_0$ .

In 1983 AGS-771 [65] accumulated an order of magnitude more statistics in nearly the same reaction: 8 GeV/c  $\pi^-p \rightarrow (K_s K^\pm \pi^-) n$ . Last year they presented [66] a partial wave analysis (PWA) of this data, finding that the 1420 is dominantly  $0^{-+}$  decaying into  $a_0\pi$ . Their analysis had a large advantage over that of Dionisi *et al.* because the higher statistics allowed the PWA to be done in 20 MeV bins of  $M(\bar{K}\bar{K}\pi)$ . This showed a large step in the  $1^{++}(\bar{K}\bar{K}^*)$  at threshold, not resembling the 1420 peak in the total  $\bar{K}\bar{K}\pi$  distribution. (Could it however be a 1420 peak on a rising background?) There was a strong peak at  $\sim 1400$  in  $0^{-+}(a_0\pi)$ , with some contribution from  $0^{-+}(\bar{K}\bar{K}^*)$ , indicated primarily by its interference with the  $a_0\pi$ . The  $0^{-+}$  wave was well described by a Breit-Wigner with  $M = 1402$  MeV and  $\Gamma = 47$  MeV, both smaller than the usual fits to the full  $\bar{K}\bar{K}\pi$  spectrum listed in Table 6. There was also a substantial peak in  $1^{++}(\bar{K}\bar{K}^*)$ . The collaboration preferred the  $0^{-+}$  as the resonance, since its relative phase showed resonance behaviour. However the  $0 - 2\pi$  ambiguity allowed one to also interpret the phase behaviour as essentially flat. Part of the problem was the lack of a smooth background to compare the phase to.

At this conference Chung of AGS-771 [63] presented a new analysis including data taken in 1985, thus almost doubling the statistics. The results with the same cuts as used before ( $|t'| < 1$  GeV<sup>2</sup>)

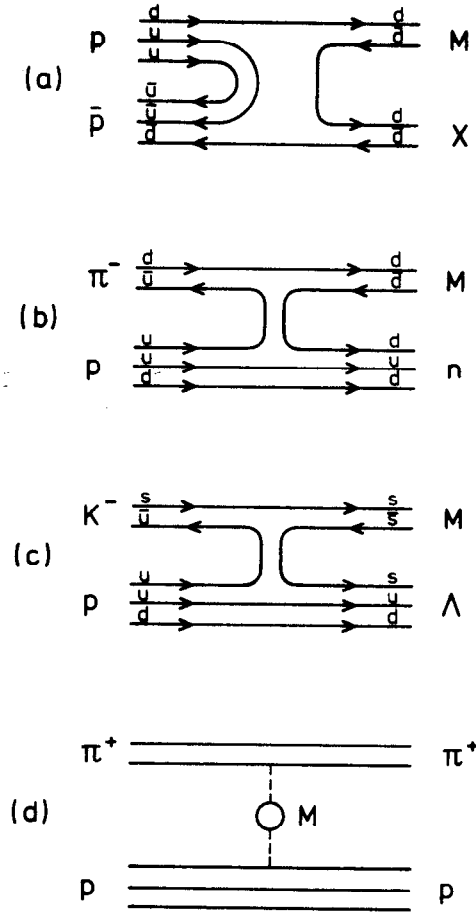


Figure 12: Diagrams for production of a meson  $M$  decaying to  $K\bar{K}\pi$  or  $\eta\pi\pi$ .

are shown in Fig. 13. The  $0^{-+}(a_0\pi)$  peak is still there, but its interference with  $0^{-+}(\bar{K}K^*)$  is gone. The peak in  $1^{++}(\bar{K}K^*)$  is now only half the size of the  $0^{-+}(a_0\pi)$ .

A second analysis, shown in Fig. 14, solves the "too little background" problem by selecting  $0.2 < |t'| < 1 \text{ GeV}^2$ . This gives a flatter  $1^{++}(\bar{K}K^*)$  background, and the phase of the  $0^{-+}(a_0\pi)$  against this shows unambiguous resonant behaviour. The  $0^{-+}(a_0\pi)$  mass distribution and its phase are well described by a B-W with  $M = 1400$  and  $\Gamma = 60 \text{ MeV}$ . Chung suggests there might be a broader resonance at  $1450 \text{ MeV}$  in  $0^{-+}(\bar{K}K^*)$ . To my eye the  $1^{++}$  looks equally interesting.

In this type of experiment the  $p$  and  $n$  spins are not measured. Because they are in principle measurable, there are two categories of waves (with and without nucleon spin flip), which do not interfere. Spin flip and non-flip correspond to different

mesons being exchanged. For example, consider the case where a spin 0 meson is exchanged. Isospin conservation at the meson-nucleon vertex requires that the exchanged meson have  $I = 1$ . If the spin flips, the meson-nucleon orbital angular momentum must be 1, and the meson's parity must be  $-$ , so it is a  $\pi$ . If the nucleon spin is not flipped,  $L$  can be 0 and the meson parity even, so the  $a_0(980)$  can be exchanged.  $a_0$  exchange with a  $\pi$  beam is an appealing mechanism for producing an  $a_0\pi$  resonance.

Originally AGS-771 required all waves of a given  $J^{PG}$  to be coherent, assuming they would come from a single resonance and a single production mechanism. When they release this requirement, they find that the fit prefers incoherent  $0^{-+}(a_0\pi)$  and  $0^{-+}(\bar{K}K^*)$ . This corresponds to the  $\eta(1400) \rightarrow a_0\pi$  and the  $\eta(1450) \rightarrow \bar{K}K^*$  being produced by different meson exchanges. As usual, more data is needed to know for sure. They have more, taken in 1986, which is still to be analysed.

The decay mode  $\eta\pi\pi$  has been investigated at KEK in  $8 \text{ GeV}/c \pi^- p \rightarrow (\eta\pi^+\pi^-) n$  [67]. The results of their PWA analysis, which allowed incoherence between the spin flip and spin non-flip waves are shown in Fig. 15.

The  $1^{++}(a_0\pi)$  contribution near 1420 is quite small. The  $0^{-+}(a_0\pi)$  has a peak at  $1420 \pm 5 \text{ MeV}$ . The width, including the  $25 \text{ MeV}$  (FWHM) experimental resolution, is only  $31 \pm 7 \text{ MeV}$ . This peak is not very evident in the total  $\eta\pi\pi$  mass spectrum, nor even in the total  $0^{-+}$ . That is because the two isobars  $a_0\pi$  and  $f_0\eta$  interfere destructively in this region. Their relative phases are shown in Fig. 16.

GAMS [68] have data on  $100 \text{ GeV}/c \pi^- p \rightarrow (\eta\pi^0\pi^0) n$ . They see a peak at  $\sim 1420 \text{ MeV}$ , as well as a much stronger one at  $\sim 1285 \text{ MeV}$ . Both have a large fraction of  $a_0\pi$ , and are produced preferentially at large  $t$  ( $|t| > 0.1 \text{ GeV}^2$ ). However they have yet to do a spin analysis.

Thus the KEK and AGS-771 experiments both see the  $E$  in  $8 \text{ GeV}/c \pi^- p \rightarrow E n$  as a  $0^{-+}$  particle decaying via  $a_0\pi$  to  $\eta\pi\pi$  and  $K\bar{K}\pi$  respectively. The mass difference ( $1400 \text{ MeV}$  for AGS-771 and  $1420$  for KEK) is a bit mysterious, as is the fact that AGS-771 sees the peak in their total  $K\bar{K}\pi$  spectrum at  $1420$ . However they do not quote an error on their  $1400 \text{ MeV}$ ; the shift may not be significant. Neither see a significant signal for a  $1^{++}$  resonance at  $1420 \text{ MeV}$ .

#### 4.1.3 $K^- p \rightarrow (K\bar{K}\pi) \Lambda$

Comparison of production by  $K^-$  and  $\pi^-$  beams is a crucial test of a meson's quark content. There

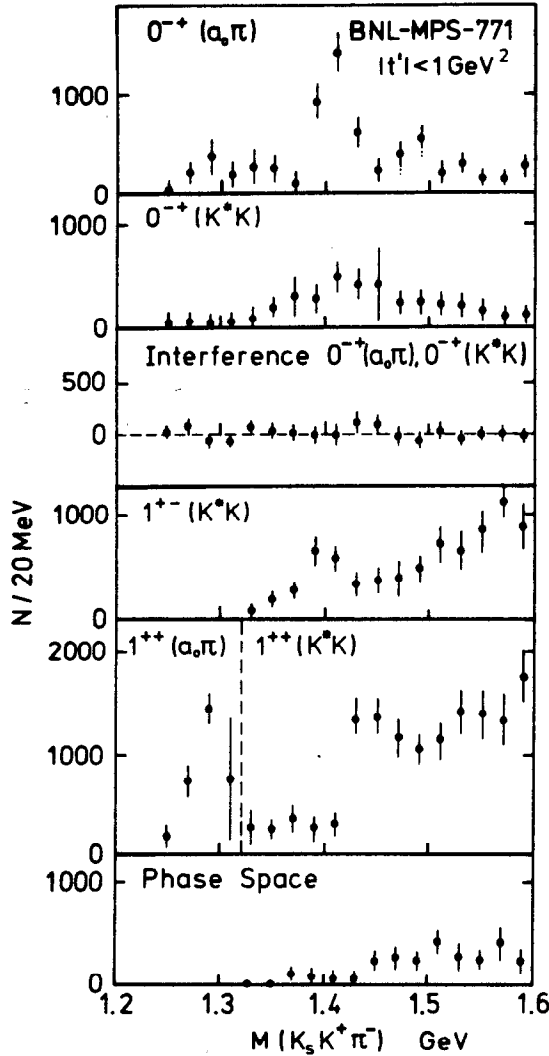


Figure 13: Partial wave analysis of AGS-771 1983+1985 data with  $|t'| < 1 \text{ GeV}^2$  [63].

should be two isosinglets in the ground state  $1^{++}$  nonet. If they are ideally mixed, the lower mass one would be  $u\bar{u}+d\bar{d}$  and the higher mass  $s\bar{s}$ . Both can decay to  $K\bar{K}\pi$ , but the former should be preferentially produced by a  $\pi^-$  beam, and the later by  $K^-$  (see Figs. 12b+c). The old D meson, now called  $f_1(1285)$ , is the undisputed candidate for the  $u\bar{u}+d\bar{d}$  state. If there is a  $1^{++}$  E, i.e. an  $f_1(1420)$ , it would presumably belong to this nonet and should be  $s\bar{s}$ . However it has a competitor for that place: the  $f_1(1526)$  [69], seen with a  $K^-$  beam.

Lepton-F [70] have published data on  $32.5 \text{ GeV}/c$   $\pi^- p \rightarrow (K^+ K^- \pi^0) n$  and  $K^- p \rightarrow (K^+ K^- \pi^0) Y$ . They perform no spin analysis, but see a peak at 1420 in the  $K^-$  beam data, and none with  $\pi^-$ . The ratio of the "E" production cross sections is  $K^-/\pi^- > 10$ .

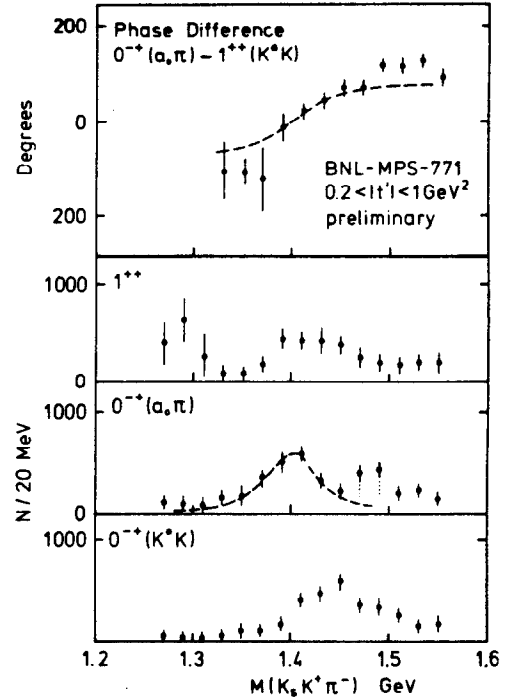


Figure 14: Preliminary PWA of AGS-771 1983+1985 data with  $0.2 < |t'| < 1 \text{ GeV}^2$  [63]. The dashed curve corresponds to a  $0^-+$  B-W with  $M = 1400$  and  $\Gamma = 60 \text{ MeV}$ .

They see no sign of the  $f_1(1526)$ .

A different picture is presented by LASS's [18] new data on  $K^- p \rightarrow (K\bar{K}\pi) \Lambda$ , shown in Fig. 17. One is not overwhelmed by the E signal. It will be difficult to tell if it is there at all. The bins are 20 MeV wide, and the one to the left of 1420 is high. That is rather narrow for a resonance with  $\Gamma=60 \text{ MeV}$  in an experiment with  $\sigma_M \sim 12 \text{ MeV}$ . More convincing is the peak at 1526 MeV in 5 of the 20 MeV bins, corresponding well to the  $f_1(1526)$  width of  $107 \pm 15 \text{ MeV}$  [69]. A preliminary partial wave analysis of the LASS data [71] indicates that the  $K\bar{K}\pi$  spectrum up to  $\sim 1.8 \text{ GeV}$  is dominated by  $1^{++}$ . The statistics in this spectrum are rather disappointing, and clearly can't compete with the  $\pi^-$  data for determining the spin of the 1420 resonance(s). However it looks like this data will confirm the existence of the  $f_1(1526)$ , and it will certainly be interesting to see the final analysis. AGS-771 have also accumulated  $K^-$  data, and the analysis should be available soon.

#### 4.1.4 $\pi^+ p \rightarrow \pi^+ f_1(1420) p$

WA76 used the  $\Omega$  spectrometer at CERN to study the reactions  $(\pi^+ \text{ or } p) p \rightarrow (\pi^+ \text{ or } p)_f (K_s K^\pm \pi^\mp)$

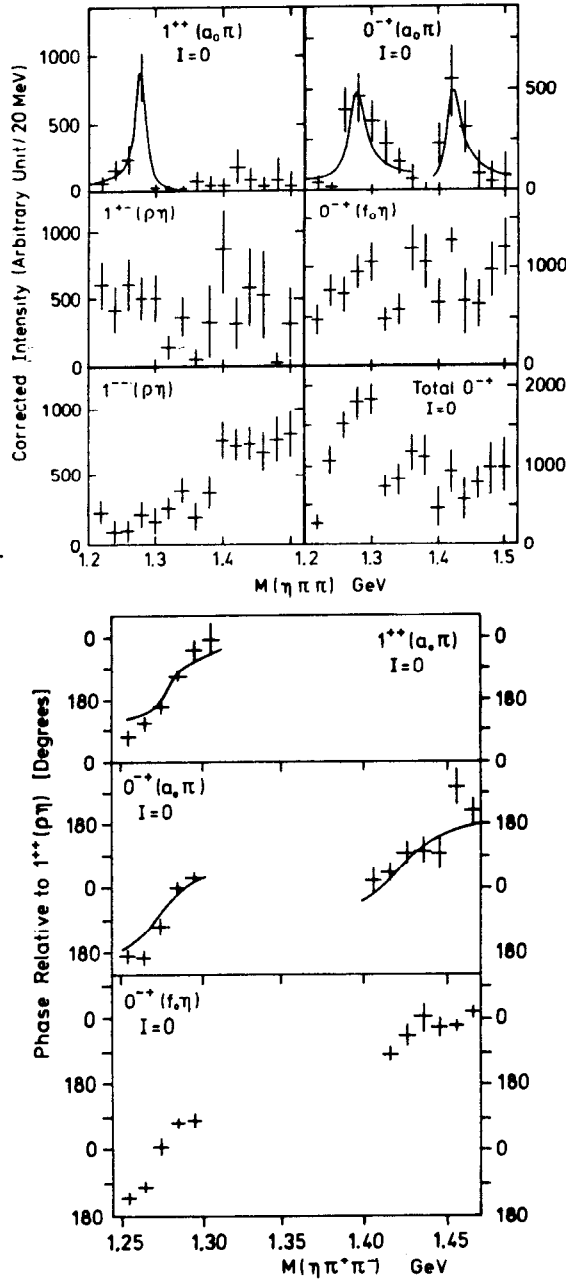


Figure 15: KEK [67] PWA of  $8 \text{ GeV}/c \pi^- p \rightarrow (\eta \pi^+ \pi^-) n$ .

$p_s$ , where  $f$  and  $s$  denote the fastest and slowest particles in the lab frame. The  $K\bar{K}\pi$  system is centrally produced (Feynman  $x \sim 0$ ), presumably by double exchange graphs as in Fig. 12d. A data selection with loose particle identification requirements is used to achieve an acceptance which is approximately flat over the Dalitz plot. Their pub-

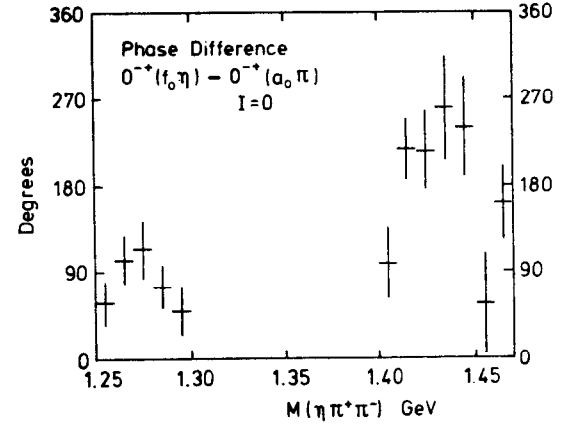


Figure 16: KEK phase difference between  $0^{--}(a_0\pi)$  and  $0^{--}(f_0\eta)$ , calculated from Fig. 15.

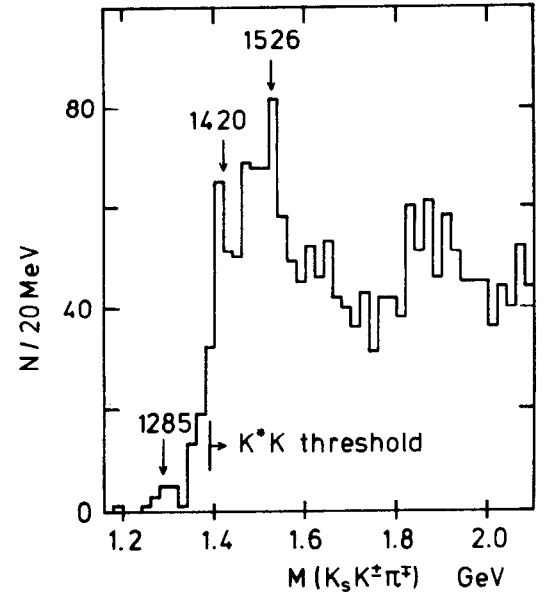


Figure 17: LASS [18]  $K_s K^\pm \pi^\mp$  mass spectrum from  $11 \text{ GeV}/c K^- p \rightarrow K_s K^\pm \pi^\mp \Lambda$ .

lished results [72] gave  $1^{++}(\bar{K}K^*)$  for the 1420 region, for which they did a Dalitz plot analysis in the  $1390 - 1470 M(K\bar{K}\pi)$  bin. Since this wide bin could have masked a step in  $1^{++}(\bar{K}K^*)$  as seen by AGS-771, they have now done the analysis in 40 MeV bins [63,62]. The results for the combined  $\pi^+$  and  $p$  beam samples are shown in Fig. 18. (The analyses done separately for  $\pi^+$  and  $p$  are similar.) The  $1^{++}(\bar{K}K^*)$  peak looks very convincing. There may be an  $\sim 10\%$  contribution from  $0^{--}$ , mostly as  $\bar{K}K^*$ . This reaction shows relatively less  $1^{++}(\bar{K}K^*)$

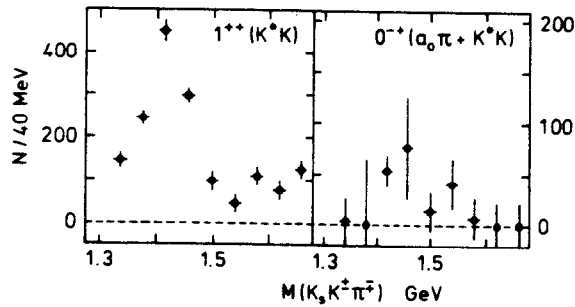


Figure 18: WA76 [62] PWA of 32.5 GeV/c  
 $(\pi^+ \text{ or } p) p \rightarrow (\pi^+ \text{ or } p)_f (K_s K^\pm \pi^\mp) p_s$ .

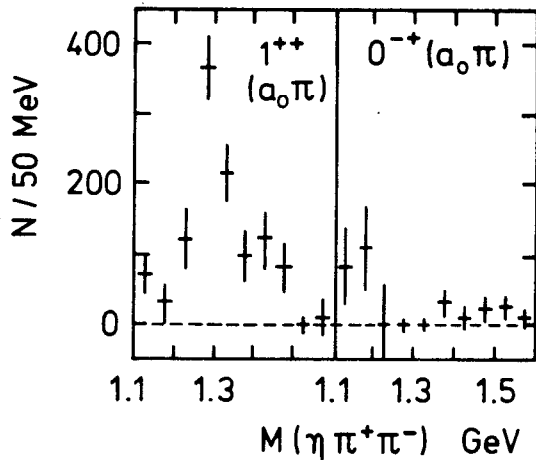


Figure 19: WA76 [73] PWA of 32.5 GeV/c  
 $(\pi^+ \text{ or } p) p \rightarrow (\pi^+ \text{ or } p)_f (\eta \pi^+ \pi^-) p_s$ .

at higher masses than seen by AGS-771. Instead the data above the 1420 peak is fit mostly by  $K\bar{K}\pi$  phase space.

They have also looked at  $\eta\pi\pi$  in the same production mechanism [73]. The results are shown in Fig. 19. They see a slight enhancement at  $\sim 1420$  MeV in the  $1^{++}(a_0\pi)$  wave, from which they obtain (correcting for missing modes assuming  $I = 0$ ):

$$\frac{f_1(1420) \rightarrow a_0\pi, a_0 \rightarrow \eta\pi}{f_1(1420) \rightarrow K\bar{K}\pi} = 0.06 \pm 0.04.$$

#### 4.1.5 Remarks on E in Hadron Collisions

Thus it seems that two different particles are seen in two different production mechanisms:

$$\begin{aligned} \pi^- p &\rightarrow \eta(1420) n \\ \pi^+ p &\rightarrow \pi^+ f_1(1420) p. \end{aligned}$$

Nevertheless there is still dispute between the collaborations on how best to handle details of the

analysis. The  $K_s K^+ \pi^-$  and  $K_s K^- \pi^+$  data can be combined two ways to make the  $K\pi$  vs  $K\pi$  Dalitz plot: either  $K_{\text{neut}}^*$  vs  $K_{\text{ch}}^*$ , or  $K^*$  vs  $\bar{K}^*$ . Although the former gives eigenstates of G-parity, Chung informs me that proper consideration of eigenstates of isospin shows that the latter combination is more useful. Also the choice of which waves are forced to be coherent could strongly influence the results, especially in the presence of backgrounds. An error in the efficiency can favor one wave over another: this is especially so when certain combinations of waves resemble each other. One of the dangerous aspects of a PWA is that one gives the fit certain waves, and it has to account for all of the data with them. For example if there were a higher spin resonance, or one which doesn't decay via the isobars, the fit would nevertheless put its contribution somewhere. Due to the orthogonality of the different waves, higher spins tend to end up in the "phase space" contribution. However this orthogonality only applies to the extent that the efficiency is independent of the 3-body configuration. Thus it is highly desirable that the groups get together and try out each others ideas, exchange programs, or analyse each others' data.

#### 4.1.6 $J/\psi$ Decays

There is a very strong  $K\bar{K}\pi$  signal at  $\sim 1460$  MeV in  $J/\psi \rightarrow \gamma K\bar{K}\pi$ , shown in Fig. 20a. It has been determined [74,12] to be dominantly  $0^{-+}$  by analysing the orientation of the 3-body decay plane, which is independent of isobars. It contains a low-mass  $K\bar{K}$  enhancement which corresponds approximately to the  $a_0(980)$ .<sup>11</sup>

Mark III [29] have noticed that the peak is not well fit by a single Breit-Wigner. Their Dalitz plots for the low and high mass sides look different, with the high side (1460 – 1580 MeV) showing clear  $K^*$  bands. The new  $\sim 1450$   $0^{-+}(K\bar{K}^*)$  enhancement of AGS-771 [63] discussed in Section 4.1.2 is on the wrong side of 1460 to explain this. There may be two separate resonances appearing in the  $J/\psi \rightarrow \gamma K\bar{K}\pi$ , or one whose shape and branching ratios are distorted by the  $K\bar{K}^*$  threshold, or a statistical fluctuation in the resonance shape.

There is no 1460 peak in  $J/\psi \rightarrow \gamma a_0 \pi \rightarrow \eta \pi \pi$  (see Fig. 21). Rather a peak at  $\sim 1390$  MeV is seen by both DM2 [28] and Mark III [29,75] and the spectra drop sharply at  $\sim 1440$  MeV. This might be the  $\eta(1460)$  showing itself through interference, but no conclusion can be made until a spin-parity analysis is available.

<sup>11</sup>Have you remembered that this was the  $\delta$ ?

Using the technique of Fig. 5 to study the quark content of  $K\bar{K}\pi$  and  $\eta\pi\pi$  resonances, Mark III [29,27,76] and DM2 [28,12] have compared the systems X in  $J/\psi \rightarrow \gamma X$ ,  $\omega X$ , and  $\phi X$ , where  $X = K\bar{K}\pi$  or  $\eta\pi^+\pi^-$ . The Mark III data are shown in Figs. 20 and 21. The  $K\bar{K}\pi$  accompanying an  $\omega$  has a clear peak with  $M = 1440 \pm 7_{-20}^{+10}$  and  $\Gamma = 40_{-13}^{+17} \pm 10$  MeV. The angular distributions do not look like  $0^{-+}$ . Perhaps it is the  $f_1(1420)$ ? The ratio of the  $K_s K^\pm \pi^\mp$  to  $K^+ K^- \pi^0$  signals is consistent with the value 2 expected for  $I = 0$ . Assuming  $I = 0$  yields  $B(J/\psi \rightarrow \omega X, X \rightarrow K\bar{K}\pi) = (6.8_{-1.6}^{+1.9} \pm 1.7) \times 10^{-4}$ .

A very similar peak is seen in  $J/\psi \rightarrow \omega \eta \pi^+ \pi^-$ , correlated with an  $a_0(980) \rightarrow \eta \pi$  subsystem, and with  $M = 1421 \pm 8 \pm 10$ ,  $\Gamma = 45_{-23}^{+32} \pm 15$  MeV, and  $B(J/\psi \rightarrow \omega X, X \rightarrow a_0 \pi \rightarrow \eta \pi \pi) = (9.2 \pm 2.4 \pm 2.8) \times 10^{-4}$ . Here no spin information is available. If it is the same X as above, then it has a slightly larger branching ratio to  $\eta \pi \pi$  than to  $K\bar{K}\pi$ . This is in contrast to WA76's ratio for the  $f_1(1420)$  of  $0.06 \pm 0.04$  [73]. Thus either the X, or one of the X's, is not the  $f_1(1420)$ .

The Mark III data for  $K\bar{K}\pi$  accompanying a  $\phi$  show no peak in the 1400 MeV region. The upper limit  $B(J/\psi \rightarrow \phi X, X \rightarrow K\bar{K}\pi) < 1.1 \times 10^{-4}$ , is obtained by fixing the X parameters to those of the peak seen accompanying an  $\omega$ , or to the  $E(1420)$ , and assuming isotropic angular distributions. The  $\eta\pi\pi$  accompanying a  $\phi$  has one high bin just below 1400 MeV. DM2 [28] see no signal in this region in  $K\bar{K}\pi$  or  $\eta\pi\pi$  accompanying  $\phi$ 's. We would have expected an  $s\bar{s}$   $f_1(1420)$  to prefer to accompany  $\phi$ 's rather than  $\omega$ 's. There is also no sign of the  $f_1(1526)$ .

These  $J/\psi$  decays, even the purely hadronic ones, escape any attempt I make to explain them by resonances seen in hadron collisions. Perhaps I am not clever enough. Perhaps some of the results are wrong. Otherwise, there are a few more particles:  $X(1390)$ ,  $X(1440)$ , and the split or whole  $\eta(1460)$ . The despair of the orderly  $q\bar{q}$  modeller rises, along with the hopes of the  $g\bar{g}$ ,  $gq\bar{q}$ , and  $q\bar{q}q\bar{q}$  fans.

#### 4.1.7 $\gamma\gamma \rightarrow f_1(1420)$

Information on the 1400 MeV region is now coming from a new source:  $\gamma\gamma$  collisions.

At an  $e^+e^-$  storage ring there are not only  $e^+e^-$  collisions, but also a great many "Bremsstrahlung"  $\gamma$ 's emitted which can collide as shown in Fig. 22. As with normal Bremsstrahlung  $\gamma$ 's, they are emitted preferentially at very small angles to the  $e^\pm$  direction. In this case, the  $e^\pm$  proceed down the beam pipe with  $\theta \sim 0$ , and are not detectable in most experimental setups. The  $\gamma$ 's are nearly massless. By

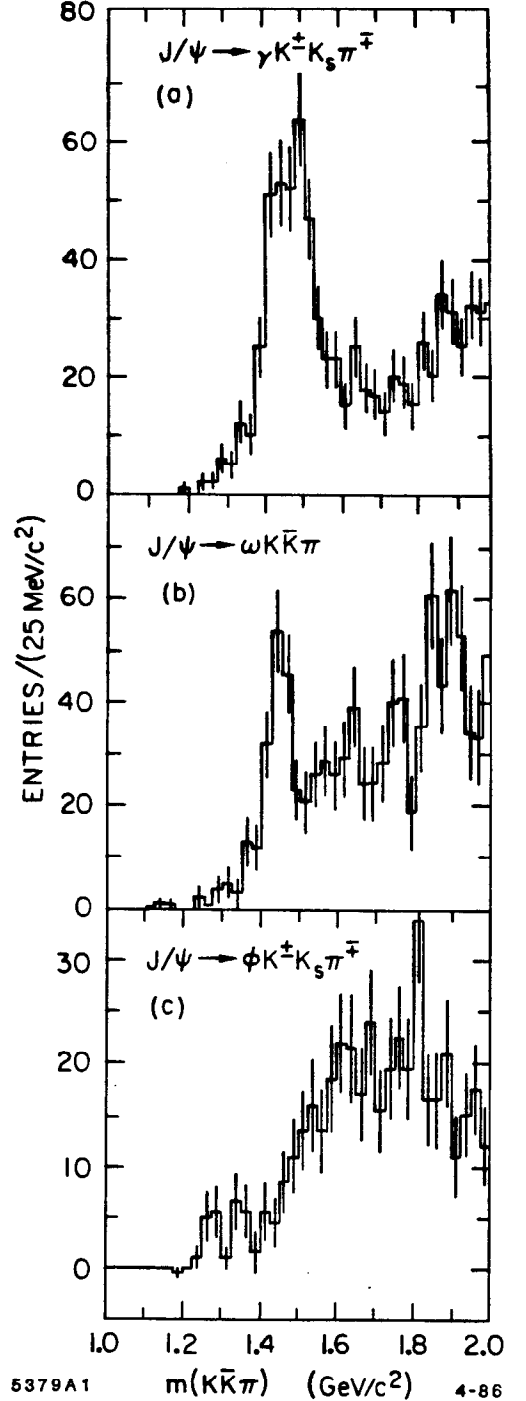


Figure 20: Mark III [27]  $X \equiv K_s K^\pm \pi^\mp$  mass plots from (a)  $J/\psi \rightarrow \gamma X$ , (b)  $J/\psi \rightarrow \omega X$  background subtracted, and (c)  $J/\psi \rightarrow \phi X$ .



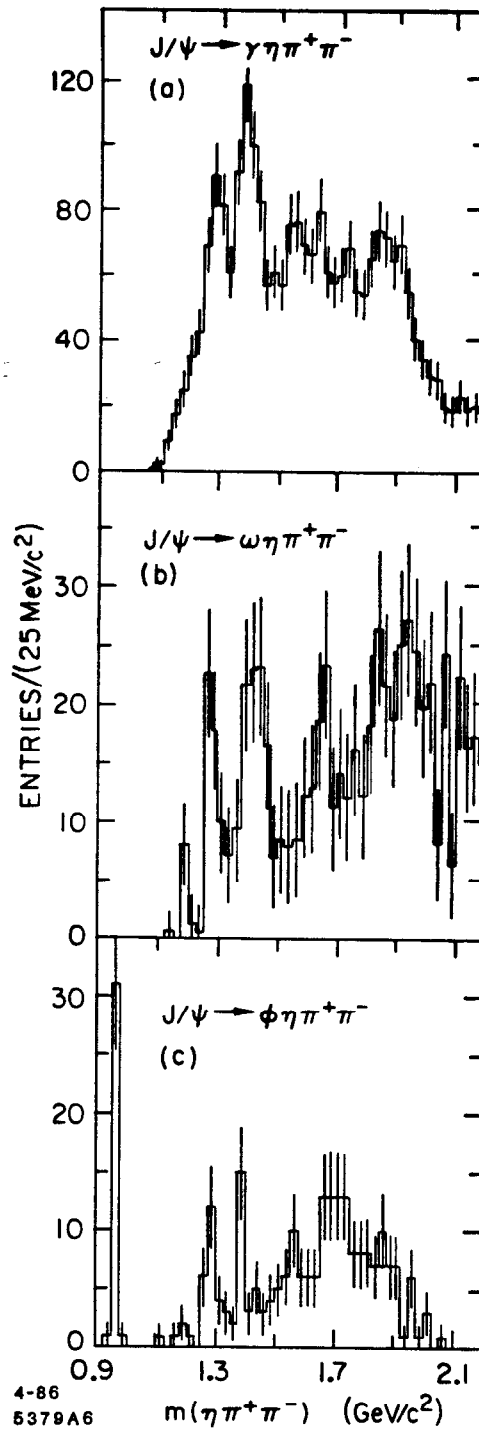


Figure 21: Mark III [27]  $X \equiv \eta\pi^+\pi^-$  mass plots from (a)  $J/\psi \rightarrow \gamma X$  for events with an  $\eta\pi$  combination consistent with the  $a_0(980)$ , (b)  $J/\psi \rightarrow \omega X$  consistent with  $a_0(980)$  and background subtracted, and (c)  $J/\psi \rightarrow \phi X$ .

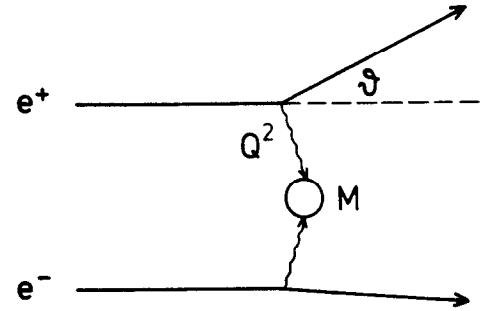


Figure 22:  $\gamma\gamma$  collision at  $e^+e^-$  storage ring with one nearly massless and one massive  $\gamma$ .

Yang's theorem [77], two massless  $\gamma$ 's cannot combine to form a  $J=1$  state. Thus we don't expect to see spin one mesons formed in  $\theta \sim 0$   $\gamma\gamma$  collisions. On the rare occasions when an  $e^\pm$  is scattered at a large enough angle to be detected, the  $\gamma$  acquires a negative mass:  $-M^2 \equiv Q^2 \approx 4EE'\sin^2(\theta/2)$ , where  $E$  and  $E'$  are the initial and final  $e^\pm$  energies and  $\theta$  is the scattering angle (see Fig. 22). Then Yang's theorem no longer applies, so that spin 1 mesons may be produced in the collision of a massless  $\gamma$  with a massive one. (The case where both  $\gamma$  acquire substantial mass is rare enough to ignore here.)

The TPC/2 $\gamma$  [78] collaboration have measured  $\gamma\gamma \rightarrow K_s K^\pm \pi^\mp$  for both  $\theta \sim 0$  and  $\theta > 0$ , shown in Fig. 23. The  $K_s K^\pm \pi^\mp$  mass distribution from  $\theta \sim 0$  data shows no structure, while that from  $\theta > 25$  mrad shows a clear peak at  $\sim 1420$  MeV. This effect has now been confirmed by Mark II [79]. In Fig. 24 the Mark II data with  $\theta > 21$  mrad are shown. The observed  $Q^2$  distribution for events with  $M(K_s K^\pm \pi^\mp)$  between 1400 and 1500 MeV is clearly different from that for all  $\gamma\gamma \rightarrow \text{hadrons}$  events. When quantified, this difference is evidence that the 1420 MeV meson being produced here has spin 1.

To make this concrete, TPC/2 $\gamma$  have compared the production of the 1420 peak as a function of the  $\gamma$  mass to that expected for spin 0 and spin 1 mesons. Massless  $\gamma$ 's always have transverse polarisation (T). Massive ones can also have longitudinal polarisation (L). Neglecting the small probability of both  $\gamma$ 's being massive, we have TT and LT scattering. A spin 0 meson cannot be formed by LT, so only TT contributes:

$$\sigma_{TT}(J=0) \sim \rho(Q^2) \quad (4)$$

$$\sigma_{LT}(J=0) = 0. \quad (5)$$

Here  $\rho(Q^2)$  is the  $\rho$ -pole photon form factor from

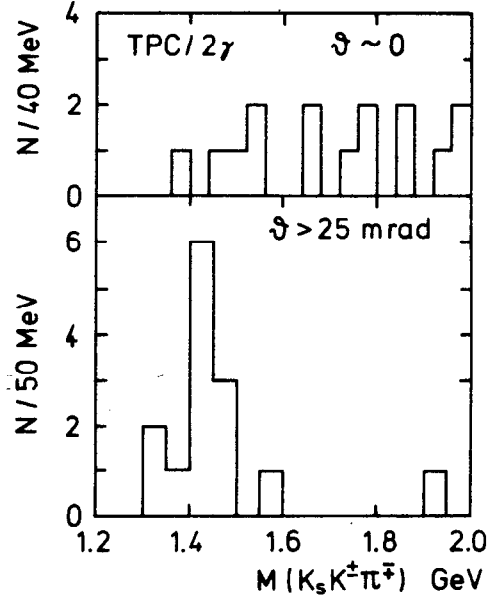


Figure 23: TPC/2 $\gamma$  [78]  $K_s K^\pm \pi^\mp$  mass distributions from  $e^+e^- \rightarrow e^+e^- \gamma\gamma$ ,  $\gamma\gamma \rightarrow K_s K^\pm \pi^\mp$  for  $e^\pm$  scattering angles (a)  $\theta \sim 0$  (nearly massless  $\gamma$ 's), and (b)  $\theta > 25$  mrad (one massive  $\gamma$ ).

VDM

$$\rho(Q^2) = \frac{1}{\left(1 - \frac{Q^2}{m_p^2}\right)^2},$$

which describes fairly well the  $Q^2$ -dependent production of other mesons (e.g. the  $f_2(1270)$  [31]).

For spin 1 both TT and LT contribute:

$$\sigma_{TT}(J=1) \sim \rho(Q^2) \frac{Q^4}{M^4} \quad (6)$$

$$\sigma_{LT}(J=1) \sim \rho(Q^2) \frac{Q^2}{M^2} \quad (7)$$

where  $M$  is the meson mass. At small  $Q^2$  LT will dominate. Fig. 25 shows a comparison of the  $J=0$  expectation and the  $J=1$  LT term with the TPC/2 $\gamma$  data on formation of the 1420 MeV peak as a function of  $Q^2$ .  $J=0$  disagrees strongly with the  $Q^2 \sim 0$  point, while  $J=1$  gives a good description of the data.

A value for the strength of the  $\gamma\gamma$  coupling of the spin 1 resonance can be obtained by extrapolating the fitted curve in Fig. 25b to  $Q^2=0$ . (This is better done after dividing out the  $Q^2/M^2$  dependence). The result is

$$\lim_{Q^2 \rightarrow 0} \frac{M^2}{Q^2} \Gamma_{\gamma\gamma} \times B(K\bar{K}\pi) = 6 \pm 2 \pm 2 \text{ keV}.$$

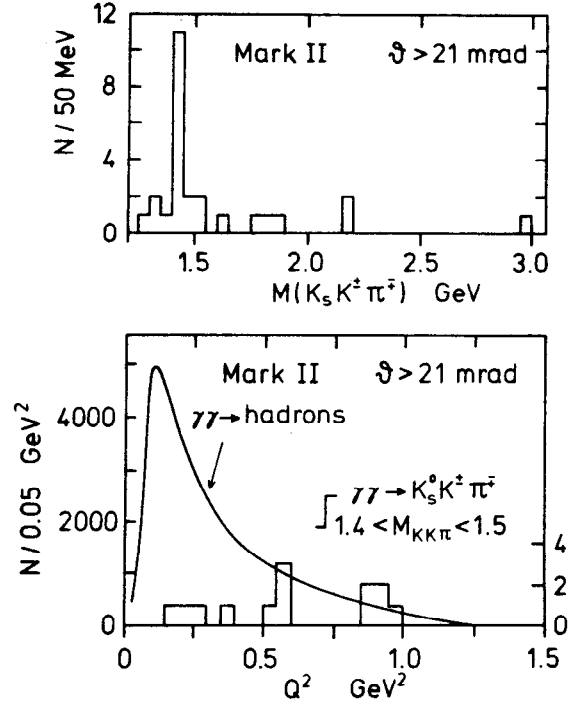


Figure 24: Mark II [79]  $\gamma\gamma$  data. (a)  $K_s K^\pm \pi^\mp$  mass distributions for events with an  $e^\pm$  detected at  $\theta > 21$  mrad. (b) Observed  $Q^2$  distributions with  $\theta > 21$  mrad for  $K_s K^\pm \pi^\mp$  events near the 1420 MeV peak compared to that for  $\gamma\gamma \rightarrow > 3$  hadrons.

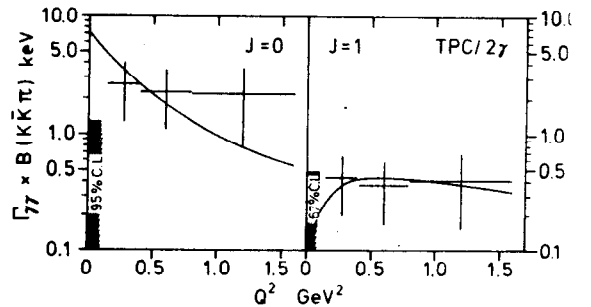


Figure 25: TPC/2 $\gamma$  [78]  $Q^2$  dependence of  $\gamma\gamma$  formation of the 1420  $K\bar{K}\pi$  peak. In (a) the data are corrected for the experimental acceptance using a  $J=0$  Monte Carlo, and in (b) using a  $J=1$  Monte Carlo. The curves are the best fits to the  $Q^2 > 0$  points using Eqs. (4) and (7) respectively.

Table 7: Stickiness of  $0^{-+}$  mesons.

The  $J/\psi$  branching ratios are from [1]. The  $\Gamma_{\gamma\gamma}$  are from [78], [1], and Table 8.

| X            | $B(J/\psi \rightarrow \gamma X)$<br>$\times 10^4$ | $\Gamma_{\gamma\gamma}$<br>[keV] | $S \times 10^4$  |
|--------------|---|----------------------------------|------------------|
| $\eta(1460)$ | $46 \pm 7$  | $< 1.6$                          | $> 4000 \pm 100$ |
| $\eta'(958)$ | $42 \pm 5$  | $4.5 \pm 0.5$                    | $23 \pm 4$       |
| $\eta(549)$  | $8.6 \pm 0.8$                                     | $0.53 \pm 0.03$                  | $6 \pm 1$        |

One is very tempted to say that this is the  $f_1(1420)$  seen by WA76 in  $\pi^+p$ . The statistics are rather sparse to test for the  $\bar{K}\bar{K}^*$  decay. The TPC Dalitz plot looks flat, while the Mark II one looks more like  $\bar{K}\bar{K}^*$ .

Besides providing independent evidence that there is a  $1^{++}(\bar{K}\bar{K}^*\pi)$  resonance at 1420 MeV,  $\gamma\gamma$  collisions also give support to the  $\eta(1460)$  glueball candidate by putting an upper limit on its  $\gamma\gamma$  coupling. TPC/2 $\gamma$  [78] have recently improved the limit to

$$\Gamma_{\gamma\gamma}[\eta(1460)] \times B(\bar{K}\bar{K}^*\pi) < 1.6 \text{ keV} \quad (95\% \text{ C.L.}).$$

Chanowitz [80] has proposed a stickiness variable as a test of glueballs. The stickiness  $S$  of a resonance is essentially the ratio of its production in radiative  $J/\psi$  decays to that in  $\gamma\gamma$  collisions, with kinematic factors divided out:

$$S_X \equiv \frac{\Gamma(J/\psi \rightarrow \gamma X)}{\text{LIPS}(J/\psi \rightarrow \gamma X)} \bigg/ \frac{\Gamma(X \rightarrow \gamma\gamma)}{\text{LIPS}(X \rightarrow \gamma\gamma)}.$$

LIPS is the Lorentz Invariant Phase Space, which for  $X=0^{-+}$  is p-wave for both channels. One advantage of this variable is that the decay branching ratio, which is unknown, divides out. The stickiness of the  $\eta(1460)$  is compared to that of other isosinglet  $0^{-+}$   $q\bar{q}$  resonances in Table 7. However here I have only listed the ground state (1S) resonances. If the  $\eta(1460)$  can find a place as  $q\bar{q}$  it will be as a radial excitation (2S). So it would be preferable to compare its stickiness to that of the 2S resonances. Unfortunately we don't have much information on them. The  $\eta(1420)$  is a candidate, but it isn't seen in either radiative  $J/\psi$  decays or  $\gamma\gamma$  collisions, so it is no quantitative help at the moment ( $S=0/0$ ). The question of 2S  $0^{-+}$  states is dealt with further in the following sections.

## 4.2 1280 MeV Region

### 4.2.1 Hadron Collisions

It may seem an unlikely coincidence to have a  $0^{-+}$  and a  $1^{++}$   $\bar{K}\bar{K}^*\pi$  resonance at  $\sim 1420$  MeV. However the same effect occurs at  $\sim 1280$  MeV. Here

we have [1] the  $1^{++}$   $f_1(1285)$ , formerly called the D, with  $M = 1283 \pm 5$  and  $\Gamma = 25 \pm 3$  MeV decaying to  $\eta\pi\pi$  (predominantly via  $a_0\pi$ ), to  $4\pi$ , and to  $\bar{K}\bar{K}^*\pi$ . In addition there is a  $0^{-+}$   $\eta(1275)$  which was discovered in its  $a_0\pi$  decay by Stanton *et al.* [81] in a PWA of 8 GeV  $\pi^-n \rightarrow (\eta\pi^+\pi^-)n$ . A better fit is obtained with the  $0^{-+}$  and  $1^{++}$  waves incoherent, indicating that they correspond to different nucleon helicity states. The same reaction, also at 8 GeV/c, confirms the  $\eta(1275)$  at KEK [67], shown in Fig. 15. Stanton *et al.* find  $M = 1275 \pm 15$  and  $\Gamma = 70 \pm 15$  MeV, while the KEK has  $M = 1279 \pm 5$  and  $\Gamma = 32 \pm 10$  MeV.

Note that this is the same production mechanism where the AGS-771 and KEK experiments also see the  $\eta(1420)$ . To complete the analogy, the  $\eta(1275)$  is not seen in the  $\pi^+p$  experiment (Figs. 18&19), where the  $f_1(1285)$  and  $f_1(1420)$  are prominent and the  $\eta(1420)$  is absent.

AGS-771 do not have evidence for the  $\eta(1275)$  in their  $\bar{K}\bar{K}^*\pi$  data (Fig. 13), but can accommodate it by changing the  $a_0(980)$  parameterisation [82].

### 4.2.2 $J/\psi$ Decays

DM2 [28] and Mark III [29,27] see a peak at  $\sim 1285$  MeV in the  $\eta\pi\pi$  spectra accompanying a  $\gamma$ ,  $\omega$ , and  $\phi$  in  $J/\psi$  decays, and in  $4\pi$  accompanying a  $\phi$ . DM2 also sees it in  $4\pi$  accompanying a  $\gamma$ . In this channel they have analysed the  $4\pi$  system and found the peak to be mostly  $\rho^0\pi\pi$ . Since this is one of the standard [1] decay modes of the  $f_1(1285)$ , it could be evidence for  $J/\psi \rightarrow \gamma f_1(1285)$ . Such a radiative decay of the  $J/\psi$  via  $J/\psi \rightarrow \gamma gg$  with both gluons massless is forbidden by Yang's theorem. However massless virtual gluons is only an approximation. Also, the determination that the  $f_1(1285)$  decays to  $\rho^0\pi\pi$  was made before the  $\eta(1275)$  was seen, and may not have allowed for the possibility that not all of the 1285 peak is due to the  $f_1(1285)$ . As usual, caution is advised before  $J^P$  measurements are available.

### 4.2.3 $\gamma\gamma \rightarrow \eta(1275)$

The  $\eta(1275)$  is a candidate  $\eta(2S)$ , although  $q\bar{q}$  models (e.g. [17]) would rather have it at a higher mass. Predictions for the  $\gamma\gamma$  coupling of an  $\eta(2S)$  are in the region of a few keV [17,83]. However Crystal Ball data [84] on  $\gamma\gamma \rightarrow \eta\pi^0\pi^0$  (Fig. 26) show no sign of the  $\eta(1275)$ . The 90% C.L. upper limit, assuming  $\Gamma_{\text{tot}} = 50$  MeV, is

$$\Gamma_{\gamma\gamma}[\eta(1275)] \times B(\eta\pi\pi) < 0.3 \text{ keV} \quad (\text{prel.})$$

This was surprising [85], but perhaps can be understood on closer inspection of the possibilities for mixing among the  $0^{-+}$  mesons.

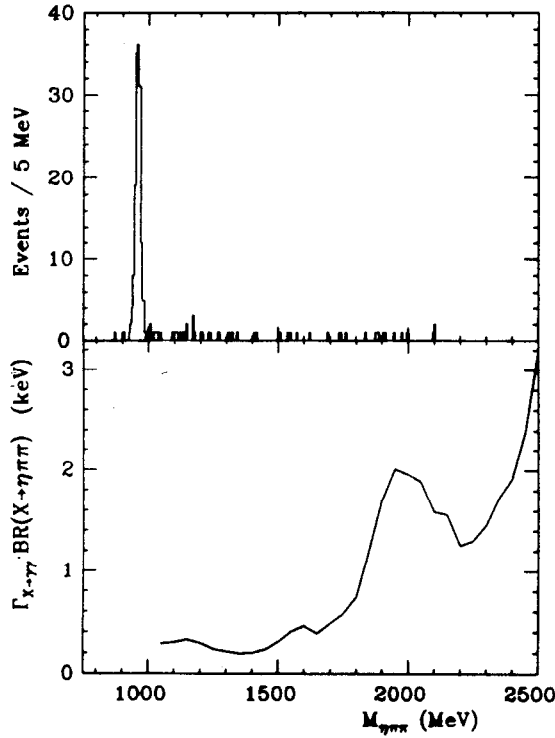


Figure 26: (a) Crystal Ball [84]  $\eta\pi\pi$  mass distribution from  $\gamma\gamma\rightarrow\eta\pi^0\pi^0$ . The large peak is the  $\eta'(958)$ . (b) Preliminary upper limits for  $\Gamma_{\gamma\gamma}(X)\times B(X\rightarrow\eta\pi\pi)$ , for  $\Gamma_{\text{tot}}(X)=50$  MeV. Although there are no events at high mass, the upper limit rises because the  $\eta\pi^0\pi^0$  reconstruction efficiency and the  $\gamma\gamma$  flux fall with increasing mass.

The  $\gamma\gamma$  coupling of a meson is the coherent sum of the  $\gamma\gamma$  couplings of its  $q\bar{q}$  components, each of which is proportional to  $e_q^2|\psi(0)|^2$ , where  $e_q$  is the quark charge and  $\psi(0)$  the  $q\bar{q}$  spatial wave function at  $r=0$ . An isosinglet always has equal amounts of  $u\bar{u}$  and  $d\bar{d}$ , so we can write the arbitrary isosinglet wave function as

$$\psi = v(u\bar{u} + d\bar{d}) + \sigma s\bar{s} \quad |v|^2 + |\sigma|^2 = 1.$$

In the approximation that the spatial wave function is the same for all  $q\bar{q}$  components we get

$$\Gamma_{\gamma\gamma} \sim \left| \frac{5v + \sigma}{9} \right|^2.$$

Thus vanishing  $\Gamma_{\gamma\gamma}$  is achieved for  $\sigma = -5v$  [86]. However that means a large  $s\bar{s}$  content for the  $\eta(1275)$ , which would make its production via a pion beam and its  $a_0\pi$  decay improbable. Also, this mixing leaves a primarily  $u\bar{u}+d\bar{d}$  partner, which should be seen in  $\gamma\gamma\rightarrow\eta\pi\pi$ . The data in Fig. 26



Figure 27: 1S-2S mixing for  $I=0$   $0^{-+}$  mesons.

don't leave much room for such a meson below  $\sim 1800$  MeV.

The Stanton *et al.* [81] and KEK [67] data on the  $\eta(1275)$  present an amusing cure for its non-appearance in  $\gamma\gamma\rightarrow\eta\pi\pi$ : They see destructive interference between the  $a_0\pi$  and  $f_0\eta$  isobars, with little sign of the  $\eta(1275)$  in the total  $\eta\pi\pi$  spectrum (see Figs. 15&16). So all the Crystal Ball have to do is perform a partial wave analysis of their 0 events to separate the interfering isobars!

Now let us be serious and look at what goes into the predictions of  $\Gamma_{\gamma\gamma}$  for the 2S states. The wave function at the origin is smaller for 2S states than for 1S, but the p-wave phase space for the decay is larger due to their higher mass. In addition, the 2S and 1S states mix, via the diagram in Fig. 27, to form the physical states we observe. Expanding the notation used above, so that for a given isosinglet meson,  $v_{1S}$  is its  $u\bar{u}+d\bar{d}$  1S component, etc.,

$$\psi = (v_{1S} + v_{2S})(u\bar{u} + d\bar{d}) + (\sigma_{1S} + \sigma_{2S})s\bar{s}.$$

Using the individual  $\gamma\gamma\rightarrow q\bar{q}$  couplings from the Godfrey&Isgur model [87] yields

$$\Gamma_{\gamma\gamma} = M^3 |2.65v_{1S} - 1.12v_{2S} + 0.58\sigma_{1S} - 0.28\sigma_{2S}|^2,$$

where inserting  $M$  in GeV gives  $\Gamma_{\gamma\gamma}$  in keV.

Notice that the 2S states enter with a minus sign in this particular model, giving an opportunity to achieve  $\Gamma_{\gamma\gamma}\sim 0$  without an  $s\bar{s}$  component. Godfrey&Isgur's prediction for  $\Gamma_{\gamma\gamma}[\eta(1440)]\approx 7$  keV was based on  $v_{1S} = -0.26$ ,  $v_{2S} = +0.79$ ,  $\sigma_{1S} = -0.17$ ,  $\sigma_{2S} = -0.44$ . However the mixing among the  $0^{-+}$  mesons is quite uncertain in their model due to the difficulty of calculating Fig. 27 at such low masses. The isosinglets are doubly difficult because they have octet-singlet mixing as well as 1S-2S. With the  $I=1$   $\pi(2S)$  we should be on firmer ground. The candidate particle is the  $\pi(1300)$  which has a width between 200 and 600 MeV, and decays to  $3\pi$ , including  $\rho\pi$ . Godfrey&Isgur predict  $\Gamma_{\gamma\gamma}[\pi(1300)]=1$  keV. Since the branching ratios are not known, a

useful measurement of its  $\Gamma_{\gamma\gamma}$  should include both the  $\pi^0\pi^+\pi^-$  and the  $3\pi^0$  channels. Next year?

Until we understand the  $\Gamma_{\gamma\gamma}$  widths of the 2S mesons, we should be very cautious in using the non-observation of the glueball candidate  $\eta(1460)$  in  $\gamma\gamma$  collision to say that it can't be 2S  $q\bar{q}$ .

## 5 $\Gamma_{\gamma\gamma}$ of Other $0^{-+}$ Mesons

### 5.1 $\pi^0$ and $\eta$

At this conference new results were presented by Crystal Ball [92], using  $\gamma\gamma \rightarrow \gamma\gamma$  scattering to measure  $\Gamma_{\gamma\gamma}$  of the  $\eta(548)$  and the  $\pi^0$ . The data are shown in Fig. 28, and the results compared to previous measurements in Table 8. Their  $\Gamma_{\gamma\gamma}(\pi^0)$  agrees well with a very precise measurement using the decay length of high energy  $\pi^0$ 's [91], and with the previous best measurement by Browman *et al.* [90] using the Primakoff effect. This agreement makes it all the more surprising that the new  $\gamma\gamma$  measurement of the  $\eta$  disagrees with that of Browman *et al.*, although all the  $\gamma\gamma$  measurements agree with each other (see Table 8).

In the Primakoff effect the  $\eta$  is formed by an incoming photon beam interacting with a virtual photon of the Coulomb field of a heavy nucleus:

$$\gamma N \rightarrow \gamma\gamma^* N \rightarrow \eta N.$$

The cross section for this process is

$$\sigma_{\text{Primakoff}} \propto \Gamma_{\gamma\gamma} |F_{\text{em}}(q)|^2 E_{\text{beam}}^4 \frac{\sin^2\theta}{q^4}, \quad (8)$$

where  $\theta$  is the angle of the  $\eta$  relative to the incoming  $\gamma$  direction. There is a minimum momentum transfer squared [97]

$$q^2 \equiv t_{\text{min}} \approx -\frac{M^4}{4E_{\text{beam}}^2}$$

for a photon of energy  $E_{\text{beam}}$  producing a meson of mass  $M$ . The  $t_{\text{min}}$ 's for the various experiments are listed in Table 8.

$F_{\text{em}}(q)$  is the electromagnetic form factor of the nucleus of charge  $Z$ . Its  $q$ -dependence must be known in order to extract  $\Gamma_{\gamma\gamma}$  from Eq. 8. A physicist of the previous generation would be able to say something wise at this point about the size of the error this is likely to introduce. The best I can do is to point out that the correction is reduced as  $|q^2|$  decreases for higher beam energies, and that the  $\eta$  needs a factor 16 higher beam energy than the  $\pi^0$  to get down to the same  $|q^2|$ . Modern Primakoff experiments are performed at hundreds of GeV (e.g. Ref. [44]), but none measure the  $\eta$ .

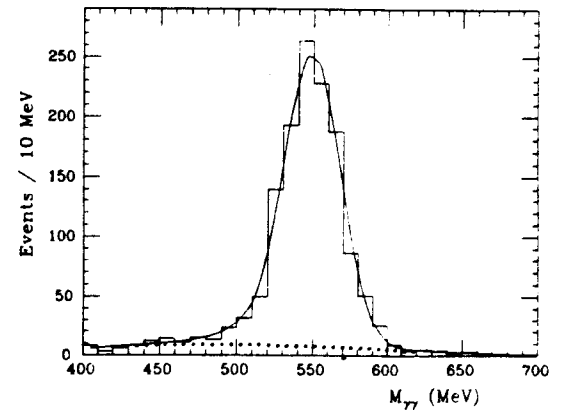
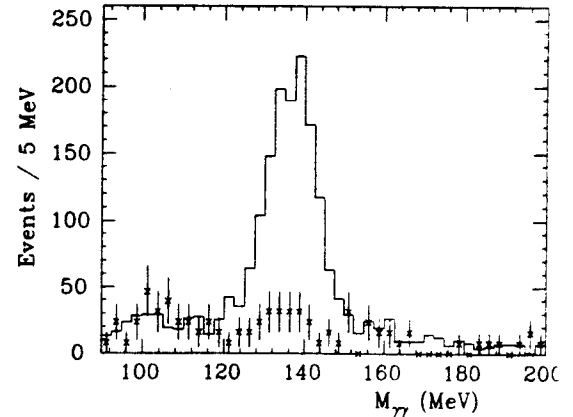


Figure 28: Crystal Ball [92] data on  $\gamma\gamma \rightarrow \gamma\gamma$  vs.  $M(\gamma\gamma)$  (a) near the  $\pi^0$  and (b) near the  $\eta$ . The crosses in (a) are the normalised single beam data, which is too sparse in (b) to plot but is well represented by the dotted background curve. The  $p_t(\gamma\gamma)$  requirement is  $<8.7$  MeV in (a) and  $<45$  MeV in (b).

Primakoff production of  $\pi^0$ 's and  $\eta$ 's has a background from  $\pi^0$ 's and  $\eta$ 's produced in the hadronic field of the nucleus, e.g.

$$\gamma N \rightarrow \gamma\rho^* N \rightarrow \eta N.$$

The Coulomb and hadronic contributions can be statistically separated by fitting the angular distributions, since that for production in the Coulomb field is peaked at smaller angles.

The most recent Primakoff experiment, that of Browman *et al.*, was able to take advantage of higher energies available by then to improve the signal to background (the Primakoff effect increases as  $E_{\text{beam}}^4$ ), and to check the systematics of the separation by comparing results from a wide range of beam energies. Therefore their  $\Gamma_{\gamma\gamma}(\eta)$  became the accepted value, although it differed substantially

Table 8: Measurements of  $\Gamma_{\gamma\gamma}$  of the  $\pi^0$  and  $\eta$ .

| $\Gamma(\pi^0)$ (eV)                          | Method       | $t_{\min}$ [MeV <sup>2</sup> ] | Reference                     |
|---|--------------|--------------------------------|-------------------------------|
| 12±1  | Primakoff    | -83                            | Bellettini <i>et al.</i> [88] |
| 7.3±0.6                                       | Primakoff    | -69                            | Kryshkin <i>et al.</i> [89]   |
| 8.0±0.4                                       | Primakoff    | -2                             | Browman <i>et al.</i> [90]    |
| 7.3±0.2±0.1                                   | Decay Length |                                | Cronin <i>et al.</i> [91]     |
| 7.8±0.4±0.9 (prel.)                           | Two Photon   |                                | Crystal Ball (DORIS) [92]     |
| $\Gamma(\eta \rightarrow \gamma\gamma)$ [keV] |              |                                |                               |
| 1.0±0.2                                       | Primakoff    | -745                           | Bemporad <i>et al.</i> [93]   |
| 0.32±0.05                                     | Primakoff    | -172                           | Browman <i>et al.</i> [90]    |
| 0.56±0.16                                     | Two Photon   |                                | Crystal Ball (SPEAR) [94]     |
| 0.53±0.04±0.04                                | Two Photon   |                                | JADE [95]                     |
| 0.64±0.14±0.13                                | Two Photon   |                                | TPC/2 $\gamma$ [96]           |
| 0.51±0.02±0.06 (prel.)                        | Two Photon   |                                | Crystal Ball (DORIS) [92]     |
| 0.53 ± 0.04                                   | Two Photon   |                                | average                       |
| $\Gamma(\eta')$ (keV)                         |              |                                |                               |
| 4.5±0.4                                       | Two Photon   |                                | average [1]                   |

from the first Primakoff measurement of the  $\eta$  by Bemporad *et al.*

In order to measure  $\Gamma_{\gamma\gamma}$  in  $\gamma\gamma$  collisions one relies on a QED calculation of the  $\gamma\gamma$  flux factor  $\mathcal{F}_{\gamma\gamma}$  to convert the  $e^+e^-$  luminosity  $\mathcal{L}$  to an equivalent  $\gamma\gamma$  luminosity:

$$N(e^+e^- \rightarrow e^+e^-M) = \mathcal{L} \mathcal{F}_{\gamma\gamma} \sigma(\gamma\gamma \rightarrow M).$$

Here  $\sigma(\gamma\gamma \rightarrow M)$  is the Breit-Wigner resonance cross section as in Eq. (1), and is proportional to  $\Gamma_{\gamma\gamma}(M)$ . The efficiency for detecting this process is typically only a few %, because the events tend to have a large Lorentz boost, and is determined using a Monte Carlo simulation of the  $e^+e^- \rightarrow e^+e^-M$  process. A possible background from beam-gas production of  $\eta$ 's, i.e.  $ep \rightarrow \eta + X$ , must be checked. The four available measurements agree with each other quite well (Table 8). Two of them have errors approaching that of the latest Primakoff experiment. The  $\gamma\gamma$  average is  $\Gamma_{\gamma\gamma}(\eta) = 0.53 \pm 0.04$ , which is a factor of  $1.7 \pm 0.3$  larger than the Primakoff result. A graphical comparison of the  $\Gamma_{\gamma\gamma}(\eta)$  results is presented in Fig. 29.

Both types of experiments have a small effect from the  $q^2$  dependence of the  $\gamma\gamma$  coupling to the  $\eta$ .  $\Gamma_{\gamma\gamma}$  is defined for the decay  $\eta \rightarrow \gamma\gamma$ , where the  $\gamma$ 's are real and massless. When we measure  $\Gamma_{\gamma\gamma}$  in  $\gamma\gamma \rightarrow \eta$ , where the photons are not quite real, we expect a  $\rho$ -pole form factor for each  $\gamma$ , so that in the above equations  $\Gamma_{\gamma\gamma}$  should be replaced by  $\rho(q) \Gamma_{\gamma\gamma}$  for the Primakoff effect (where only one  $\gamma$  is virtual) and by  $\rho(q_1) \rho(q_2) \Gamma_{\gamma\gamma}$  for  $\gamma\gamma$  collisions. In the latter, the  $\gamma$ 's have small  $q^2$ , especially after typical cuts on the net  $p_t$  of the observed  $\eta$ . The Crystal Ball

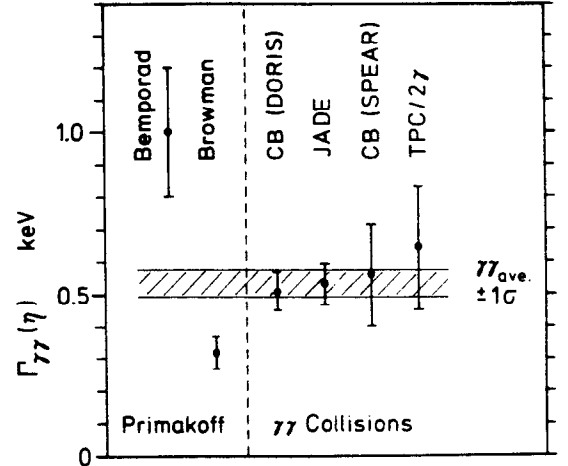


Figure 29: Comparison of Primakoff and  $\gamma\gamma$  measurements of  $\Gamma_{\gamma\gamma}(\eta)$ . The points are not drawn in chronological order, but rather so as to put the most precise measurements next to each other.

[92] requires  $p_t(\eta) < 45$  MeV, for which the form factors reduce the observed cross section by less than 0.3%.

We are left with two different types of precise measurements which don't agree with each other as well as we would like. It is tempting to take the  $\gamma\gamma$  results as correct, saying that even the Browman *et al.* experiment was at too low a beam energy for a reliable  $\eta$  measurement. However it would be preferable to first obtain a realistic estimate of how much the uncertainty in the nuclear form factor affects the Primakoff results.

Table 9:  $\eta_c$  Decay Branching Ratios.

The  $K\bar{K}\pi$  branching ratios assume  $I=0$ ; thus  $(K\bar{K}\pi)^0 = \frac{1}{3}K_s K^\pm \pi^\mp + \frac{1}{3}K_L K^\pm \pi^\mp + \frac{1}{6}K^+ K^- \pi^0 + \frac{1}{6}K^0 \bar{K}^0 \pi^0$ . The  $2(\pi^+ \pi^-)$  includes  $\rho^0 \rho^0$ . Additional Mark III branching ratios are in Ref. [99].

| X                | $10^4 \times B(J/\psi \rightarrow \gamma \eta_c, \eta_c \rightarrow X)$ |                 |                 |
|------------------|---|-----------------|-----------------|
|                  | Mark III<br>[99]  | DM2<br>[100]    | average         |
| $K\bar{K}\pi$    | $6.4 \pm 1.4$   | $7.5 \pm 1.6$   | $6.9 \pm 1.1$   |
| $p\bar{p}$       | $0.14 \pm 0.07$   | $0.13 \pm 0.04$ | $0.13 \pm 0.03$ |
| $2(\pi^+ \pi^-)$ | $1.6 \pm 0.6$   | $1.3 \pm 0.3$   | $1.4 \pm 0.3$   |
| $\rho^0 \rho^0$  | $< 0.6$   | $1.1 \pm 0.2$   | ?               |
| $\phi\phi$       | $1.02 \pm 0.29$   | $0.41 \pm 0.12$ | ?               |

## 5.2 $\Gamma_{\gamma\gamma}(\eta_c)$

The  $\gamma\gamma$  flux falls with increasing mass, so that data on the heavier mesons is scarce. This year we have first results on  $\gamma\gamma \rightarrow \eta_c$ . They don't agree with each other terribly well, but they are all low statistics measurements, so fluctuations are expected.

Before comparing the various  $\Gamma_{\gamma\gamma}(\eta_c)$  measurements, it is necessary to update the  $\eta_c$  decay branching ratios. This is done in Table 9. The DM2 and Mark III results for the  $\rho\rho$  and  $\phi\phi$  decays are in disagreement. However the decay modes we need here,  $K\bar{K}\pi$  and  $p\bar{p}$ , agree well. The values in Table 9 are product branching ratios  $B(J/\psi \rightarrow \gamma \eta_c, \eta_c \rightarrow X)$ . To get  $B(\eta_c \rightarrow X)$  we need to divide by  $B(J/\psi \rightarrow \eta_c) = (1.27 \pm 0.36)\%$  [98]. The 28% error on this will be common to most of the  $\Gamma_{\gamma\gamma}$  measurements, and must be treated as such in making the average.

PLUTO have published [101] their 7 observed  $\gamma\gamma \rightarrow K_s K^\pm \pi^\mp$  events, shown in Fig. 30. TASSO are still working on their analysis, but reported a preliminary result this spring [102]. Now Mark II have a preliminary result [79] from 4 observed events in the  $\eta_c$  region (Fig. 31). All three  $\Gamma_{\gamma\gamma}(\eta_c)$  values are listed in Table 10.

The MD-1 collaboration [104] at the VEPP-4  $e^+e^-$  storage ring in Novosibirsk have looked for  $e^+e^- \rightarrow e^+e^- \gamma\gamma \rightarrow e^+e^- \eta_c$ . Instead of observing the  $\eta_c$  decay products, they measure the energies and angles of the scattered electrons and calculate the missing mass  $X$  in  $e^+e^- \rightarrow e^+e^- X$ . This is possible because, unlike the standard detector with solenoidal magnetic field parallel to the  $e^\pm$  beams, MD-1 has a perpendicular field which bends off-energy electrons out of the beam. The analysis is done for events with the  $e^+$  and  $e^-$  detected at scattering angles  $\theta > 0.5$  mrad, and two additional tracks (charged or neutral) at large angles to the beam.

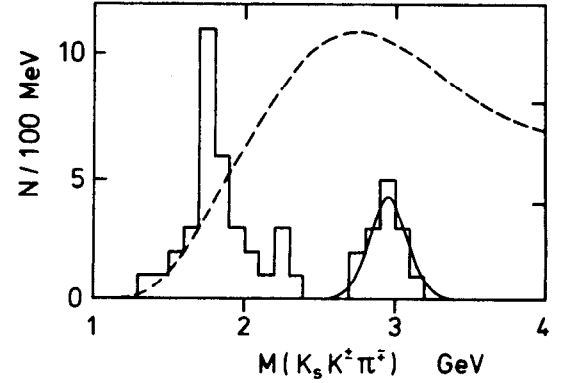


Figure 30: PLUTO evidence for  $\gamma\gamma \rightarrow \eta_c$  [101].  $K_s$ 's are identified by their reconstructed  $\pi^+ \pi^-$  decay, requiring that the decay vertex be clearly separated from the interaction point. No particle identification is used for the charged particles, so each event appears twice, once for the  $K_s K^\pm \pi^\mp$  hypothesis, once for  $K_s \bar{K}^\pm \pi^\mp$ . The two hypotheses tend to lie close to each other in  $M(K_s K^\pm \pi^\mp)$ . Thus the 14 entries in the  $\eta_c$  peak are from only 7 events. Events consistent with  $K_s K_s$  have been rejected. The dashed curve shows the mass dependence of the efficiency times  $\gamma\gamma$  flux.

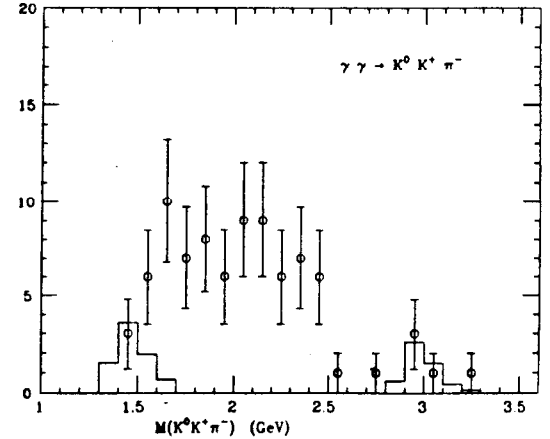
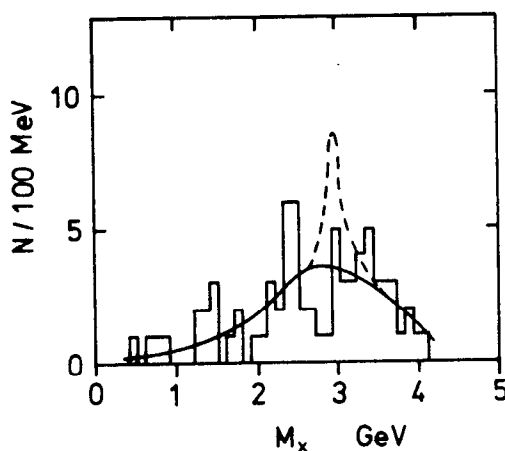


Figure 31: The points are the Mark II data on  $\gamma\gamma \rightarrow \eta_c$  [79]. Only 6 out of the 84 events have more than one combination of tracks consistent with  $K_s K^\pm \pi^\mp$ . The solid histograms are Monte Carlo simulations of  $\gamma\gamma \rightarrow \eta(1460)$  and  $\gamma\gamma \rightarrow \eta_c$ .

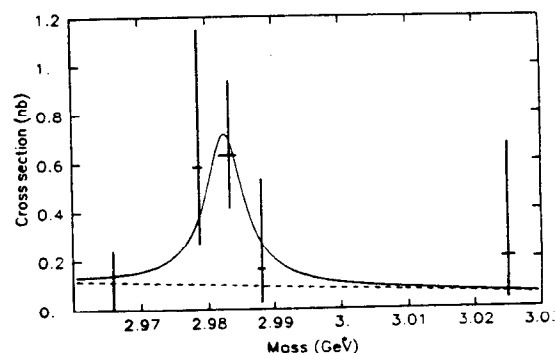
Table 10: Measurements of the  $\gamma\gamma$  width of the  $\eta_c$ 

|  | $\Gamma_{\gamma\gamma}(\eta_c)$ [keV]                  | Reference    |
|--|--|--------------|
| $\Gamma_{\gamma\gamma}(\eta_c) \times B(\eta_c \rightarrow K_s K^\pm \pi^\mp)$ [keV]                           |  |              |
| $0.5_{-0.15}^{+0.2} \pm 0.1$   | $30 \pm 13^*$  | PLUTO [101]  |
| $1.2 \pm 0.6 \pm 0.4$ (prel.)  | $71 \pm 43^*$  | TASSO [102]  |
| $0.15_{-0.08}^{+0.11} \pm 0.05$ (prel.)  | $9 \pm 7^*$  | Mark II [79] |
|  | * neglecting $B(\eta_c \rightarrow K\bar{K}\pi)$ error |              |
| $B(\eta_c \rightarrow \gamma\gamma) \times B(\eta_c \rightarrow p\bar{p})$<br>$(0.57 \pm 0.26) \times 10^{-6}$ | $6 \pm 4$  | R704 [103]   |
|  | neglecting $B(\eta_c \rightarrow p\bar{p})$ error      |              |
|  | $9 \pm 4$  | average      |
|  | including all errors                                   |              |
|  | $< 11$ (90% C.L., prel.)                               | MD-1 [104]   |


 Figure 32: Preliminary MD-1 missing mass (X) spectrum in  $e^+e^- \rightarrow e^+e^-X$  [104]. The dashed curve corresponds to the upper limit  $\Gamma_{\gamma\gamma}(\eta_c) < 11$  keV.

The missing mass spectrum is shown in Fig. 32. The resolution in missing mass is  $\sigma_m \approx 90$  MeV at the  $\eta_c$ . They obtain a preliminary 90% C.L. upper limit of 14 events, or  $\Gamma_{\gamma\gamma}(\eta_c) < 11$  keV. This limit is independent of the  $\eta_c$  decay branching ratios, requiring only a reasonable simulation of  $\eta_c \rightarrow$  hadrons in order to obtain the detection efficiency, which is about 20%.

Yet another way of measuring  $\Gamma_{\gamma\gamma}(\eta_c)$  has been developed by R704 at the ISR. They produce the  $\eta_c$ 's directly in  $p\bar{p}$  annihilation, scanning the beam energy over the  $\eta_c$  region. The ISR beam gives them a mass resolution of  $\sim 0.3$  MeV. To measure  $p\bar{p} \rightarrow \eta_c \rightarrow \gamma\gamma$ , they must suppress the background from  $p\bar{p} \rightarrow \pi^0\pi^0$  with two  $\gamma$ 's outside the detector, or  $\pi^0 \rightarrow \gamma\gamma$  with the  $\gamma$ 's so close together that they are indistinguishable from a single  $\gamma$ . They were only able to collect small numbers of events before the ISR shut down. Slight changes in the cuts, which


 Figure 33: R704 [103]  $\eta_c$  data. Note that this is a scan so that where there are no points the cross section is not necessarily 0; rather there is no information there. The dashed line is the background level determined from a study of  $p\bar{p} \rightarrow \pi^0\pi^0$  events.

cause a few events more or less to be accepted, make noticeable changes in  $\Gamma_{\gamma\gamma}(\eta_c)$ . Thus several values have been quoted as the analysis has progressed; however they are all compatible within the statistical error. Their  $\eta_c$  scan is shown in Fig. 33. The total width of the  $\eta_c$  cannot be very well determined from this data: a fit gives  $\Gamma_{tot} = 7.0_{-7.0}^{+7.5}$  MeV; while the peak height is better determined:  $B(\eta_c \rightarrow \gamma\gamma)B(\eta_c \rightarrow p\bar{p}) = 0.68_{-0.31}^{+0.42} \times 10^{-6}$ . The value in Table 10 is from a fit with  $\Gamma_{tot}$  fixed at the Crystal Ball [98] value of  $11.5 \pm 4.5$  MeV.

The various  $\Gamma_{\gamma\gamma}(\eta_c)$  measurements are compared in Fig. 34. They exhibit the usual effect that the first experiment that sees a significant signal is observing an upward fluctuation, and the value tends to decrease as more information comes in. The present average is  $\Gamma_{\gamma\gamma}(\eta_c) = 9 \pm 4$  keV ( $\chi^2/d.f. = 5/3$ ). This may be a biased average, since experiments with even lower values may not bother to



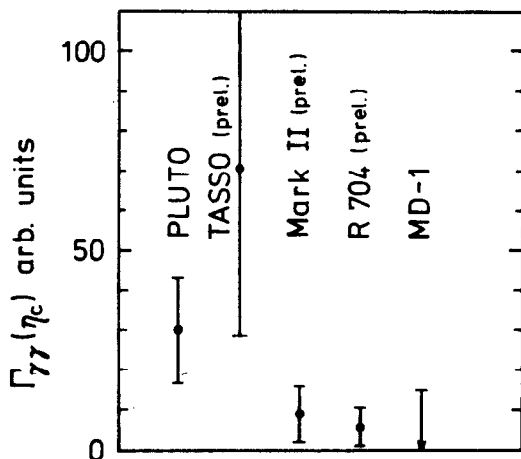


Figure 34:  $\Gamma_{\gamma\gamma}(\eta_c)$  measurements. The comparison is complicated by common systematic errors. I have put no error for  $B(\eta_c \rightarrow K\bar{K}\pi)$  on the 3  $K\bar{K}\pi$  points, and assigned the relative error between it and  $B(\eta_c \rightarrow p\bar{p})$  to the single  $p\bar{p}$  point. The MD-1 upper limit has been increased by the full error on  $B(K\bar{K}\pi)$ . This confuses the absolute y-scale, but is (I think) the fairest comparison between the measurements, which is the point here.

report them.

Clearly all the experiments need more statistics. The most promising opportunity is with experiment E760 [105] being built to repeat the  $p\bar{p}$  annihilation measurement at the Fermilab  $\bar{p}$  accumulator ring.

The expected  $\Gamma_{\gamma\gamma}(\eta_c)$  can be related to  $\Gamma_{ee}(J/\psi)$ . Both the  $\eta_c$  and the  $J/\psi$  are bound  $c\bar{c}$  states, the former is the  $1^1S_0$  and the latter is the  $1^3S_1$ . The approximation where they have the same wave function at the origin gives [106]

$$\Gamma_{\gamma\gamma}(\eta_c) = 3 e_q^2 \Gamma_{ee}(J/\psi) \times \left(1 + 1.96 \frac{\alpha_s}{\pi}\right),$$

where the last factor is the  $1^{st}$  order QCD correction. The measured [1]  $\Gamma_{ee}(J/\psi) = 4.7 \pm 0.3$  keV leads to a predicted  $\Gamma_{\gamma\gamma}(\eta_c) \sim 7$  keV for  $\alpha_s = 0.22$ . QCD sum rules [107] give  $\sim 4$  keV.

## 6 $b\bar{b}$ Mesons

### 6.1 Limits on Other Narrow $1^{--}$ Resonances in the $\Upsilon$ Region

The  $\Upsilon$ 's are the  $n^3S_1$  bound states of  $b\bar{b}$  quarks. The ground state ( $n=1$ ), called the  $\Upsilon(1S)$ , was discovered via its  $\mu^+\mu^-$  decay in  $pN \rightarrow \mu^+\mu^- X$  [108]. There indications were also seen for the first two excited states, the  $\Upsilon(2S)$  and  $\Upsilon(3S)$  [109]. Since

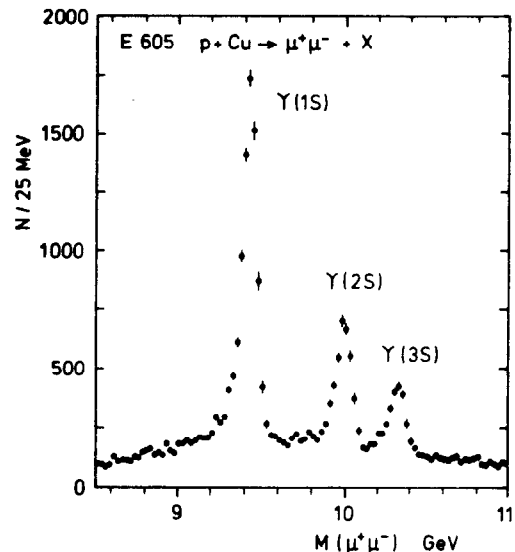


Figure 35: E605 [110]  $M(\mu^+\mu^-)$  distribution from  $p \text{ Cu} \rightarrow \mu^+\mu^- X$ .

then the  $\Upsilon$  family has been largely the domain of the  $e^+e^-$  machines. However now E605 at Fermilab [110] have achieved  $\sim 0.3\%$  mass resolution and clearly separated the first three  $\Upsilon$ 's in the reaction  $p \text{ Cu} \rightarrow \mu^+\mu^- X$ , as shown in Fig. 35.

These data have been used to extract upper limits for the production of other resonances in the  $\Upsilon$  region (Fig. 36) relative to the Drell-Yan production of  $\mu^+\mu^-$ . Although they are not sensitive enough to rule out Higgs particle or Technipion production, the expected levels for which are also shown in Fig. 36, they are useful for testing other hypotheses that come up.

One such hypothesis was suggested by Tye and Rosenfeld [111] after the 1984 report by Crystal Ball [112] of a narrow resonance  $\zeta$  seen at 8.3 GeV in radiative  $\Upsilon(1S)$  decays.

Tye and Rosenfeld speculated that the  $\zeta$  was the  $1S$  bound state of a pair of scalar quarks,  $\bar{Q}Q$ , and that it was coming not from  $\Upsilon(1S)$  decays, but from those of the  $\bar{Q}Q(3P) 1^{--}$  state which would be close to the  $\Upsilon(1S)$  in mass. This explained the  $\zeta$ 's non-appearance in  $\Upsilon(2S)$  decays [112]; and also the fact that it wasn't seen [113] by CLEO or CUSB at the CESR  $e^+e^-$  machine, which has a  $\sim 4$  MeV center of mass resolution compared to DORIS's  $\sim 8$  MeV. The resolution difference was perhaps even greater, since the original Crystal Ball  $\Upsilon(1S)$  data was accumulated in 3 short run periods, a situation not conducive to precise setting of the beam energy on the  $\Upsilon(1S)$  mass.

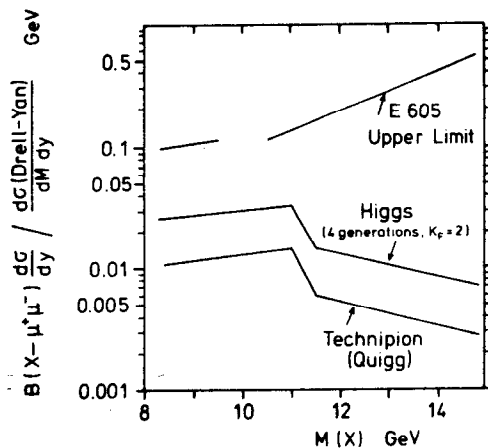


Figure 36: E605 [110] upper limits for narrow resonance (X) production times  $B(X \rightarrow \mu^+ \mu^-)$  in  $p \text{ Cu} \rightarrow \mu^+ \mu^- + \text{anything}$ , relative to the Drell-Yan  $\mu^+ \mu^-$  cross section.

Later in 1984 Crystal Ball took more data on the  $\Upsilon(1S)$ , taking great care to put the beam energy at the peak of the  $\Upsilon(1S)$ . No  $\zeta$  was seen, and an upper limit set which contradicted the previous signal, assuming it came from the  $\Upsilon(1S)$  [114,115]. Elimination of the  $\bar{Q}Q$  explanation of the  $\zeta$  signal was achieved in 1986 with data taken 12 MeV above and 12 MeV below the  $\Upsilon(1S)$ , where again no peak was seen [116]. Thus the original peak must have been a statistical fluctuation.

The idea of other bound states besides the  $\Upsilon$  remains an interesting possibility however, and wherever one can look for new phenomena one should. MD-1 [117] have scanned the  $e^+e^-$  center-of-mass region from 7.2 to 10 GeV setting the limits shown in Fig. 37 on  $\Gamma_{ee}$  of a narrow resonance. Their data are a substantial improvement over what was previously available in this energy region.

## 6.2 $\Gamma_{ee}$ and Radiative Corrections Corrections

A part of Crystal Ball's  $\Upsilon(1S)$  running this year was a careful scan over the resonance to measure its leptonic width  $\Gamma_{ee}$ . That result is not ready yet, but I report on our progress on understanding how to extract  $\Gamma_{ee}$  from the scan data. In principle  $\Gamma_{ee}$  is proportional to the area of the  $e^+e^- \rightarrow \text{hadrons}$  resonance curve, just as described previously for  $K\bar{K}$  scattering (Eq. (2)). However in the case of the  $\Upsilon$ , the resonance width is much smaller than the energy resolution  $\Delta$  of the  $e^+e^-$  machine, and the  $\Upsilon$

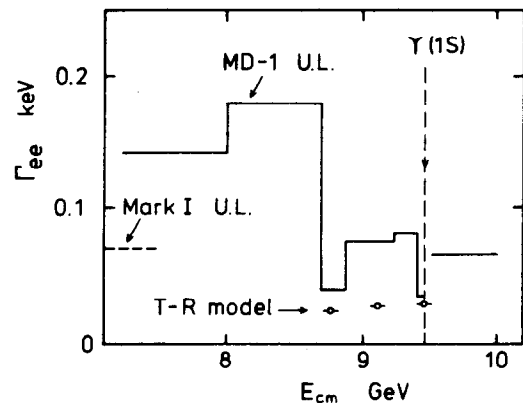


Figure 37: MD-1 [117] preliminary 90% C.L. upper limits on  $\Gamma_{ee}$  of a narrow resonance ( $\Gamma < 4$  MeV). The energy range is divided into 7 regions with equal integrated luminosity (excluding the  $\Upsilon(1S)$ ); for each region the maximum  $\Gamma_{ee}$  is plotted. The Mark I [118] upper limit is also sketched. The LENA upper limit [119] is off scale. The points are the predicted masses and  $\Gamma_{ee}$ 's of the 1P, 2P and 3P scalar quark states in the Tye-Rosenfeld model [111].

Breit-Wigner curve is replaced by the Gaussian of the machine resolution:

$$\begin{aligned} \bar{\sigma}(W) &= H_0 e^{-(W-M)^2/2\Delta^2}, \text{ where} \\ H_0 &= \Gamma_{ee} \frac{\Gamma_{\text{had}}}{\Gamma_{\text{tot}}} \frac{6\pi^2}{M^2} \frac{1}{\Delta\sqrt{2\pi}} \end{aligned} \quad (9)$$

is the new peak height. The area of the resonance curve is not changed by this smearing.

Initial state radiation (Fig. 38d) adds to the Gaussian a high energy tail, as shown in Fig. 39, because at a nominal setting above the  $\Upsilon$ , radiation of a photon before the  $e^+e^-$  annihilation can bring the effective energy down to the  $\Upsilon$ . Until now, almost all  $\Upsilon$ -experimenters relied on the formulation of Jackson and Scharre [120] for this radiative correction. Last year rumors reached us of a Russian paper by Kuraev and Fadin which claimed to find significant deviations from the Jackson-Scharre result. Even after translation into English [121] it remained a formidable obstacle. However now the VEPP-4 experimenters [122] have published a paper using an approximation to the Kuraev-Fadin form, and very considerably give their formula explicitly. It is this last which I shall use in the following.

As shown in Fig. 39, the new and old formulations agree quite well in the shape. However the normalisation is significantly affected. Evaluated for  $\Delta=4$  MeV, the peak height of the Jackson-Scharre curve is  $0.645 H_0$ , while that of VEPP-4 is  $0.584 H_0$ , a 10%

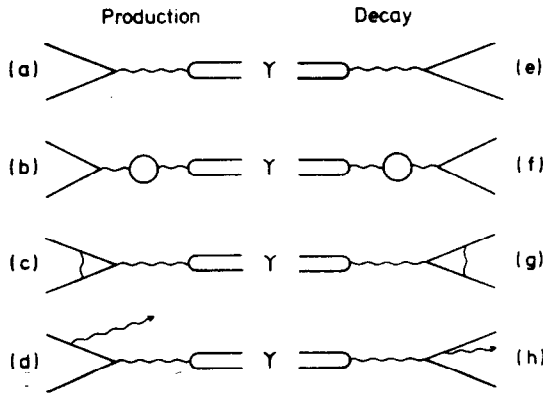


Figure 38: Diagrams for  $e^+e^- \rightarrow \Upsilon$  and for  $\Upsilon \rightarrow e^+e^-$ .

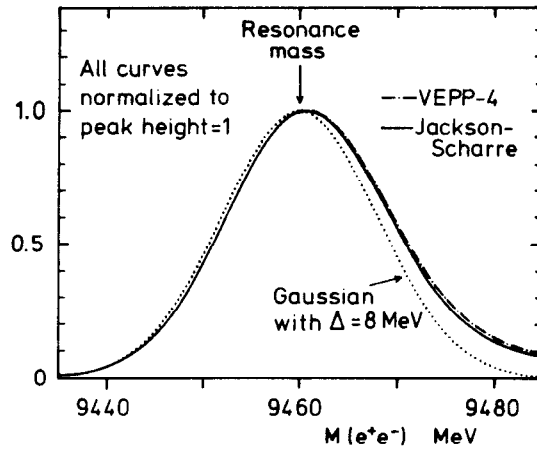


Figure 39: Shape of  $e^+e^- \rightarrow \Upsilon$  peak ignoring initial state radiation (Gaussian curve of  $\sigma = \Delta$ ), and with radiation according to the Jackson-Scharre [120] and VEPP-4 [122] formulas.

change<sup>12</sup>. The difference turns out to be partly a matter of definition, and partly a problem with the treatment of low energy photons.

The matter of definition was pointed out by Tsai [123] in 1983, but overlooked by the experimenters. Although we measure  $\Gamma_{ee}$  in  $e^+e^- \rightarrow \text{hadrons}$ , we use it to extract the  $\Upsilon$  total width  $\Gamma_{\text{tot}}$  from  $B(\Upsilon \rightarrow e^+e^-) \equiv \Gamma_{ee}/\Gamma_{\text{tot}}$ . For this equivalence to hold, the definition of  $\Gamma_{ee}$  must include all the diagrams which contribute to the  $\Upsilon \rightarrow e^+e^-$  decay, shown in Fig. 38. The  $e^+e^- \gamma$  final state has been included in both the calculation and the experimental branching ratio, and is not the problem. Rather

<sup>12</sup>Note that the lowest order QED corrections have reduced the peak height by  $\sim 35\%$  from the Gaussian's  $H_0$ , an astonishingly large effect for  $\alpha = 1/137$ .

it is the vacuum polarisation diagram (Fig. 38b), which has been handled in an inconsistent manner. It clearly belongs to the  $\Upsilon \rightarrow e^+e^-$  decay, and should therefore be included in the definition of  $\Gamma_{ee}$ . It also occurs in the  $e^+e^- \rightarrow \text{hadrons}$  process. However here Jackson and Scharre treated it as part of the radiative correction instead. CLEO [130] "improved" upon Jackson-Scharre by including not only electron but also  $\mu, \tau$ , and hadron vacuum polarisation loops, obtaining a normalisation of  $0.693 H_0$ . With the vacuum polarisation put back into  $\Gamma_{ee}$  where it belongs, the Jackson-Scharre normalisation becomes  $0.617 H_0$ .

The second problem is disagreement among theorists on how to do the "soft-photon exponentiation". Jackson-Scharre applied it only to diagram 38d, while current majority vote (e.g. [124,121]) favors applying it (or something very close to it [123]) to all terms. The proper resolution to the dispute will come from a calculation of the next order. For now I will take the majority opinion, with its peak normalisation of  $0.584 H_0$ , and the caution that there remains an  $\sim 5\%$  theoretical uncertainty.

Since the shapes of all the curves agree so well, we can renormalise the published results to the new consistent definition of  $\Gamma_{ee}$ . As can be seen from Eq. (9), the observed peak height is proportional to  $\Gamma_{ee} \Gamma_{\text{had}}/\Gamma_{\text{tot}}$  times the radiative corrections normalisation factor. Reducing that factor from its original  $0.645$  to  $0.584$  increases the extracted  $\Gamma_{ee} \Gamma_{\text{had}}/\Gamma_{\text{tot}}$  values by  $10\%$ . The re-normalised values are given in Table 11.

In order to get  $\Gamma_{ee}$ , we need the  $\Gamma_{\text{had}}/\Gamma_{\text{tot}}$  factor which accounts for the fact that in this measurement we use only decays  $\Upsilon \rightarrow \text{hadrons}$ . Assuming lepton universality and that the  $\Upsilon$  decays only to charged lepton pairs or to hadrons gives  $\Gamma_{\text{tot}} = 3\Gamma_{ee} + \Gamma_{\text{had}}$ , or  $\Gamma_{\text{had}}/\Gamma_{\text{tot}} = 1 - 3B_{\mu\mu}$ .

New world averages for  $B_{\mu\mu}$  are calculated in Table 12, including the new values presented at this conference: a new  $B_{\mu\mu}(1S)$  measurement from ARGUS [137], and the first statistically significant  $B_{\mu\mu}(3S)$ , provided by CUSB [141]. In Table 13 the average  $\Gamma_{ee} \Gamma_{\text{had}}/\Gamma_{\text{tot}}$  and  $B_{\mu\mu}$  values are combined to get  $\Gamma_{ee}$  and  $\Gamma_{\text{tot}}$ . The results are significantly different from those in the latest PDG tables [1].

There are several applications of these measurements. Both  $\Gamma_{ee}$  and  $\Gamma_{\text{tot}}$  are proportional to the  $Q\bar{Q}$  wave function at the origin;  $\Gamma_{\text{tot}}$  is also proportional to  $\alpha_s^3$ . Thus  $\Gamma_{ee}$  is a good test of the  $Q\bar{Q}$  potential, subject of course to the usual cautions when QCD gets in the picture. In  $B_{\mu\mu}$ , the ratio of the two, the effect of the wave function drops out leaving only the  $\alpha_s$  dependence, but unfortunately

Table 11: Measurements of  $\Gamma_{ee} \Gamma_{had}/\Gamma_{tot}$  (in keV)

The type of radiative correction that was used in each published  $\Gamma_{ee} \Gamma_{had}/\Gamma_{tot}$  value is listed, and the new value with VEPP-4 normalisation is given.

| Published $\Gamma_{ee} \Gamma_{had}/\Gamma_{tot}$ | Rad. corr.              | new value       | Experiment            |
|---|-------------------------|-----------------|-----------------------|
| <b><math>\Upsilon(1S)</math></b>                  |                         |                 |                       |
| ?   | Greco                   | -               | PLUTO [125]           |
| $1.00 \pm 0.23$                                   | JS                      | $1.09 \pm 0.25$ | DESY-Heidelberg [126] |
| $1.10 \pm 0.07 \pm 0.11$                          | Greco                   | $1.13 \pm 0.13$ | LENA [127,128]        |
| $1.12 \pm 0.07 \pm 0.04$                          | JS                      | $1.23 \pm 0.09$ | DASP II [129]         |
| $1.17 \pm 0.05 \pm 0.08$                          | JS, full $\delta_{vac}$ | $1.37 \pm 0.11$ | CLEO [130]            |
| $1.04 \pm 0.05 \pm 0.09$                          | JS                      | $1.17 \pm 0.11$ | CUSB [131] (unpub.)   |
|   |                         | $1.22 \pm 0.05$ | average               |
| <b><math>\Upsilon(2S)</math></b>                  |                         |                 |                       |
| $0.37 \pm 0.16$                                   | JS                      | $0.41 \pm 0.18$ | DESY-Heidelberg [126] |
| $0.53 \pm 0.07^{+0.09}_{-0.05}$                   | Greco                   | $0.54 \pm 0.12$ | LENA [132,128]        |
| $0.55 \pm 0.11 \pm 0.06$                          | JS                      | $0.60 \pm 0.14$ | DASP II [129]         |
| $0.49 \pm 0.03 \pm 0.04$                          | JS, full $\delta_{vac}$ | $0.58 \pm 0.06$ | CLEO [130]            |
| $0.53 \pm 0.03 \pm 0.05$                          | JS                      | $0.59 \pm 0.06$ | CUSB [131] (unpub.)   |
|   |                         | $0.57 \pm 0.04$ | average               |
| <b><math>\Upsilon(3S)</math></b>                  |                         |                 |                       |
| $0.38 \pm 0.03 \pm 0.03$                          | JS, full $\delta_{vac}$ | $0.45 \pm 0.05$ | CLEO [130]            |
| $0.35 \pm 0.02 \pm 0.03$                          | JS                      | $0.39 \pm 0.04$ | CUSB [131] (unpub.)   |
|   |                         | $0.41 \pm 0.03$ | average               |

Table 12: Measurements of  $B_{\mu\mu}$  (in %)

| <b><math>\Upsilon(1S)</math></b>  |                          |                     |
|---|--------------------------|---------------------|
| Reaction  |                          | Experiment          |
| $\Upsilon \rightarrow \mu^+ \mu^-$  | $2.2 \pm 2.0$            | PLUTO [125]         |
| $\Upsilon \rightarrow \mu^+ \mu^-$  | $1.4^{+3.4}_{-1.4}$      | DESY-Heid. [126]    |
| $\Upsilon \rightarrow \mu^+ \mu^-$  | $3.2 \pm 1.3 \pm 0.3$    | DASP II [129]       |
| $\Upsilon \rightarrow \mu^+ \mu^-$  | $3.8 \pm 1.5 \pm 0.2$    | LENA [127]          |
| $\Upsilon \rightarrow \mu^+ \mu^-$  | $2.7 \pm 0.3 \pm 0.3$    | CLEO [133]          |
| $\Upsilon \rightarrow \mu^+ \mu^-$  | $2.7 \pm 0.3 \pm 0.3$    | CUSB [134]          |
| $\Upsilon \rightarrow ee$   | $5.1 \pm 3.0$            | PLUTO [135]         |
| $\Upsilon' \rightarrow \pi^+ \pi^- \Upsilon, \Upsilon \rightarrow \mu^+ \mu^-, e^+ e^-$ | $2.84 \pm 0.18 \pm 0.20$ | CLEO [136]          |
| $\Upsilon' \rightarrow \pi^+ \pi^- \Upsilon, \Upsilon \rightarrow \mu^+ \mu^-, e^+ e^-$ | $2.39 \pm 0.12 \pm 0.14$ | ARGUS [137] (prel.) |
| $\Upsilon \rightarrow \tau\tau$   | $3.4 \pm 0.4 \pm 0.4$    | CLEO [138]          |
|   | $2.63 \pm 0.13$          | average             |
| <b><math>\Upsilon(2S)</math></b>  |                          |                     |
| $\Upsilon' \rightarrow \mu\mu$  | $1.8 \pm 0.8 \pm 0.5$    | CLEO [139]          |
| $\Upsilon' \rightarrow \mu\mu$  | $1.9 \pm 0.3 \pm 0.5$    | CUSB [134]          |
| $\Upsilon' \rightarrow \mu\mu$  | $1.0 \pm 0.6 \pm 0.5^*$  | ARGUS [140]         |
| $\Upsilon' \rightarrow \tau\tau$  | $1.7 \pm 1.5 \pm 0.6$    | CLEO [139]          |
|   | $1.6 \pm 0.4$            | average             |
| <b><math>\Upsilon(3S)</math></b>  |                          |                     |
| $\Upsilon'' \rightarrow \mu\mu$   | $3.3 \pm 1.3 \pm 0.7$    | CLEO [133]          |
| $\Upsilon'' \rightarrow \mu\mu$   | $1.53 \pm 0.29 \pm 0.21$ | CUSB [141]          |
|   | $1.6 \pm 0.4$            | average             |

\* The ARGUS 2S value is scaled to the average 1S value with  $B_{\mu\mu}(2S) = 1.57 \pm 0.59 \pm 0.53 + 2.1(B_{\mu\mu}(1S) - 2.9)$  (in %) [140].

Table 13: Average values of  $B_{\mu\mu}$ ,  $\Gamma_{ee}$  and  $\Gamma_{tot}$ .

| Resonance      | New Values       |                     |                      | PDG Values [1]   |                     |                      |
|----------------|------------------|---------------------|----------------------|------------------|---------------------|----------------------|
|                | $B_{\mu\mu}$ [%] | $\Gamma_{ee}$ [keV] | $\Gamma_{tot}$ [keV] | $B_{\mu\mu}$ [%] | $\Gamma_{ee}$ [keV] | $\Gamma_{tot}$ [keV] |
| $\Upsilon(1S)$ | $2.63 \pm 0.13$  | $1.33 \pm 0.06$     | $51 \pm 3$           | $2.8 \pm 0.2$    | $1.22 \pm 0.05$     | $43 \pm 3$           |
| $\Upsilon(2S)$ | $1.6 \pm 0.4$    | $0.60 \pm 0.04$     | $37 \pm 10$          | $1.8 \pm 0.4$    | $0.54 \pm 0.03$     | $30 \pm 7$           |
| $\Upsilon(3S)$ | $1.6 \pm 0.4$    | $0.43 \pm 0.03$     | $27 \pm 6$           | $3.3 \pm 1.5$    | $0.40 \pm 0.03$     | $12^{+10}_{-4}$      |

also a large sensitivity to QCD problems. My not-yet-updated but still relevant thoughts on  $\Gamma_{ee}$  and  $B_{\mu\mu}$  can be found in Ref. [142]. The latest  $\Lambda_{QCD}$  values were given by J. Lee-Franzini at this conference [141].

The interest in  $\Gamma_{tot}$  is more subtle, but pervasive. Experimenters measure  $\Upsilon$  decay branching ratios, while theorists calculate partial widths. All comparisons between the two rely on  $\Gamma_{tot}$ !

### 6.3 $\chi_b(2P)$ States

The CLEO and CUSB experiments have been running on the  $\Upsilon(3S)$ . Their results presented at this conference represent about 1/3 of the total luminosity they hope to accumulate this year.

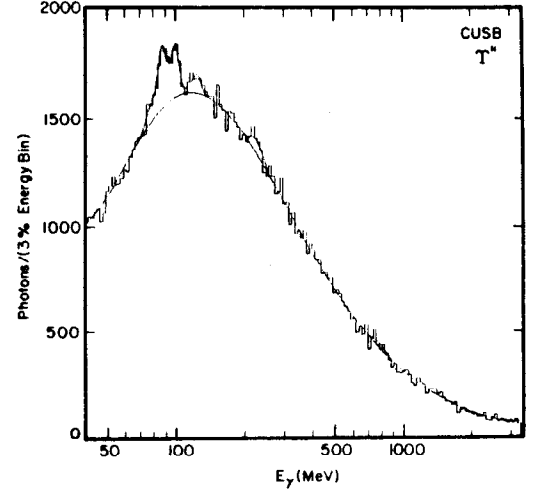
For this run the CUSB detector was upgraded to CUSB-II by the installation of a BGO inner detector. The energy resolution for electromagnetically showering particles is now  $\sigma_E/E = 2.2\%/\sqrt{E}$ , for  $E$  up to  $\sim 1$  GeV [141]. This resolution is about 3 MeV in the range  $E_\gamma = 85 - 100$  MeV, sufficient to separate the three  $\gamma$  lines corresponding to  $\Upsilon(3S) \rightarrow \gamma \chi_{bJ}(2P)$ ,  $J = 2, 1, 0$  in the inclusive  $\gamma$  spectrum from  $\Upsilon(3S) \rightarrow \gamma + \text{hadrons}$  (Fig. 40). The  $\gamma$  energies obtained from a fit to that spectrum are:

$$\begin{aligned} \chi_{b2} &: 86.5 \pm 0.7 \text{ MeV} \\ \chi_{b1} &: 99.3 \pm 0.8 \text{ MeV} \\ \chi_{b0} &: 124.2 \pm 2.3 \text{ MeV} \end{aligned}$$

This spectrum, along with the data on the exclusive decays  $\Upsilon(3S) \rightarrow \gamma \chi_b(2P)$ ,  $\chi_b(2P) \rightarrow \gamma \Upsilon$ ,  $\Upsilon \rightarrow \ell^+ \ell^-$ , provide several branching ratios which can be compared to those expected from potential model calculations, and also can be used to extract total widths of the  $\chi_b(2P)$  states for comparison with QCD calculations. All of these tests will be significantly improved when the full data sample is available. The current status was fully covered in the talk of J. Lee-Franzini at this conference. Here I will concentrate on the relative mass splitting of the  $\chi_b(2P)$  states and what it means for the heavy quark potential.

Combining their inclusive and exclusive measurements of the  $\chi_b(2P)$  states, CUSB obtain

$$r(2P) \equiv \frac{M_2 - M_1}{M_1 - M_0} = 0.57 \pm 0.06,$$


 Figure 40: CUSB-II [141] inclusive  $\gamma$  spectrum from  $\Upsilon(3S) \rightarrow \gamma + \text{hadrons}$ .

where  $M_J$  is the mass of the spin  $J$   $\chi_b(2P)$  state. The parameter  $r$  is sensitive to the Lorentz form of the confining part<sup>13</sup>  $kr + C$  of the  $Q\bar{Q}$  potential [143], which can be written approximately as

$$V(r) = -\frac{4\alpha_s}{3r} + kr + C.$$

The  $\alpha_s/r$  term is expected in perturbative QCD to come from the exchange of a gluon, which is a vector particle. However the confining part is non-perturbative and not that well understood, although most theorists expect it to behave as a scalar. Without any confining term in the potential,  $r=0.8$ . Adding scalar confinement reduces  $r$ , while vector confinement increases it. Although the earlier CUSB measurements [144] had large errors:  $r(2P) = 0.85 \pm 0.1 \pm 0.3$  and  $r(1P) = 0.93 \pm 0.1 \pm 0.2$ , their tendency to favor vector confinement caused some consternation. The new more precise CUSB 2P value, last year's world average of  $r(1P) = 0.66 \pm 0.05$  [143], and the  $\chi_c$  value of  $0.48 \pm 0.01$  are all well on the side of scalar confinement.

However now that the data is behaving, the theory is not. N. Byers [145] reported that scalar con-

<sup>13</sup>I use bold-face  $r$  for the ratio, and italic  $r$  for the distance in the potential  $V(r)$ .

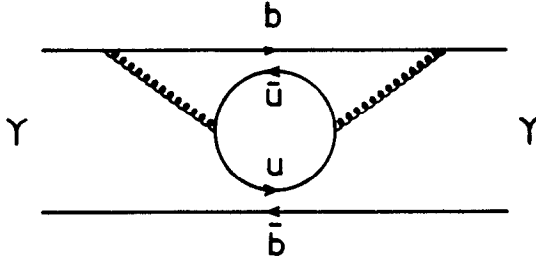


Figure 41: Pair creation diagram contributing to  $\Upsilon$  mass. The high  $k$  part is taken into account by the running of  $\alpha_s$ . Calculations of the low  $k$  part assume it is saturated by mesons, e.g.  $\Upsilon \rightarrow B\bar{B} \rightarrow \Upsilon$  [145].

finement, although providing the best description of the spin splittings, can no longer fit the gross features of the spectrum: the  $\Upsilon$  masses and the spin-averaged  $\chi_b$  masses. In the following I give my interpretation of what she and others [85] said.

The above discussion has ignored the effect of light quark pair creation<sup>14</sup> (Fig. 41) on the heavy meson masses. This is the mechanism by which the  $b\bar{b}$  mesons above threshold decay, e.g.  $\Upsilon(4S) \rightarrow B\bar{B}$ . The decay is forbidden for the lighter  $\Upsilon$ 's, but can exist as a virtual intermediate state, and thus affect the mass. Again it is clear how to treat the perturbative part. A gluon exchanged in the  $t$ -channel is what makes the  $\alpha_s/r$  part of the potential. Exchanged in the  $s$ -channel as in Fig. 41, it creates a light-quark pair. The use of the same exchange particle in the  $t$  and  $s$  channels is called "crossing", and is uncontroversial in the perturbative case.

Less clear is how to calculate the pair creation by the confining part of the potential. Confinement is probably not due to single particle exchange, but to the collective action of many gluons. The term scalar confinement is to be understood as "effective", i.e. its Lorentz properties are as though a scalar particle were being exchanged. But this is not enough to tell us how to create pairs. Byers makes the simplest approximation: that a scalar particle really is being exchanged in the  $t$  channel for the potential, and in the  $s$  channel to make pairs. The scalar particle is described by the  $kr+C$  terms in the potential.  $C$  sets the zero of the mass scale, and is large and negative. Pair production by a scalar particle is proportional to the potential, and both the  $kr$  and the  $C$  terms contribute strongly, with opposite sign. The net shift in masses is large. No successful fit to the measured masses could be found with scalar confinement model when the mass

<sup>14</sup>Vacuum polarisation come back to haunt us again!

shifts due to pair creation were included. (Previous fits ignored pair creation; then the type of confinement has no effect on the  $\Upsilon$  and average  $\chi_b$  masses.)

If confinement is via a vector particle exchange, the pair creation by that particle is proportional to the derivative of the potential, so the  $C$  term doesn't contribute. The mass shifts are still substantial: 126 MeV for the  $\chi_b(1P)$  center of gravity. However they can be accommodated by changing the parameters of the potential. A good fit was found with the following potential (where I have put in the  $\hbar c$ 's,  $r$  is in fm, and  $V$  in GeV):

$$V(r) = \frac{-0.097}{r} + 1.57 r - 0.97 .$$

Thus Byers concludes that the spin-averaged masses require vector confinement, while the spin-splittings need scalar confinement, so that we are in trouble. This conclusion depends however on the "crossing" assumption. Models with different treatment of pair creation can fit the data. For example the  ${}^3P_0$  model [85] finds only a  $\sim 20$  MeV shift for the  $\chi_b$  states using scalar confinement.

#### 6.4 Search for the ${}^1P_1$

Still missing in heavy quark spectroscopy are the  ${}^1P_1$  states of  $c\bar{c}$  and  $b\bar{b}$  [146]. They have  $J^{PC}=1^{+-}$ , and thus cannot be produced directly in  $e^+e^-$  annihilation or in radiative decays of the  $\Upsilon$ 's or  $\psi$ 's.

The  ${}^1P_1$  is an  $L=1$  state like the  ${}^3P_J$   $\chi_c$  and  $\chi_b$ , but with the quark spins anti-parallel instead of parallel. Since the net quark spin  $S=0$ , there is no  $\vec{L} \cdot \vec{S}$  force contributing to the  ${}^1P_1$  mass. The  $\vec{L} \cdot \vec{S}$  contribution to  ${}^3P_J$  averages to 0 in taking the spin-weighted average (usually referred to as the center-of-gravity):

$$M({}^3P_{\text{cog}}) \equiv \frac{5M({}^3P_2) + 3M({}^3P_1) + M({}^3P_0)}{9} .$$

The only contribution to a mass difference between the  ${}^3P_{\text{cog}}$  and the  ${}^1P_1$  is the  $s_1 \cdot s_2$  force. In lowest order it is proportional to the square of the wave function at the origin, which is 0 for  $P$  states. Thus we expect the  ${}^1P_1$  to be very close to the  ${}^3P_{\text{cog}}$ .

R704 [147] have looked for the  $c\bar{c}$   ${}^1P_1$  in  $p\bar{p} \rightarrow {}^1P_1 \rightarrow J/\psi + \text{anything}$ . They have 5 events at the right mass, corresponding to a  $2.3\sigma$  effect. If this signal is real, their new experiment E760 at Fermilab should be able to confirm it with many more events, and provide a statistically reliable mass determination.

A possibility for observing the  $b\bar{b}$   ${}^1P_1$  state is the reaction  $\Upsilon(3S) \rightarrow \pi\pi {}^1P_1$  [149]. The new CLEO [148] recoil mass spectrum against  $\pi^+\pi^-$  in

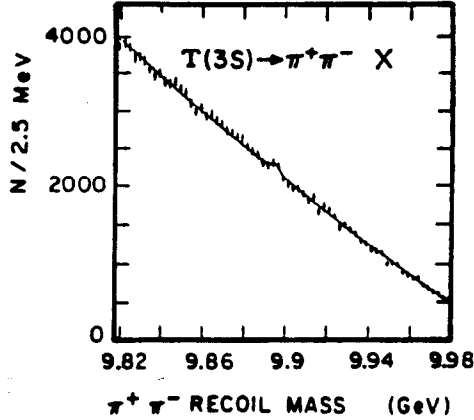


Figure 42: CLEO [148] missing mass spectrum against  $\pi^+\pi^-$  from  $\Upsilon(3S) \rightarrow \pi^+\pi^- + \text{hadrons}$ .

$\Upsilon(3S) \rightarrow \pi^+\pi^- + \text{hadrons}$  is shown for the  $^1P_1$  region in Fig. 42. The peak near the expected  $^1P_1$  mass contains  $\sim 330$  events, but due to the large background is only a  $2.5\sigma$  effect. Again, if it is real, more data will tell, and CLEO hopes to at least double the data sample by the end of this year. The present effect corresponds to a branching ratio  $B(3S \rightarrow \pi^+\pi^- X) \sim 0.4\%$  or an upper limit of  $0.6\%$ .

Theoretically the  $\Upsilon(3S) \rightarrow \pi\pi^1P_1$  decay is treated as a two step process (Fig. 43): the  $Q\bar{Q}$  system emits two gluons, which then turn into pions. Kuang and Yan [149] assume that the  $gg \rightarrow \pi\pi$  transition occurs with probability 1. This assumption works well for the  $\Upsilon(3S,2S) \rightarrow \pi\pi\Upsilon(1S)$  decays, but predicts too large a rate for  $\Upsilon(3S) \rightarrow \pi\pi\Upsilon(2S)$ , where the smaller energy available makes ignoring mass effects more risky. For  $B(\Upsilon(3S) \rightarrow \pi\pi^1P_1)$  it gives  $\sim 1\%$ .

Voloshin [150] has disputed the validity of this picture. The ITEP group have analysed the matrix elements  $\langle \pi\pi | \theta | 0 \rangle$ , where  $\theta$  is the QCD stress tensor, containing products of color electric and magnetic fields, analogous to the stress tensor used in textbook electricity and magnetism. The  $E1 \cdot E1$  element, which is used in  $\Upsilon(3S) \rightarrow \pi\pi\Upsilon(1S)$ , is enhanced by the triangle anomaly. This enhancement does not apply to the  $E1 \cdot M1$  of  $\Upsilon(3S) \rightarrow \pi\pi^1P_1$ , so its rate should be relatively suppressed. Voloshin estimates  $B(\Upsilon(3S) \rightarrow \pi\pi^1P_1) \leq 10^{-4}$  and  $B(\Upsilon(3S) \rightarrow \pi^0^1P_1) \sim 10^{-3}$ .

## 7 Conclusions

Light mesons:

- Time reversal invariance tells us that mesons which decay to  $K\bar{K}$  are also produced in  $K\bar{K}$

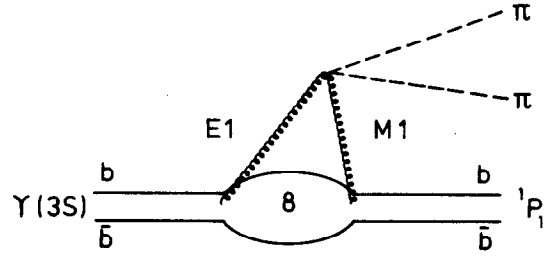


Figure 43: Diagram for  $\Upsilon(3S) \rightarrow \pi\pi^1P_1$ . Note that the gluons are emitted from the  $Q\bar{Q}$  system as a whole. Gluons of such low energy don't have enough spatial resolution to see the individual quarks. Physical states must be color singlets, but since a gluon carries color, the  $Q\bar{Q}$  after the first gluon emission is in a color octet state. Upon emitting the second gluon, it becomes a color singlet again.

collisions, even if they are glueballs.

- The 2.2 GeV region is populated by  $\phi\phi$ ,  $K\bar{K}$ , and  $\eta\eta'$  resonances, largely with  $J^{PC}=2^{++}$ . Along with the  $f_2(1720)$  seen in radiative  $J/\psi$  decay, there are too many neutral  $2^{++}$  mesons for a  $q\bar{q}$  nonet.
- Systematic comparisons of the production of final states  $X$  in  $J/\psi \rightarrow \gamma X$ ,  $\omega X$ , and  $\phi X$  are very promising, but need spin-parity measurements.
- 2 high-statistics experiments have seen  $\eta(1420) \rightarrow a_0\pi$ ; 1 has seen  $f_1(1420) \rightarrow K^*K$ . The production mechanisms are different, so it is quite possible that there are two particles at 1420 MeV. However cross-checks between the experiments would help us to be convinced, or not.
- Evidence from  $Q^2 > 0$   $\gamma\gamma$  collisions supports the existence of an  $f_1(1420)$ . However in its hadronic production and decay it doesn't behave like the partner of the  $f_1(1285)$ .  $f_1(1285)$ ,  $f_1(1420)$ , and  $f_1(1525)$  are one too many  $I=0$   $1^{++}$  mesons for one  $q\bar{q}$  nonet.
- $Q^2=0$   $\gamma\gamma$  collisions show no sign of any of the radially excited  $0^{-+}$  candidates:  $\eta(1275)$ ,  $\eta(1420)$ ,  $\eta(1460)$ . Especially if the new  $\eta(1450)$  is confirmed, we have too many for a  $q\bar{q}$  nonet.

We have been frustrated in looking for a pure glueball candidate. But a complicated spectrum due to mixtures of  $q\bar{q}$ ,  $gg$ , and  $gq\bar{q}$  is a more reasonable expectation, and a better match to the chaos which is emerging (again) in light meson spectroscopy. Will

a modern version of the eight-fold way straighten it out?

#### Heavy Quark Spectroscopy:

- The  $\gamma\gamma$  width of the  $\eta_c$  is roughly as expected, the primary problem being lack of statistics.
- Statistics are also plaguing the search for the  $c\bar{c}$  and  $b\bar{b}$   $^1P_1$  states, but more data is coming. Calculations of  $\Upsilon(3S) \rightarrow \pi\pi ^1P_1$  should be done soon if they are to count as predictions.
- The leptonic branching ratio of the  $\Upsilon(3S)$  has been measured, and the leptonic and total widths of the  $\Upsilon(1S) - \Upsilon(3S)$  updated with corrected use of radiative corrections.
- The  $\chi_b(2P)$  mass splitting has now been well measured, and agrees with theorists' (previous) preference for scalar confinement. But now there are theoretical doubts in some quarters.

The heavy quark spectroscopy measured so far is a gratifying confirmation of the heavy quark potential model, and demonstrates that, at least in this domain, meson spectroscopy can be understood.

#### Acknowledgements

This talk is based on information presented by the speakers in the Two Photon, Heavy Quark, and Light Quark parallel sessions, and on discussions with many of them. For help in clarifying various issues after the conference, I thank C. Bemporad, F. Berends, N. Byers, R. Cester, S.-U. Chung, S. Godfrey, N. Isgur, K. Königsmann, L. Köpke, R. Longacre, D. Morgan, V. Obraztsov, B. Ratcliff, M. Reidenbach, H.-W. Siebert, Y. S. Tsai, and D. Williams. In particular I am grateful for many discussions with Helmut Marsiske, and for the drawings by Ursula Rehder.

#### References

- [1] Review of Particle Properties, Particle Data Group, Phys. Lett. **170B** (1986).
- [2] A. Etkin *et al.*, Phys. Rev. Lett. **49**, 1620 (1982) S. J. Lindenbaum, Proc. Int. Conf. on HEP, Bari, July 1985, p. 311.
- [3] F. Binon (GAMS), talk 10FB; D. Alde *et al.*, Nucl. Phys. **B269**, 485 (1986).
- [4] R. Longacre, talk 10RL; A. Etkin *et al.*, paper 1899, sub. to Phys. Lett. **B**.
- [5] J. D. Jackson, Nuovo Cim. **34**, 1644 (1964).
- [6] R. A. Lee (Crystal Ball), Stanford Ph.D. thesis, SLAC-282 (1985).
- [7] M.E.B. Franklin (Mark II), Stanford Ph.D. thesis, SLAC-254 (1982).
- [8] D. M. Coffman *et al.* (Mark III), SLAC-PUB-3720 (1986), Sub. to Phys. Rev. **D**.
- [9] R. M. Baltrusaitis *et al.* (Mark III), Phys. Rev. **D33**, 1222 (1986).
- [10] R. M. Baltrusaitis *et al.* (Mark III), Phys. Rev. Lett. **55**, 1723 (1985).
- [11] K. F. Einsweiler (Mark III), Stanford Ph.D. Thesis, SLAC-272, May 1984.
- [12] J. E. Augustin *et al.* (DM2), Orsay preprint LAL/85-27, July 1985.
- [13] C. Edwards *et al.* (Crystal Ball), Phys. Rev. Lett. **48**, 458 (1982).
- [14] J. J. Becker *et al.* (Mark III), paper 3409.
- [15] V. F. Obraztsov (GAMS), talk 10VO.
- [16] E. D. Bloom and C. W. Peck (Crystal Ball), Ann. Rev. Nucl. Part. Sci. **33**, 143 (1983).
- [17] S. Godfrey and N. Isgur, Phys. Rev. **D32**, 189 (1985).
- [18] D. Aston (LASS), talk 10DA.
- [19] M. Gell-Mann and K. M. Watson, Ann. Rev. Nucl. Sci. **4**, 219 (1954); K. M. Watson *et al.*, Phys. Rev. **101**, 1159 (1956); Hamilton, *The Theory of Elementary Particles*, p. 358, Oxford Univ. Press (1959).
- [20] R. Longacre, private communication.
- [21] G. W. Brandenburg *et al.*, Nucl. Phys. **B104**, 413 (1976); M. Aguilar-Benitez *et al.*, Z. Phys. **C8**, 313 (1981).
- [22] F. C. Porter (Crystal Ball), Proc. Summer Inst. on Particle Physics, Stanford, 1981. SLAC Report 245.
- [23] E. D. Bloom (Crystal Ball), SLAC-PUB-3573, Proc. Aspen Winter Physics Conf., Jan. 1985.
- [24] T. A. Armstrong *et al.* (WA76), Phys. Lett. **167B**, 133 (1986). This data has peaks in  $K\bar{K}$  at 1629 and 1742 MeV.
- [25] K. L. Au, D. Morgan and M. R. Pennington. Rutherford preprint RAL-86-076 (1986).
- [26] J. J. Becker *et al.* (Mark III), paper 3441.
- [27] L. Köpke (Mark III), Proc. XXI Rencontre de Moriond, Les Arcs, 9-16 March 1986, Santa Cruz preprint SCIPP 86/61; U. Mallik, Les Arcs, 16-22 March 1986, SLAC-PUB-3946.



- [28] B. Jean-Marie (DM2), talk 10BJ.
- [29] L. Köpke (Mark III), talk 10LK.
- [30] M. Althoff *et al.* (TASSO), Phys. Lett. **121B**, 216 (1983).
- [31] H. Aihara *et al.* (TPC/2 $\gamma$ ), Phys. Rev. Lett. **57**, 404 (1986).
- [32] D. Cords (Mark II), talk 19DC and contributed paper.
- [33] T. D. Lee, Proc. 21<sup>st</sup>/ Int. School of Subnuclear Physics, Erice, 3-14 Aug. 1983. See also S. J. Lindenbaum, BNL 37412 and in Superstrings, Supergravity and Unified Theories, pub. by World Scientific, p. 570.
- [34] R. Sinha, S. Okubo, S. F. Tuan, UH-511-592-86 (1986).
- [35] J. J. Becker *et al.* (Mark III), paper 3468.
- [36] A. Etkin *et al.*, Phys. Rev. **D25**, 1786 (1982).
- [37] F. Binon (GAMS), talk 10FB; D. Alde *et al.*, paper 9822, CERN-EP/86-71, June 1986.
- [38] S. Godfrey, R. Kokoski and N. Isgur, Phys. Lett. **141B**, 439 (1984).
- [39] R. M. Baltrusaitis *et al.* (Mark III), Phys. Rev. Lett. **56**, 107 (1986).
- [40] J. Sculli, talk 10JS; J. H. Christenson *et al.*, paper 5975.
- [41] S. S. Gershtein, A. A. Likhoded and Yu. D. Prokoshkin, Z. Phys. **C24**, 305 (1984).
- [42] S. I. Bitjukov *et al.*, (Lepton-F), Serpukov preprint 86-110 (1986), sub. to Phys. Lett. **B**; JETP Lett. **42**, 384 (1985); Sov. J. Nucl. Phys. **38**, 727 (1983).
- [43] H. Primakoff, Phys. Rev. **81**, 899 (1951).
- [44] J. Huston *et al.*, Phys. Rev. **D33**, 3199 (1986).
- [45] T. Ferbel, talk 10TF.
- [46] M. Bourquin *et al.* (WA62), Phys. Lett. **172B**, 113 (1986); H.-W. Siebert, private communication.
- [47] A. N. Aleev *et al.* (BIS-2), paper 11207.
- [48] R. Brandelik *et al.* (TASSO), Phys. Lett. **97B**, 448 (1980); M. Althoff *et al.*, Z. Phys. **C16**, 13 (1982).
- [49] D. L. Burke *et al.* (Mark II), Phys. Lett. **103B**, 153 (1981); H. J. Behrend *et al.* (CELLO), Z. Phys. **C21**, 205 (1984).
- [50] W. G. J. Langeveld (TPC/2 $\gamma$ ), talk 19WL.
- [51] N. N. Achasov, S. A. Devyanin and G. N. Shestakov, Z. Phys. **C16**, 55 (1982) and Z. Phys. **C27**, 99 (1985); B. A. Li and K. F. Liu, Phys. Rev. **D30**, 613 (1984).
- [52] J. E. Olsson (JADE), cont. paper to EPS Conf., Brighton, 1983. The data is shown in H. Kolanoski, Proc. Int. Symp. on Lepton Photon Interactions, Kyoto, 1985.
- [53] G. Alexander, U. Maor and P. G. Williams, Phys. Rev. **D26**, 1198 (1982).
- [54] G. Alexander, A. Levy and U. Maor, Z. Phys. **C30**, 65 (1986).
- [55] H. Aihara *et al.* (TPC/2 $\gamma$ ), Phys. Rev. Lett. **54**, 2564 (1985); M. Althoff *et al.* (TASSO), Z. Phys. **C32**, 11 (1986).
- [56] P. M. Patel (ARGUS), talk 19PP; H. Albrecht *et al.*, paper 7986.
- [57] T. A. Armstrong *et al.* (WA76), K<sup>+</sup>K<sup>\*</sup>: paper 7854;  $\phi\phi$ : Phys. Lett. **166B**, 245 (1986).
- [58] D. Bridges *et al.*, Phys. Rev. Lett. **56**, 211 and 215 (1986); Phys. Lett. **180B**, 313 (1986).
- [59] K.-F. Liu and B.-A. Li, paper 2283, Stonybrook preprint ITP-SB-86-48 (1986).
- [60] P. Baillon *et al.*, Nuovo Cim. **50A**, 393 (1967); P. Baillon, CERN/EP 82-127, Proc. XXI Int. Conf. on High Energy Physics, Paris, 1982.
- [61] C. Dionisi *et al.*, Nucl. Phys. **B169**, 1 (1980).
- [62] T. A. Armstrong *et al.* (WA76), paper 7870.
- [63] S. U. Chung (AGS-771), talk 10SC and private communication.
- [64] D. F. Reeves *et al.* (AGS-771), Phys. Rev. **D34**, 1960 (1986).
- [65] S. U. Chung *et al.* (AGS-771), Phys. Rev. Lett. **55**, 779 (1985).
- [66] D. Zieminska (AGS-771), Proc. Int. Conf. on Hadron Spectroscopy, College Park, Maryland, April 1985.
- [67] A. Ando *et al.* (KEK), Phys. Rev. Lett. **57**, 1296 (1986); K. Takamatsu, private communication.
- [68] Th. Mouthuy (GAMS), Proc. Int. Conf. on HEP, Bari, July 1985, p. 320.
- [69] Ph. Gavillet *et al.*, Z. Phys. **C16**, 119 (1982).
- [70] S. I. Bitjukov *et al.* (Lepton-F), Sov. J. Nucl. Phys. **39**, 735 (1984).
- [71] B. Ratcliff (LASS), talk at SLAC Summer Institute, 1986.

- [72] T. A. Armstrong *et al.* (WA76), Phys. Lett. **146B**, 273 (1984).
- [73] O. Villalobos Baille (WA76), Proc. Int. Conf. on HEP, Bari, July 1985, p. 314.
- [74] J. D. Richman (Mark III), CalTech Ph.D. Thesis, CALT-68-1231 (1985).
- [75] J. J. Becker *et al.* (Mark III), paper 3433.
- [76] J. J. Becker *et al.* (Mark III), paper 3476.
- [77] L. D. Landau, Soviet Physics "Doklady" **60**, 207 (1948). C. N. Yang, Phys. Rev. **77**, 242 (1950).
- [78] A. M. Eisner (TPC/2 $\gamma$ ), talk 19AE; H. Aihara *et al.*, Phys. Rev. Lett. **57**, 51 and 2500 (1986).
- [79] G. Gidal (Mark II), talk 19GG and contributed paper.
- [80] M. S. Chanowitz, Proc. VI Int. Workshop on Photon-Photon Collisions, Lake Tahoe, Sept. 1984.
- [81] N. Stanton *et al.*, Phys. Rev. Lett. **42**, 346 (1979).
- [82] S. D. Protopopescu (AGS-771), Proc. XXI Rencontre de Moriond, Les Arcs, 16-22 March 1986.
- [83] M. Frank and P. J. O'Donnell, Phys. Rev. **D32**, 1739 (1985); S. B. Gerasimov and A. B. Govorkov, Z. Phys. **C29**, 61 (1985).
- [84] R. Clare (Crystal Ball), Proc. XXI Rencontre de Moriond, Les Arcs, 16-22 March 1986.
- [85] N. Isgur, private communication.
- [86] S. Meshkov, W. F. Palmer and S. S. Pinsky, DOE/ER/01545-382 (1986), sub. to Phys. Rev. Lett.
- [87] S. Godfrey and N. Isgur, private communication and Ref. [17].
- [88] G. Bellettini *et al.*, Nuovo Cim. **40A**, 1139 (1965).
- [89] V. I. Kryshkin *et al.*, Soviet Physics JETP **30**, 1037 (1970).
- [90] A. Browman *et al.*, Phys. Rev. Lett. **32**, 1067 (1974) and **33**, 1400 (1974).
- [91] H. W. Atherton *et al.*, Phys. Lett. **158B**, 81 (1985).
- [92] D. Williams (Crystal Ball), talk 19DG and private communication.
- [93] C. Bemporad *et al.*, Phys. Lett. **25B**, 380 (1967), corrected for  $B(\eta \rightarrow \gamma\gamma) = (38.9 \pm 0.4)\%$  [1].
- [94] A. Weinstein *et al.* (Crystal Ball), Phys. Rev. **D28**, 2869 (1983).
- [95] W. Bartel *et al.* (JADE), Phys. Lett. **160B**, 417 (1985).
- [96] H. Aihara *et al.* (TPC/2 $\gamma$ ), Phys. Rev. **D33**, 844 (1986).
- [97]  $t_{\min}$  occurs when the  $\eta$  is produced parallel to the incoming  $\gamma$  direction ( $\theta=0$ ). Then  $t = m_{\eta}^2 - 2E_{\gamma}(E_{\eta} - p_{\eta})$ . Approximating the nucleus as infinitely heavy,  $E_{\eta} = E_{\gamma}$  in the lab frame. Expanding  $p_{\eta}$  according to  $\sqrt{1-x} \approx 1-x/2 - x^2/8$  yields  $t_{\min} \approx -M_{\eta}^4/4E_{\gamma}^2$ .
- [98] J. E. Gaiser *et al.* (Crystal Ball), Phys. Rev. **D34**, 711 (1986).
- [99] R. M. Baltrusaitis *et al.* (Mark III), Phys. Rev. **D33**, 629 (1986).
- [100] B. Jean-Marie (DM2), talk 9BJ
- [101] Ch. Berger *et al.* (PLUTO), Phys. Lett. **167B**, 120 (1986).
- [102] U. Karshon (TASSO), Cont. to VIIth Int. Workshop on Photon-Photon Collisions, Paris, April 1986.
- [103] C. Baglin *et al.* (R704), CERN/EP/0061P (1986).
- [104] A. E. Blinov *et al.* (MD-1), Novosibirsk preprint 86-107.
- [105] R. Cester, E760 spokesperson.
- [106] R. Barbieri *et al.*, Phys. Lett. **95B**, 93 (1980).
- [107] L. J. Reinders, H. R. Rubinstein, and S. Yazaki, Phys. Lett. **113B**, 411 (1982).
- [108] S. W. Herb *et al.*, Phys. Rev. Lett. **39**, 252 (1977).
- [109] W. R. Innes *et al.*, Phys. Rev. Lett. **39**, 1240 (1977); K. Ueno *et al.*, Phys. Rev. Lett. **42**, 486 (1979).
- [110] M. Alex (E605), talk 9MA.
- [111] S.H.H. Tye and C. Rosenfeld, Phys. Rev. Lett. **53**, 2215 (1984).
- [112] C. Peck *et al.* (Crystal Ball), SLAC-PUB-3380 and DESY 84-064; H.-J. Trost, Proc. XXII Int. Conf. on HEP, Leipzig, July 1984.
- [113] D. Besson *et al.* (CLEO), Phys. Rev. **D33**, 300 (1986). J. Lee-Franzini (CUSB), Proc. 5<sup>th</sup> Int. Conf. on Physics in Collision, Autun, France, July 1985.
- [114] E. D. Bloom (Crystal Ball), SLAC-PUB-3686, Proc. 5<sup>th</sup> Topical Workshop on Proton Antiproton Collider Physics, St. Vincent, Italy, Feb. 1985.

- [115] H. Albrecht *et al.* (ARGUS), Phys. Lett. **154B**, 452 (1985); Z. Phys. **C29**, 167 (1985).
- [116] U. Strohbusch (Crystal Ball), DESY seminar, 1986.
- [117] A. E. Blinov *et al.* (MD-1), Novosibirsk preprint 85-99.
- [118] J. Siegrist *et al.* (Mark I), Phys. Rev. **D26**, 969 (1982).
- [119] B. Niczyporuk *et al.* (LENA), Z. Phys. **C15**, 299 (1982).
- [120] J. D. Jackson and D. L. Scharre, Nucl. Inst. and Meth. **128**, 13 (1975).
- [121] É. A. Kuraev and V. S. Fadin, Sov. J. Nucl. Phys. **41**, 466 (1985).
- [122] S. E. Baru *et al.* (VEPP-4), Z. Phys. **30**, 551 (1986).
- [123] Y. S. Tsai, SLAC-PUB-3129 (1983).
- [124] M. Greco, G. Pancheri-Srivastava, Y. Srivastava, Phys. Lett. **56B**, 367 (1975).
- [125] Ch. Berger *et al.* (PLUTO), Z. Phys. **C1**, 343 (1979). Only  $\Gamma_{ee}$  is quoted, not  $\Gamma_{ee} \Gamma_{had}/\Gamma_{tot}$ . The description of the radiative corrections used does not obviously correspond to any presented here. Therefore the PLUTO value could not be corrected or included in the average.
- [126] P. Bock *et al.* (DESY-Heid.), Z. Phys. **C6**, 125 (1980).
- [127] B. Niczyporuk *et al.* (LENA), Phys. Rev. Lett. **46**, 92 (1981). In Z. Phys. **C15** 299 (1982), this group revised their  $\Gamma_{ee}(1S)$  value, normalising to their new measurement of the continuum R. However the R they originally used is closer to the current average R see Ref. [130]; therefore I use their original  $\Gamma_{ee}$ .
- [128] B. Niczyporuk (LENA), private communication: The LENA  $\Gamma_{ee}$  measurements used a modified Jackson-Scharre radiative correction formula with full soft photon exponentiation.
- [129] H. Albrecht *et al.* (DASP II), Phys. Lett. **116B**, 383 (1982).
- [130] R. Giles *et al.* (CLEO), Phys. Rev. **D29** 1285(1984). The values for  $\Gamma_{ee} \Gamma_{had}/\Gamma_{tot}$  before correction for  $B_{\mu\mu}$  are quoted in Ref. [133]. The value of  $\delta_{vac}^{had}$  used was 0.034, as quoted in R. K. Plunkett, Cornell Ph.D. thesis (1983).
- [131] P. M. Tuts, Int. Symp. on Lepton and Photon Interactions at High Energy, Ithaca, N.Y. (1983), p. 284; and private communication.
- [132] B. Niczyporuk *et al.* (LENA), Phys. Lett. **99B**, 169 (1981).
- [133] D. Andrews *et al.* (CLEO), Phys. Rev. Lett. **50**, 807 (1983).
- [134] J. E. Horstkotte *et al.*, CUSB-83-09, quoted in Ref. [131].
- [135] Ch. Berger *et al.* (PLUTO), Phys. Lett. **93B**, 497 (1980).
- [136] D. Besson *et al.* (CLEO), Phys. Rev. **D30**, 1433 (1984).
- [137] D. MacFarlane (ARGUS), talk at XXIII Int. Conf. on HEP, Berkeley, July 1986; and R. Waldi, private communication.
- [138] R. Giles *et al.* (CLEO), Phys. Rev. Lett. **50**, 877 (1983).
- [139] P. Haas *et al.* (CLEO), Phys. Rev. **D30**, 1996 (1984).
- [140] H. Albrecht *et al.* (ARGUS), Z. Phys. **C28**, 45 (1985).
- [141] J. Lee-Franzini (CUSB), talk 9JL; and CUSB contributed papers:  $B_{\mu\mu}$ -T. Kaarsberg *et al.*, paper 7480;  $\chi_b(2P)$  inclusive-C. Yanagisawa *et al.*, paper 7501;  $\chi_b(2P)$  exclusive-T. Zhao *et al.*, paper 7498.
- [142] S. Cooper, SLAC-PUB-3555, in Proc. 12<sup>th</sup> SLAC Summer Inst. on Particle Physics, Stanford, July 1984.
- [143] I have given a more thorough discussion of this with references: S. Cooper, SLAC-PUB-3819, Proc. Int. Conf. on HEP, Bari, July 1985.
- [144] C. Klopfenstein *et al.* (CUSB), Phys. Rev. Lett. **51**, 160 (1983).
- [145] N. Byers, talk 9NB; N. Byers and V. Zambetakis, UCLA/86/TEP/24.
- [146] A recent review is R. H. Datitz and S. F. Tuan, Proc. 10<sup>th</sup> Hawaii Conf. on HEP, 1985.
- [147] C. Baglin *et al.* (R704), Phys. Lett. **171B**, 135 (1986).
- [148] T. Bowcock *et al.* (CLEO), paper 6173, Cornell preprint CLNS-86/740.
- [149] Y.-P. Kuang and T.-M. Yan, Phys. Rev. **D24**, 2874 (1981); G.-Z. Li and Y.-P. Kuang, Commun. Theor. Phys. **5**, 79 (1986).
- [150] M. B. Voloshin, Moscow preprint ITEP-166 (1985).